TECHNICAL REPORT

ISO/TR 13571-2

First edition
2016-07-01

Life-threatening components of fire —

Part 2: **Methodology and examples of tenability assessment**

Composants dangereux du feu —

Partie 2: Méthodologie et exemples d'analyse de tenabilité

Reference number
ISO/TR 13571-2:2016(E)

Contents

Page

Foreword

ISO (the International Organization for Standardization) is a worldwide federation of national standards bodies (ISO member bodies). The work of preparing International Standards is normally carried out through ISO technical committees. Each member body interested in a subject for which a technical committee has been established has the right to be represented on that committee. International organizations, governmental and non-governmental, in liaison with ISO, also take part in the work. ISO collaborates closely with the International Electrotechnical Commission (IEC) on all matters of electrotechnical standardization.

The procedures used to develop this document and those intended for its further maintenance are described in the ISO/IEC Directives, Part 1. In particular the different approval criteria needed for the different types of ISO documents should be noted. This document was drafted in accordance with the editorial rules of the ISO/IEC Directives, Part 2 (see www.iso.org/directives).

Attention is drawn to the possibility that some of the elements of this document may be the subject of patent rights. ISO shall not be held responsible for identifying any or all such patent rights. Details of any patent rights identified during the development of the document will be in the Introduction and/or on the ISO list of patent declarations received (see www.iso.org/patents).

Any trade name used in this document is information given for the convenience of users and does not constitute an endorsement.

For an explanation on the meaning of ISO specific terms and expressions related to conformity assessment, as well as information about ISO's adherence to the World Trade Organization (WTO) principles in the Technical Barriers to Trade (TBT) see the following URL: www.iso.org/iso/foreword.html.

The committee responsible for this document is ISO/TC 92 *Fire Safety*, Subcommittee 3, *Fire threat to people and environment*.

Introduction

Tenability of people in case of fire is an essential safety objective of regulations. Reasons that could lead to compromised tenability conditions are loss of visibility, thermal and toxic effects. ISO 13571 is a tool that has been developed to quantify the performance level related to these criteria in case of a fire.

This document presents application cases of ISO 13571. It is structured as follows:

— Clause 4 explains the principle of the application;

— Clause 5 presents the selection of performance criteria;

— Clause 6 presents the evaluation of the impact of fire to people according to ISO 13571;

— Clause 7 introduces the examples detailed in Annexes A, B, D and E.

Examples of application are presented in annexes. The first case of application concerns comparison of tenability in real-scale fire tests (Annex A and Annex B). The second case presents the methodology (Annex C) and two example cases (Annex D and Annex E) for application of ISO 13571 as performance criteria in Fire Safety Engineering studies according to ISO 23932. Annex F presents information on experimental production of input data.

Life-threatening components of fire —

Part 2: Methodology and examples of tenability assessment

1 Scope

This document describes the practical application of ISO 13571 as a tool to evaluate effects of fire effluents on people. The method of application, performance criteria and evaluation of the impact are explained and illustrated by two families of examples: application to real-scale tests (Annex A and Annex B) and application to Fire Safety Engineering (Annex C, D and E).

2 Normative references

The following documents, in whole or in part, are normatively referenced in this document and are indispensable for its application. For dated references, only the edition cited applies. For undated references, the latest edition of the referenced document (including any amendments) applies.

There are no normative references in this document.

3 Terms and definitions

For the purposes of this document, the terms and definitions given in ISO 13943 and ISO 13571 apply. ISO and IEC maintain terminological databases for use in standardization at the following addresses:

— IEC Electropedia: available at http://www.electropedia.org/

— ISO Online browsing platform: available at http://www.iso.org/obp

4 Principle

Smoke toxicity, to a certain degree, is not a material property. Depending on the environment, availability of oxygen, thermal attack, flow conditions and surface areas available for combustion, the chemistry of the combustion of a given material can proceed along various routes and produce species in very different quantities.[1][2][3] It is then a systemic parameter, which need a systemic approach, as stated in ISO 19706.

It is also appropriate to keep the following points in mind:

— The production rates of various gaseous species change according to the combustion regime. In particular the influential parameters (not exhaustive) are:

  — Fuel nature

  — Oxygen availability

  — Temperature

- Flows received and lost
- The species produced by the combustion are carried away from the initial fire source, and their effect is related to:
  - Sensitivity and activity of people
  - Concentrations (instantaneous)
  - Exposure times (accumulation)

Furthermore, the thermal effects related to the heat of the gases and smoke produced, along with the radiant fluxes, which they emit, play a role in the safety of people who are evacuating.

For a given design fire, it is therefore necessary to determine one or more exposure scenarios, which will make it possible to answer questions about the effects on people according to:

- The fire source and its development;
- The species produced by this fire source and their movement away from the original fire source;
- The evacuation of the people, their path and the toxic and thermal elements to which they are subject as a function of time.

Finally, it is useful to recall that toxic hazard in enclosures is mainly caused by the combustion of the contents and furnishings in the enclosure rather than the enclosure itself in the early phases of a fire. Furthermore, changes in regulations can lead to better insulation of the rooms, modification of the ventilation, and resistance of windows to bursting, all of which notably change the conditions for the accumulation of thermal energy and the generation of toxic species.

The following are the objectives of the application of ISO 13571:

- Assess effects of fire on people as a principal criterion for performance evaluation in Fire Safety Engineering studies, or in comparison of real-scale fire tests,
- Involve realistic fire sources in terms of:
  - Kinetics
  - Species produced, in particular by including data concerning the toxic species related to the burning of the contents and furnishings in building fires
- Be able to process all the materials present and not just certain ones
- Consider all potential toxic species, not only CO, as is often seen in practice
- Consider the aspects of production kinetics, movement of gases, and availability of oxygen
- Be able to process several scenarios and their possible variations:
  - “Typical” materials/”risky” materials
  - Risk in the room of fire origin room and outside the room of origin
  - Different fire regimes (smouldering, well ventilated, post-flashover)
  - Evacuation plans
- Consider the various risks for people and the associated sanction criteria as a function of thermal and toxic effects, both instantaneous and by accumulation.

5 Performance criteria

The selection of criteria to consider is conducted in early phases of a project, before any detailed study.

These criteria will make it possible to determine whether a given exposure scenario (i.e. a fire scenario combined with an evacuation scenario) is a success or failure. This concept depends above all on the susceptibility of the people to the fire effluent. In the application of ISO 13571, the objective that a person could realize his/her own evacuation without any assistance.

In fact, each person is different and according to their constitution, age, gender, possible underlying conditions, etc. the FEC and FED which they can endure before being incapacitated varies. There is, however, no feedback from experience which can be used in statistical terms. Due to the lack of precise knowledge in this field, approximating the distribution of individual susceptibilities by a log-normal distribution with a median value of one as thresholds for the FED and FEC is proposed. Half the population is therefore considered as being able to tolerate FED and FEC each having a value of one, and the other half is more sensitive and cannot tolerate values of FED and FEC equal to or above one.

As an example of a safety criterion that provides protection for a larger fraction of the population, ISO 13571:2012, A.5.2 shows that a value 0,3 protects a significant portion of the more sensitive people. At this value, 11,4 % of the population remains vulnerable to incapacitation by exposure to the fire effluent. It should be kept in mind that one of the consequences of the distribution described by the ISO 13571:2012 standard for the sensitivity of individuals (log-normal law) is that there is no value for the criterion which is low enough to guarantee protection of all occupants in an evacuation situation. Designing a facility such that the FED and FEC values are kept to extremely low values is likely to require immediate detection and suppression or to preclude otherwise desirable construction and furnishing products. It is the regulator’s role to weigh these considerations.

6 Evaluation of the impact

6.1 Effects of fire on people

The impact of fire effluent on a person depends on two interacting components. The first is the location of a person and how that location might change during the course of the fire. The second is the evolving concentrations of the effluent constituents where the person is located.

A fire safety assessment could be made considering the evolution of tenability for a person who is stationary at one position in a room. This would apply to people who are asleep or medically confined. Such an application in real-scale fire tests is presented in Annex A. Assessment could also consider the exposure of a person moving along an egress path with its travel path in real-scale fire tests (Annex B) or included in a Fire Safety Engineering approach (Annexes C to E).

The exposure models used are those described in ISO 13571:2012. In particular, they cover the toxic and thermal models, but do so independently. For the toxic models, the effects of the asphyxiating and irritating gases are considered separately. See ISO 19706 for more details on the relevance of these models.

6.2 Models for toxic impact

Toxic effluents can have two principal mechanisms of action on people when considering acute exposure. Depending on their nature, they are classified into two categories:

— asphyxiating gases (CO, HCN, etc.)

— irritating gases (HCl, HBr, etc.)

There are also indirect effects like those of the low oxygen concentration (hypoxia) or high CO_2 concentration (hyperventilation). Other effects exist, like clogging of the respiratory tracts because of the presence of soot.

The evaluation of the effects related to exposure to smoke requires knowledge of the central concepts. The References [4] and [5] present a review of the art of these concepts.

Because of the complexity of the problem, there are various models incorporating toxic effects. Although all of them can be used, a first consensus was established on the models given in ISO 13571. In the ISO 13571 models, the asphyxiating gases, incorporated using the calculation of a Fractional Effective Dose (FED), and the irritating gases, incorporated using the calculation of Fractional Effective Concentration (FEC), are considered separately.

Thus, the asphyxiating gases (mainly CO, and HCN) are considered from the perspective of an accumulation mechanism, and the irritants (mainly HCl, HBr, HF, SO_2, NO, NO_2, acrolein, and formaldehyde) from that of their instantaneous effect. These assumptions are only valid when considering short-term acute effects at an incapacitating level of exposure. For irritants, other, dose-related aspects need to be included when considering long exposures or lethality levels.

One of the limits of the ISO 13571 asphyxiant gas model is that it does not incorporate the rarefaction of oxygen, O_2, which also has an asphyxiating effect. However, in many situations this effect can be considered to be minor compared with the effects of CO and HCN. CO_2 is considered as producing a hyperventilation factor in ISO 13571.

6.3 Models for thermal impact

Three mechanisms are considered: hyperthermia linked to exceeding the body's thermal regulation capacity, skin burns, and burns in the bronchial tubes. In most cases, bronchial tube burns take place at higher exposure levels than skin burns.

There are two models proposed in ISO 13571 one for radiant flux exposure and one for exposure to convective heat exchange – and they are synthesized in the form of an FED making it possible to calculate the cumulative dose.

6.3.1 Radiant flux exposure model

Two formulas are proposed in ISO 13571. The first makes it possible to calculate the time to get second-degree burns on the skin; the second makes it possible to calculate the time to reach the pain threshold.

It should be noted that the skin temperature depends on the applied flux density at the surface and the ease with which the blood carries away the energy reaching under the skin. Because of this there is a threshold located around 2,5 $kW.m^{-2}$, below which exposure to the flux does not cause a significant temperature increase of the skin and above which the temperature increase occurs quickly. A greater exposure can however be acceptable with the exposure time is short, especially when considering passing before an opening leading to an area on fire. Further details can be found in ISO 13571.

6.3.2 Temperature exposure model

Two formulas are included in ISO 13571, according to whether the subject is dressed normally or lightly dressed (even naked) for calculating the time necessary to become incapacitated (for an air environment at less than 10 % relative humidity).

6.3.3 Dose calculation model

The dose effect linked to the accumulation of the temperature is calculated using the thermal model FED equation of ISO 13571.

7 Examples of application

Annex A presents an example of application of ISO 13571 to a series of real-scale fire tests performed on houses with different designs of floors between the basement and the rest of the house, in two different basement fire scenarios. The objective of the study was to better understand the impact of basement fires on the ability of occupants on the upper storeys to escape. ISO 13571 models are used to monitor tenability conditions at various locations in the upper storeys. The example gives a relative comparison between different designs, using FED as the comparison criterion, without considering any specific evacuation scenario.

Annex B presents the application of ISO 13571 to different real-scale fire scenarios on a single sleeping room. Analysis is based on the time to reach compromised tenability conditions using thermal and toxic models of ISO 13571 and different evacuation strategies. The results identify the main factor comprising tenability for each scenario, according to occupant's behaviour.

Annex C presents a methodology to apply ISO 13571 to Fire Safety Engineering studies. It refers to ISO 23932 and proposes a mathematical approach that allows obtaining tenability data as performance criteria. This methodology is based on a construction of a source term of toxic gases in addition to a source term of heat release in the Design Fire Scenario studied. It proposes ways to obtain data for each fire stage and presents the input data in a matricial shape.

Annex D is a first application of methodology proposed in Annex C. The situation is a fire in a hotel room connected to a corridor equipped with mechanical smoke control devices. Tenability assessment in the corridor is studied according to the ISO 13571 models. Various scenarios of occupant behaviour are tested, such as different departure times, a travel trough the corridor or turn back depending on the conditions. The different evacuation strategies and occupant behaviour lead to contrasted results: in some scenarios, tenability is driven by thermal effects, and in some other, toxic effects prevails.

Annex E is a second application of the methodology proposed in Annex C. The situation is a fire in a restaurant equipped with natural smoke control openings and an operating heating, ventilating, and air conditioning (HVAC) system. The fire starts in a hidden technical room (dishwashing room). Tenability assessment is performed along two escape routes, considering various pre-movement delays. The different evacuation strategies and occupant behaviour lead to contrasted results: depending on route chosen and pre-movement delay, tenability is driven by either thermal effects or toxic effects. Results are also expressed as success (FED, FEC < 0,3) versus pre-movement delay.

Annex A
(informative)

Example of application to real-scale fire scenarios - FED and ASET calculations for fire experiments conducted in a full-scale test house under two basement fire scenarios

A.1 General

An experimental program was undertaken to study the fire performance of various engineered floor systems used in single-family houses as construction moves away from the traditional solid sawn wood joists[6]. The experimental program was conducted using a test facility representing a two-storey detached single-family house with a basement (referred to as the test house hereafter). It involved full-scale fire experiments with unprotected floor assemblies located over the basement (unsheathed on the basement side) using two specific basement fire scenarios. The objective of the study was to better understand, from the perspective of tenability and structural integrity of the floor assemblies as egress routes, the impact of basement fires on the ability of occupants on the upper storeys to escape.

The experimental program used a timeline approach to establish the sequence that affects the life safety and egress of occupants under two specific basement fire scenarios. This sequence included fire initiation, smoke alarm activation, onset of untenable conditions on upper storeys, and structural failure of the test floor assembly as a viable egress route on the first storey. The experimental approach was designed to determine how long egress routes would remain viable from the perspective of both tenability and structural integrity of the test floor assembly. With the use of engineered joists and trusses in floor construction, it is desirable that the time to incapacitation of occupants should not be adversely affected. Structural failure of the floors constructed with alternative engineered products should not occur prior to the time taken to reach incapacitating levels of smoke, gases and heat. This involved FED and ASET calculations using experimental data and comparison between ASET and the floor failure time.

A.2 Experiments

Brief descriptions of the experiments are provided in the following sections. Further details of the experimental setup can be found in reference[6].

A.2.1 Facility

Each storey of the test house had a floor area of 95 m^2 and a ceiling height of 2,4 m. The basement was partitioned to create a fire compartment representing a 27,6 m^2 basement living area; the remaining area was not used during the experiments. The fire compartment had a rectangular exterior opening (2,0 m wide by 0,5 m high) covered with a removable non-combustible panel. The walls of the fire compartment were lined with 12,7 mm thick regular gypsum board. The gypsum board met ASTM C1396 and CAN/CSA-A82.27 material standards and consisted of a solid set gypsum core enclosed in face paper and liner back paper with a weight of 7,8 kg/m^2, a Flame Spread rating of 15 and Smoke Developed rating of 0 in accordance with ASTM E84 (UL 723, UBC 8-1,NFPA 255, CAN/ULC-S102). An enclosed stairwell connected the fire compartment to the first storey. At the top of this stairwell, a 0,81 m wide by 2,05 m high doorway led to the first storey. This doorway either had a door in the closed position (closed basement doorway) or had no door at all (open basement doorway), depending on the scenario being studied.

The first storey had an open-plan layout with no partitions. A test floor assembly was constructed on the first storey directly above the basement fire compartment for each experiment. A range of engineered floor systems, including wood I-joist, steel C-joist, metal plate wood truss and metal web wood truss assemblies as well as solid wood joist assemblies were used in the full-scale fire experiments. A 0,89 m wide by 2,07 m high doorway led to the exterior. The staircase to the second storey was not enclosed.

The second storey had a corridor (measuring 4,45 m long by 1,10 m wide) and bedrooms. Two bedrooms (each having a floor area of 16,8 m^2) were used as target bedrooms in the experiments. The door to one of the bedrooms was kept open whereas the door to the other bedroom remained closed. Each bedroom doorway was 0,81 m wide by 2,05 m high.

A.2.2 Fire scenarios

Two fire scenarios were used in the full-scale fire experiments:

— the doorway from the first storey to the basement had no door (referred to as the open basement doorway scenario);

— a hollow-core interior door was used in the doorway in the closed position (referred to as the closed basement doorway scenario).

A simple and repeatable fuel package was developed for use in full-scale experiments to fuel a fire that simulated a basement living area fire. This fuel package consisted of a mock-up sofa constructed with 9 kg of flexible polyurethane foam without any upholstery fabric, and 190 kg of wood cribs beside and underneath the mock-up sofa. The polyurethane blocks used were furniture grade flexible foam with a chemical formula of $CH_{1,91}\ O_{0,263}\ N_{0,055}$ and a density of 32,8 kg/m^3. The fuel package was located at the centre of the fire compartment in order to provide a greater challenge to the unprotected floor assemblies above. The mock-up sofa was ignited in accordance with the ASTM 1537 test protocol [7] and the wood cribs provided the remaining fire load to sustain the fire for a desired period of time.

To provide the ventilation necessary for combustion and to simulate the fire-induced breakage and complete fall-out of the window glass, the non-combustible panel that initially covered the exterior window opening of the fire compartment was manually removed when the temperature reached 300 °C at the opening. This condition was normally reached within 90 s to 120 s after ignition in the experiments. The exterior door on the first storey was opened at 180 s after ignition and left open to simulate some occupants evacuating the test house.

A.2.3 Measurements

Various measurement devices were used and data was collected at 5 s intervals in the experiments. Extensive thermocouple arrays were installed throughout the test house to measure temperatures. Flame-sensing devices and floor deflection devices were installed on the test floor assemblies. Residential ionization and photoelectric smoke alarms were installed on each level and in each bedroom.

Measurements of smoke density and gas concentrations were focused on upper storeys. On the first storey, smoke and gas sampling ports were located at a quarter point at 0,9 m and 1,5 m above the floor. On the second storey, smoke and gas sampling ports were located at the centre of the corridor at 0,9 m and 1,5 m above the floor. Smoke and gas samples from these sampling locations were connected to nondispersive infrared CO/CO_2 gas analyzers, O_2 gas analyzers and smoke density meters. Detailed gas analysis using Fourier Transform Infrared (FTIR) spectrometers was only conducted in a limited number of experiments.

A.2.4 Fire development in the basement fire compartment

Figure A.1 and Figure A.2 show the temperature profiles measured at the centre of the four quadrants of the basement fire room at the ceiling height for all of the tests. The polyurethane foam used for the mock-up sofa dominated the initial fire growth. The fast development of the fire from ignition to attainment of the first temperature peak was consistent for all of the tests. The temperatures at the ceiling height exceeded 600 °C at approximately 120 s in all of the tests, indicating that the basement fire compartment reached flashover conditions. Following this initial stage, the effects of ventilation became more pronounced and the fire became wood-crib-dominated and also involved the unprotected floor assemblies. Both fire scenarios provided relatively severe and consistent fire exposure to the unprotected floor assemblies in all experiments.

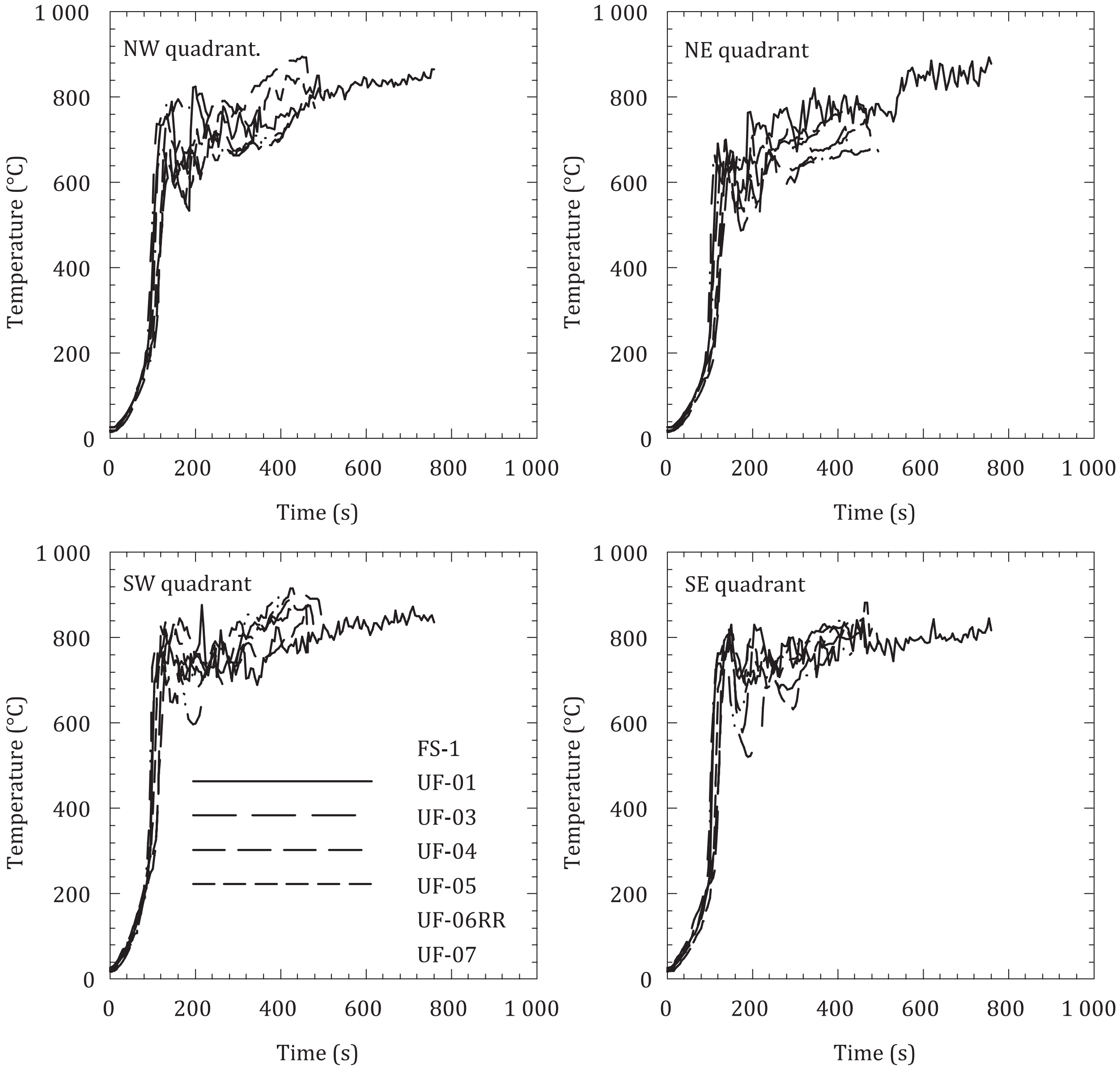

Figure A.1 — Temperatures in basement fire compartment at 2,4 m height (open basement doorway)

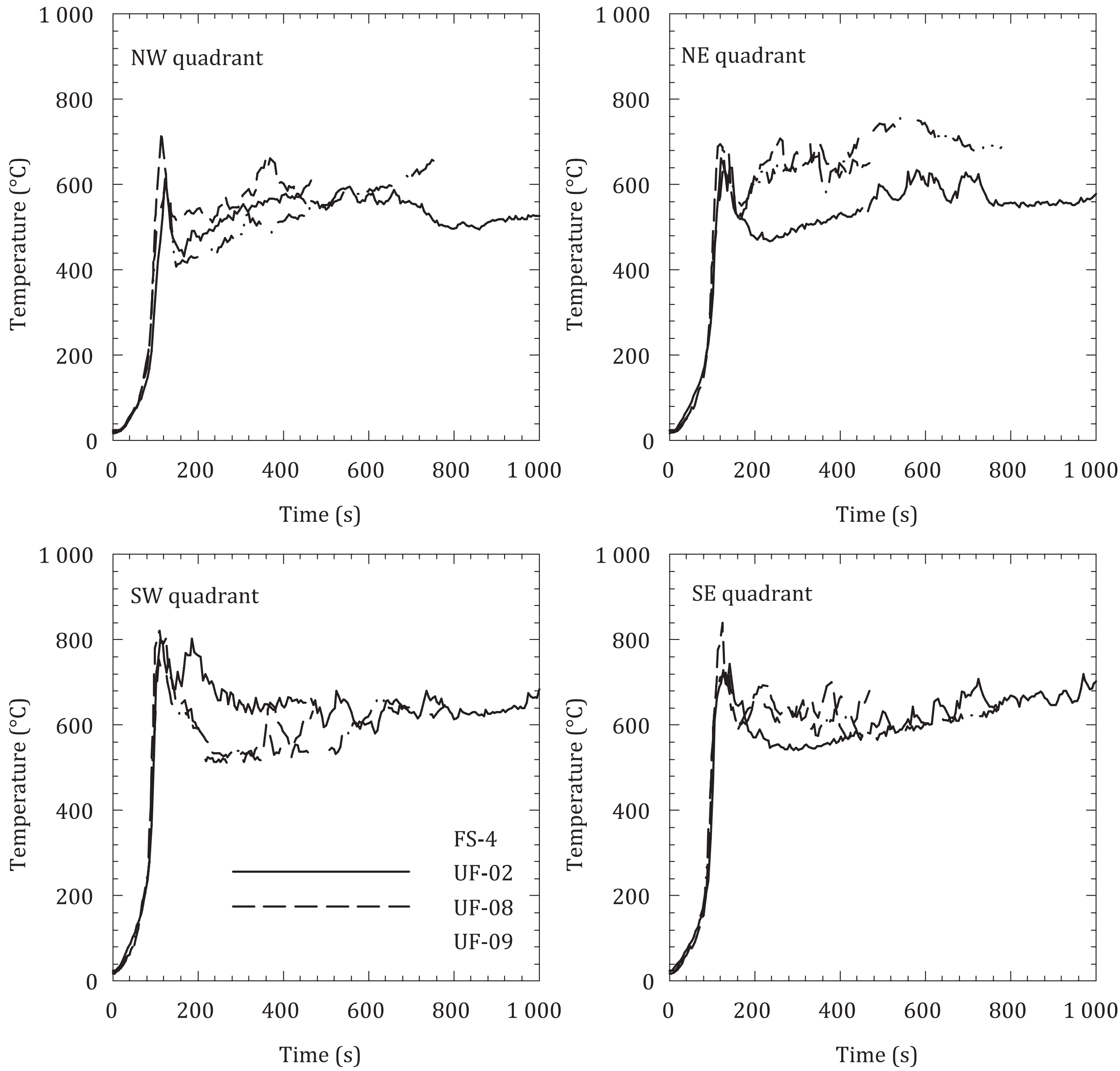

Figure A.2 — Temperatures in basement fire compartment at 2,4 m height (closed basement doorway)

A.3 Upper storey conditions and tenability analysis

Heat, combustion products and smoke produced from fires can, either individually or collectively, create conditions that are potentially untenable for occupants. Tenability analysis was conducted using temperatures, concentrations of combustion products and smoke optical densities measured during the experiments to provide an estimation of the ASET with incapacitation as the end point. The analysis focused on the conditions on the upper storeys of the test house. The conditions in the basement fire room would not be survivable once flashover occurred.

Potential exposure to the toxic and asphyxiant gases, heat and smoke obscuration under the test conditions was analysed independently. Each component was treated as acting independently on the occupant to create incapacitating conditions and the ASET was the shortest of the times estimated from consideration of exposure to combustion gas products, heat and smoke obscuration.

A.3.1 Exposure to toxic gases

In regards to the fuel package used in this study, with the combined flaming combustion of polyurethane foam and wood cribs, the primary gaseous products were expected to be carbon monoxide (CO), carbon dioxide (CO_2) and hydrogen cyanide (HCN) in a vitiated oxygen (O_2) environment. Although HCN could be produced from the combustion of the polyurethane foam in the fuel package, FTIR spectroscopy measurements in selected tests indicated that the HCN concentrations on the upper storeys were well below 30 ppm. These concentrations would not be a concern for occupant life safety on the upper storeys in the timeframe for incapacitation by CO exposure. As the polyurethane foam has a chemical formula of $CH_{1,91}O_{0,263}N_{0,055}$, the fuel package contained no chemical components that would produce acid halide irritants in the combustion gases. Other potential irritant gases transported to the upper storeys, such as NO, NO_2 and acrolein, were below the detection limits of the FTIR spectrometers used in the experiments.. Therefore, the analysis for the upper storeys involved CO and CO_2 and oxygen vitiation only. Figure A.3 shows exemplar concentration-time profiles for CO, CO_2 and O_2 measured during experiments.

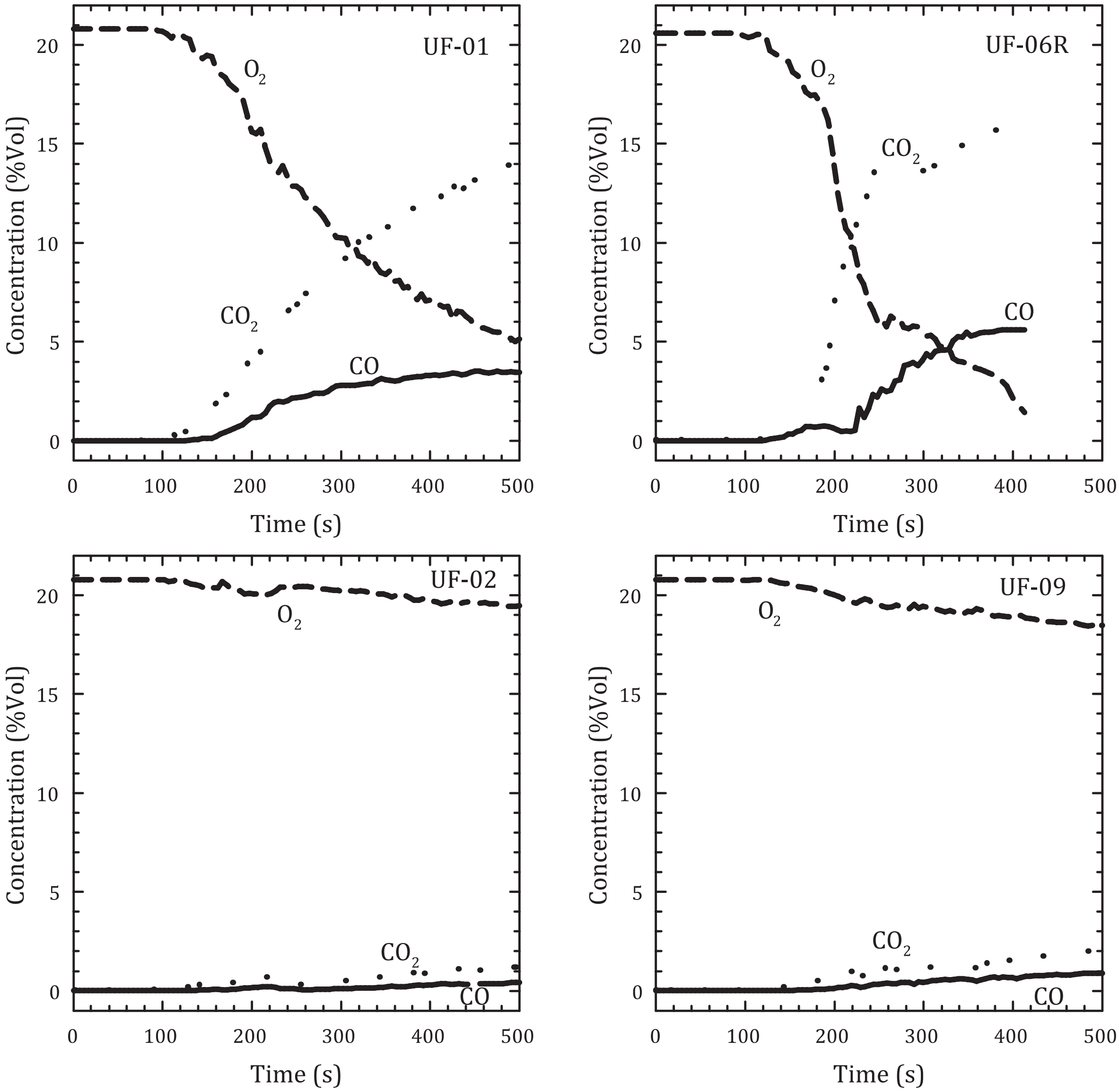

Figure A.3 — Exemplar CO, CO_2 and O_2 concentrations measured at a quarter point on the first storey at 1,5 m height

The fractional effective dose for incapacitation due to CO was calculated as follows with the CO_2-induced hyperventilation factor:

$$FED_{\text{in,CO}} = \sum_{t_0}^{t} \frac{[CO] \times \Delta t}{35\ 000} \exp\left(\frac{\%CO_2}{5}\right)$$

Since data were collected at 5 s intervals in the experiments, Δt = *0,0833 min*. The uncertainty in the calculation of $FED_{\text{in,CO}}$ is estimated to be ± 40 %, which takes into consideration of 20 % uncertainty for hyperventilation factor in addition to the normal 35 % uncertainty for FED.

Table A.1 shows the calculated times for the fractional effective dose to reach two typical values (FED = 1 for healthy adults of average susceptibility, and FED = 0,3 for some susceptible people), including the uncertainty in the estimated times. The times associated with other FED values can be calculated, if required.

Table A.1 — Time (in seconds) to the specified FED for exposure to CO with CO_2 hyperventilation

	1st storey SW quadrant		2nd storey corridor	
FED $_{\text{in, CO}}$ =	**0,3**	**1,0**	**0,3**	**1,0**
Tests with open basement doorway				
Solid wood joist	205 ± 10	235 ± 15	225 ± 10	255 ± 15
Wood I-joist A	209 ± 5	240 (−15, +5)	225 ± 10	247 ± 15
Steel C-joist	220 (−10, +5)	260 ± 20	245 ± 10	280 ± 20
Metal-plate wood truss	206 ± 7	232 ± 13	235 ± 7	260 ± 10
Wood I-joist B	198 ± 10	233 (−15, +5)	208 ± 12	241 ± 10
	198 ± 10	228 ± 5	207 ± 15	241 ± 10
	203 ± 10	233 ± 10	218 ± 10	248 ± 15
Metal web wood truss	225 ± 25	265 ± 7	230 ± 25	275 ± 10
Tests with closed basement doorway				
Solid wood joist	466 ± 60	676 ± 90	362 ± 30	501 ± 70
Metal web wood truss	400 (−55, +40)	510 (−25, +[a])	375 ± 35	510 (−50, +[a])
Wood I-joist A	329 ± 40	484 ± 70	364 ± 35	504 (−70, +60)

NOTE Calculated based on concentrations at 1,5 m height above the floor

[a] Upper range of uncertainty in timing is unavailable due to commencement of fire suppression

For the tests with the open basement doorway, the calculated time difference between $FED_{\text{in,CO}}$ = 0,3 and $FED_{\text{in,CO}}$ = 1,0 was 40 s or less at any measurement location for any given test. The calculations were associated with the fixed positions where the concentrations were measured and an occupant would move through different locations in real fire situations. The time difference between the second storey and first storey reaching either of the two doses was less than 30 s for any given test. Moreover, the time difference between tests reaching either of the two doses was less than 40 s at any measurement location. These results indicate a consistent time frame for reaching the incapacitation doses for exposure to CO in this fire scenario.

For the experiments with the closed basement doorway, the calculated times were at least 60 % longer to reach $FED_{\text{in,CO}}$ = 0,3 and at least doubled to reach $FED_{\text{in,CO}}$ = 1, compared with the open basement doorway experiments. The closed door impeded the migration of smoke and hot fire gases into the upper storey(s) and delayed the onset of untenable conditions.

The fractional effective doses for incapacitation due to O_2 vitiation alone, and due to asphyxiant effect of CO_2 alone, were also calculated using the methodology given in reference[8]. Under the experimental conditions of this study, these calculations indicated that the effect of O_2 vitiation and the asphyxiant effect of CO_2 would cause incapacitation at a later time than the toxic effect of CO.

A.3.2 Exposure to heat

Figure A.4 and Figure A.5 show exemplar temperature profiles measured on the first and second storeys during the experiments. The temperatures depended on the locations inside the test house. In the bedroom with the door closed, the temperatures never exceeded 50 °C in any experiment.

The presence of the closed door in the basement doorway made a significant difference in the thermal conditions on the first and second storeys. The closed door impeded the migration of smoke and hot fire gases into the upper storeys until it was breached by the fire, and thereby delayed the onset of untenable thermal conditions on the upper storeys.

Assuming unclothed or lightly clothed subjects, the fractional effective dose for incapacitation due to the convected heat exposure was calculated using the following equation:

$$FED_{\text{in,heat}} = \sum_{t0}^{t} \frac{T^{3,4}}{5 \times 10^7} \Delta t$$

The uncertainty in the calculation of $FED_{\text{in,heat}}$ is estimated to be ± 25 %. Since there was temperature stratification, the temperatures at the 1,4 m height on each storey were used for the analysis of convected heat exposure, as this simulated the height of the nose/mouth of an average height individual.

Radiant heat is important when the hot smoke layer is over 200 °C, which corresponds to the threshold radiant heat flux of 2,5 kW·m^{-2} to produce second degree burning of skin[9]. The calculation indicated that the convected heat exposure would result in incapacitation before the radiant heat began to play a major role on the first and second storeys. Convected heat was the most important source of heat exposure for occupants on the first and second storeys for the fire scenarios used.

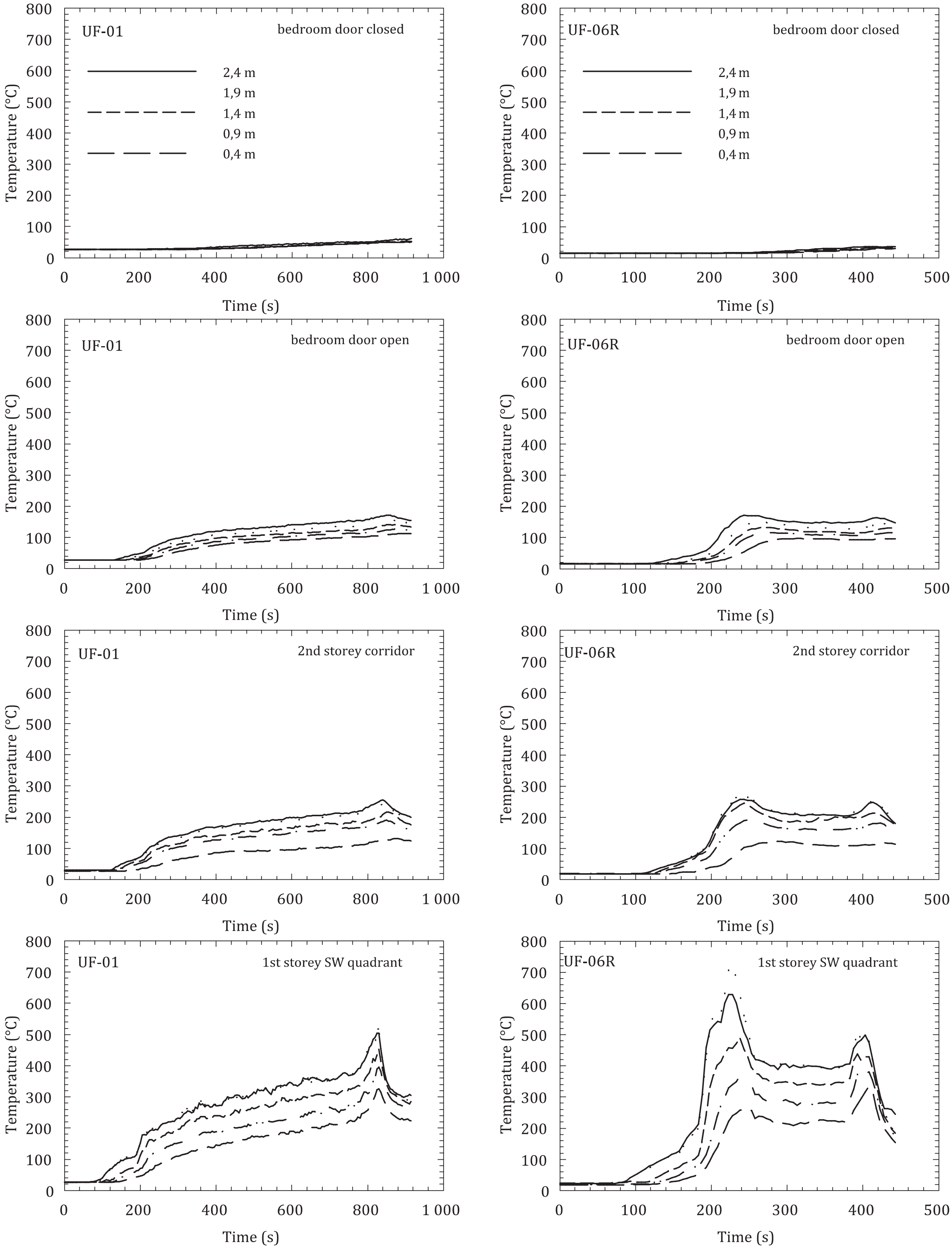

Figure A.4 — Exemplar temperature profiles on upper storeys (open basement doorway)

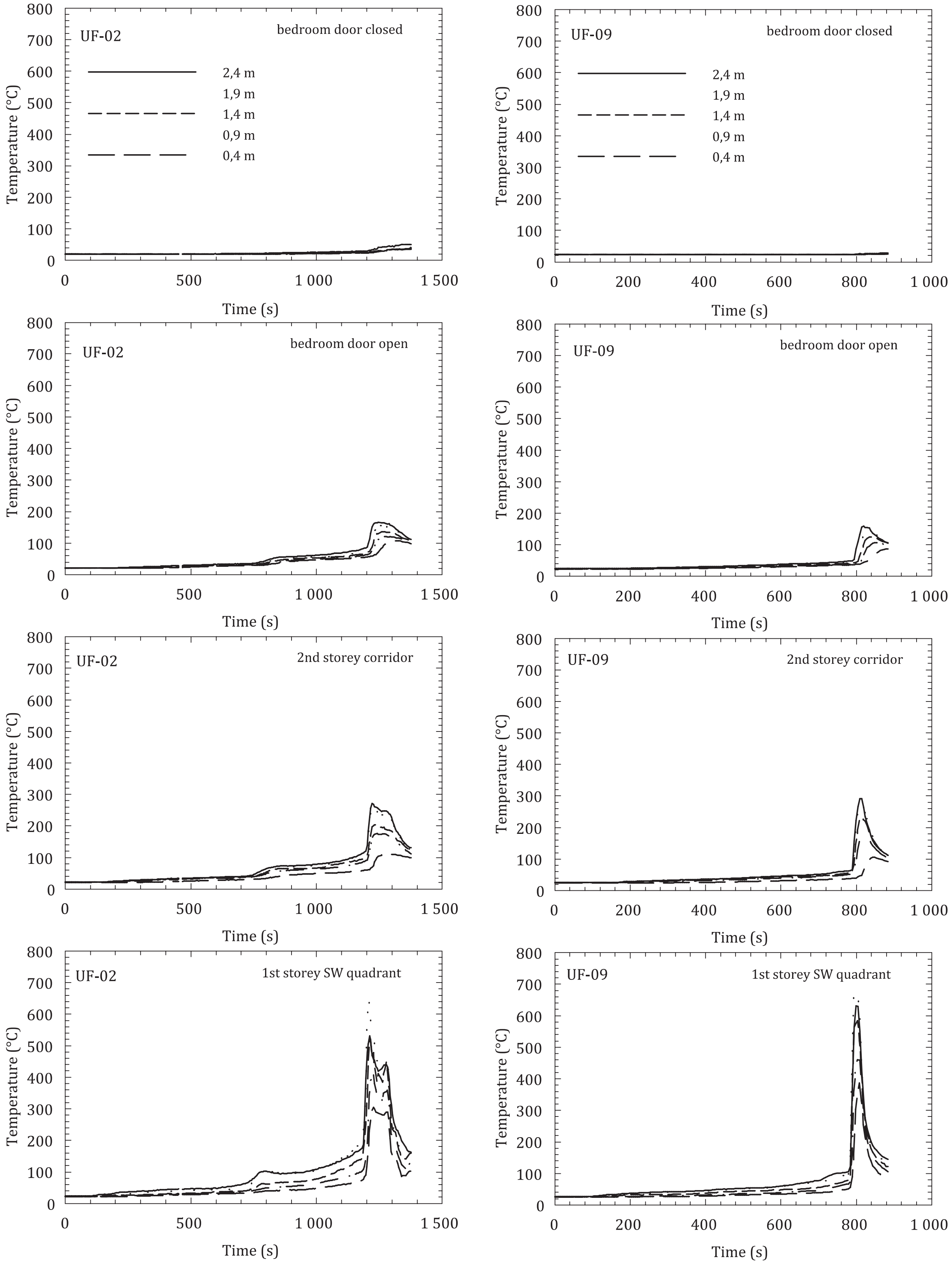

Figure A.5 — Exemplar temperature profiles on upper storeys (closed basement doorway)

The convective heat exposure depended on the location in the test house. In the closed bedroom, heat exposure would not cause incapacitation ($FED_{\text{in,heat}}$ < 0,07 in all experiments). On the first storey, in the corridor or in the open bedroom on the second storey, the calculated times to incapacitation due to exposure to the convected heat are given in Table A.2 for $FED_{in,heat}$ = 0,3 and $FED_{in,heat}$ = 1, including the uncertainty in the estimated times. Depending on the test conditions (floor assembly type, condition of doorway to the basement) and locations in the test house, the heat exposure could cause incapacitation before CO exposure or vice versa.

For the tests with the open basement doorway, the calculated times to reach the heat incapacitation doses on the first storey were comparable to those for CO exposure and, in most cases, the time difference for $FED_{in,heat}$ to change from 0,3 to 1,0 was also much shorter than that for $FED_{in,CO}$. In the corridor on the second storey, except for one test, the calculated times for heat exposure to reach the incapacitation doses were longer than those for CO exposure.

For the tests with the closed basement doorway, the incapacitation doses for heat exposure on the first storey were reached much later than for the CO exposure. The calculated times for heat incapacitation were at least double that for the tests with the open basement doorway. The closed door to the basement impeded the heat transfer to the upper storey(s) and delayed the onset of untenable heat conditions. The CO exposure dominated incapacitation on both storeys.

Table A.2 — Time (in seconds) to the specified FED for exposure to convective heat

	1st storey SW quadrant		2nd storey corridor		2nd storey open bedroom	
$FED_{in, heat}$ =	**0,3**	**1,0**	**0,3**	**1,0**	**0,3**	**1,0**
Tests with open basement doorway						
Solid wood joist	230 ± 7	280 ± 15	320 ± 15	435 ± 30	455 ± 30	690 ± 60
Wood I-joist A	205 ± 3	213 ± 3	252 ± 5	330 ± 25	370 ± 30	(FED < 0,8)
Steel C-joist	207 ± 2	215 ± 3	250 ± 5	290 ± 10	325 ± 15	460 (−35, +[a])
Metal-plate wood truss	220 ± 3	240 ± 5	270 ± 10	320 ± 15	345 ± 15	500 (−60, +[a])
Wood I-joist B	202 ± 2	211 ± 3	229 ± 3	254 ± 10	315 ± 20	(FED < 0,8)
	193 ± 2	199 ± 2	217 ± 3	238 ± 6	293 ± 15	(FED < 0,8)
	209 ± 2	216 ± 2	234 ± 3	298 ± 25	393 ± 30	(FED < 0,4)
Metal web wood truss	192 ± 2	207 ± 5	225 ± 5	255 ± 10	305 ± 15	(FED < 0,9)
Tests with closed basement doorway						
Solid wood joist	1086 ± 30	1196 (−10, +5)	1171 (−55, +35)	1241 (−10, +5)	1263 ± 10	(FED < 0,5)
Metal web wood truss	482 ± 1	486 ± 1	507 ± 2	(FED < 0,5)	(FED < 0,1)	(FED < 0,1)
Wood I-joist A	786 ± 1	796 ± 1	(FED < 0,2)	(FED < 0,2)	(FED < 0,1)	(FED < 0,1)

NOTE Calculated based on temperatures at 1,4 m height above the floor

[a] Upper range of uncertainty in timing is unavailable due to commencement of fire suppression

A.3.3 Visual obscuration by smoke

Visual obscuration by the optically dense smoke tended to be the first hazard to arise that could impede evacuation by the occupants.

In ISO 13571, the minimum visible brightness difference between an object and its background is used to estimate the smoke obscuration limit at which occupants cannot see their hands in front of their faces (a distance of 0,5 m or less). These calculations indicate that occupants cannot see their hands in front of their faces and become disoriented at a smoke optical density (OD) of 1,7.

During the experiments, the smoke optical density was measured at 0,9 and 1,5 m heights above the floor on the first and second storeys (simulating the height of the nose/mouth of an average height individual crawling and standing, respectively). Figure A.6 shows exemplar smoke optical density-time profiles with a 0,5 m optical path length. It was observed that in the experiments with the open basement doorway, the optical density temporarily decreased shortly after the exterior door on the first storey was opened at 180 s, and then increased again.

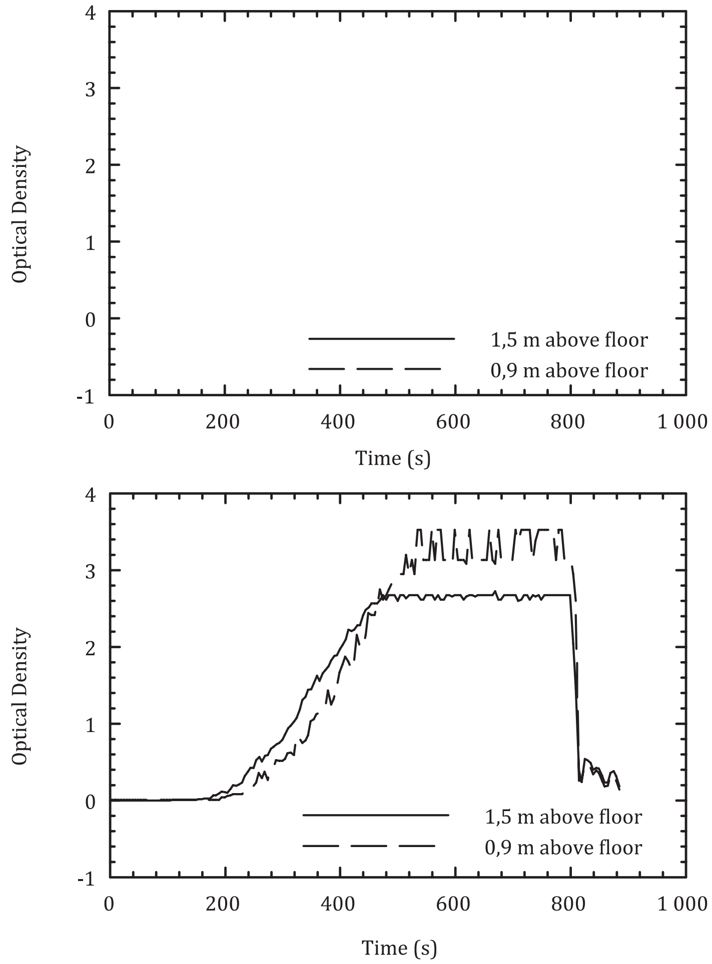

Figure A.6 — Exemplar data of smoke optical density (in the corridor on the second storey)

Table A.3 shows the times to reach various optical density levels at the 1,5 m height, which were very similar from one experiment to another. The increase in the optical density was faster with the open basement doorway than with the closed basement doorway. It is worth noting that the smoke density meters used for the first storey had a narrow working range and could not measure the smoke obscuration of OD = 1 and beyond. It is reasonable to assume that the first storey lost the visibility shortly before the second storey, given the comparable times for reaching the OD's of 0,5 and 0,85 on both storeys. It can be seen from Table A.1 and Table A.3 that the times when the optical density reached 1,7 were generally very close to the times when $FED_{\text{in,CO}}$ = 0,3, which is a CO incapacitation dose for some susceptible persons.

Table A.3 — Time (in seconds) to the specified smoke optical density

	1st storey SW quadrant		2nd storey corridor			
OD =	**0,5**	**0,85**	**0,5**	**0,85**	**1**	**1,7**
Tests with open basement doorway						
Solid wood joist	155	170	170	185	185	200
Wood I-joist A	158	168	173	178	183	198
Steel C-joist	160	n.a.	180	190	195	210
Metal-plate wood truss	160	n.a.	175	186	190	200
Wood I-joist B	147	155	160	167	170	185
	133	153	150	158	161	178
	168	n.a.	168	178	184	198
Metal web wood truss	134	140	155	165	170	330
Tests with closed basement doorway						
Solid wood joist	187/342[a]	n.a.	247	277	297	377
Metal web wood truss	220	325	265	330	360	450
Wood I-joist A	186	n.a.	254	304	319	374

NOTE Determined based on optical density measurements at 1,5 m height above the floor

NOTE n.a. – not available due to limited measurement range of the smoke meters used for the first storey

[a] OD = 0,5 first reached at 187 s on the first storey but OD then decreased due to the exterior door was opened at 180 s, then reached again at 342 s

A.3.4 Summary of tenability analysis

Table A.4 summarizes the estimated times to the onset of various conditions. With the fast-growing fire used in the experiments, the resulting uncertainty in the estimated time is much smaller than the uncertainty in the calculated fractional effective dose ($FED_{\text{in,CO}}$ or $FED_{\text{in,heat}}$) due to the nonlinear relationship. The uncertainty in the timing of the optical density measurement is 5 s.

Table A.4 — Summary of time to specified $\mathbf{FED_{in}}$ and OD (in seconds)

Test	OD = 1,7	$FED_{in,\ CO}$ or $\mathbf{FED_{in,\ heat}}$ = 0,3		$FED_{in,\ CO}$ or $\mathbf{FED_{in,\ heat}}$ = 1	
	2nd storey	1st storey	2nd storey	1st storey	2nd storey
Tests with open basement doorway					
Solid wood joist	200 ± 5	*205 ± 10*	*225 ± 10*	*235 ± 15*	*255 ± 15*
Wood I-joist A	198 ± 5	**205 ± 3**	*225 ± 10*	**213 ± 3**	*247 ± 15*
Steel C-joist	210 ± 5	**207 ± 2**	*245 ± 10*	**215 ± 3**	*280 ± 20*
Metal-plate wood truss	200 ± 5	*206 ± 7*	*235 ± 7*	*232 ± 13*	*260 ± 10*
Wood I-joist B	185 ± 5	*198 ± 10*	*208 ± 12*	**211 ± 3**	*241 ± 10*
	178 ± 5	*198 ± 10*	*207 ± 15*	**199 ± 2**	*241 ± 10*
	198 ± 5	*203 ± 10*	*218 ± 10*	**216 ± 2**	*248 ± 15*
Metal web wood truss	330 ± 5	**192 ± 2**	*230 ± 25*	**207 ± 5**	**255 ± 10**
Tests with closed basement doorway					

NOTE Values determined using the measurements at 1,5 m height (for gas concentrations and OD) or 1,4 m height (for temperatures)

NOTE The number with the Italic font represents the calculated time for reaching the CO incapacitation dose, while the number in bold represents the calculated time for reaching the heat incapacitation dose, whichever occurred first

[a] Upper range of uncertainty in timing is unavailable due to commencement of fire suppression

Table A.4 *(continued)*

Test	OD = 1,7	*FED$_{in, CO}$* or **FED$_{in, heat}$** = 0,3		*FED$_{in, CO}$* or **FED$_{in, heat}$** = 1	
	2nd storey	1st storey	2nd storey	1st storey	2nd storey
Solid wood joist	377 ± 5	*466 ± 60*	*362 ± 30*	*676 ± 90*	*501 ± 70*
Metal web wood truss	450 ± 5	*400 (−55, +40)*	*375 ± 35*	**486 ± 1**	*510 (−50, +[a])*
Wood I-joist A	374 ± 5	*329 ± 40*	*364 ± 35*	*484 ± 70*	*504 (−70,+60)*

NOTE Values determined using the measurements at 1,5 m height (for gas concentrations and OD) or 1,4 m height (for temperatures)

NOTE The number with the Italic font represents the calculated time for reaching the CO incapacitation dose, while the number in bold represents the calculated time for reaching the heat incapacitation dose, whichever occurred first

[a] Upper range of uncertainty in timing is unavailable due to commencement of fire suppression

Smoke obscuration was the first hazard to arise in most of the experiments. Although smoke obscuration would not directly cause incapacitation, it could impede evacuation and prolong exposure of occupants to other hazards.

The calculated times for reaching the specific FED, either due to the heat exposure or due to the CO exposure (exacerbated by CO_2-induced hyperventilation), whichever occurred first, are listed in Table A.4. Heat exposure tended to be more severe on the first storey than on the second storey. In most cases, the time difference for heat exposure and CO exposure to reach the specific FED was not significant with the open basement doorway.

For the experiments with the open basement doorway, the time for FED to change from 0,3 to 1 was no more than 40 s. The times to reach each FED level were also very consistent for the different experiments. The tenability data indicates that, regardless what test floor assemblies were used, the untenable conditions (for incapacitation) were reached in a consistent timeframe soon after smoke obscuration. Depending on the susceptibility and location of occupants, the untenable conditions generally occurred within 180 s to 240 s after ignition under this fire scenario (shortly after smoke obscuration).

The presence of the closed door to the basement limited the air available for combustion and also reduced the rate at which combustion products were conveyed to the upper storeys. The ASET was at least doubled for an occupant of average susceptibility (FED = 1) and was increased by at least 60 % for a more susceptible occupant (FED = 0,3) with the closed basement doorway, compared to the scenario with the open basement doorway.

For the closed bedroom on the second storey, based on the temperature measurements in all experiments and the heat exposure calculation, the conditions in the closed bedroom would not reach untenable conditions associated with FED = 0,3 or 1.

The location of the occupant in the test house has an effect on the time available for escape. The analysis focused on the fire conditions affecting tenability, as measured on the first and second storeys of the test facility, and the impact on any occupant assumed to be present at the time of ignition. Each calculation was associated with a particular position where the concentration or temperature was measured. In real fire situations, the occupant would move through different locations during egress. Therefore, the time to incapacitation would be in-between the times calculated for different locations.

A.4 The sequence of events

Table A.5 summarizes the chronological sequence of the fire events in the full-scale experiments — fire initiation, smoke alarm activation, onset of untenable conditions, and structural failure of the test floor assembly. In all experiments except one, fire events followed a chronological sequence: initiation and growth of the fire, activation of smoke alarms, loss of tenable conditions in open areas on upper storeys, and finally structural failure of the test floor assembly over the basement (loss of the main egress route on first storey). However the time gap between the onset of untenable conditions and the structural failure of the floor assembly was smaller for the engineered floor assemblies than for the solid wood joist assembly used in the experiments. In the closed basement doorway scenario, one engineered floor assembly experienced structural failure before untenable conditions (FED = 1) were reached in the open areas on the upper storeys. In the second storey bedroom where the door to the bedroom was kept closed, untenable conditions were not reached in any of the experiments.

The FED and ASET calculations along with this timeline approach enabled the establishment of the key sequence of the fire events in the experiments to better understand the impact of the basement fires on the ability of occupants on the upper storeys to escape in houses with alternative floor construction.

Table A.5 — Summary of sequence of events (in seconds)

Floor Assembly Type	Test	First Alarm	OD = 1,7	FED = 0,3–1 1st storey	FED = 0,3–1 2nd storey	Structural Failure
Tests with open basement doorway						
Solid wood joist	UF-01	40	200	*205–235*	*225–255*	740
Wood I-joist A	UF-03	48	198	**205–213**	*225–247*	490
Steel C-joist	UF-04	30	210	**207–215**	*245–280*	462
Metal-plate wood truss	UF-05	40	200	*206–232*	*235–260*	469
Wood I-joist B	UF-06	45	185	*198*-**211**	*208–241*	382
	UF-06R	38	178	*198*-**199**	*207–241*	380
	UF-06RR	43	198	*203*-**216**	*218–248*	414
Metal web wood truss	UF-07	40	330	**192–207**	*230*-**255**	325
Tests with closed basement doorway						
Solid wood joist	UF-02	42	377	*466–676*	*362–501*	1200
Metal web wood truss	UF-08	50	450	*400*-**486**	*375–510*	474
Wood I-joist A	UF-09	44	374	*329–484*	*364–504*	778
NOTE Values determined using the measurements at 1,5 m height (for gas concentrations and OD) or 1,4 m height (for temperatures)						
NOTE The number with the Italic font represents the calculated time for reaching the CO incapacitation dose, while the number in bold represents the calculated time for reaching the heat incapacitation dose, whichever occurred first						
NOTE All values shown in the table are before fire suppression						

Annex B
(informative)

Example of application to real-scale fire scenarios - FED calculations for fire experiments conducted in a full-scale test of single sleeping rooms

B.1 General

Small rooms fires are frequent situations that could lead to fatal consequences. People have to be alerted, then evacuated before reaching conditions that are not tenable. Adverse effects of fire on people are linked to thermal and/or toxic effects, enhanced by the loss of visibility as an indirect one. Annex B presents a series of tests performed in order to estimate tenability conditions according to ISO 13571 in single-room fire situations. This Annex is issued from Reference [10].

The studied room is a small 9 m^2 room, equipped with finishes and furniture as in everyday life. Various scenarios of ignition source, origin and events such as door openings have been tested. The room has been instrumented with a large number of sensors, in order to measure physical and chemical parameters of such fire scenarios, and then to produce tenability data.

B.2 Description of test enclosure

The tested room is a realistic 9 m^2 sleeping room (3 m x 3 m ground surface) with a ceiling height of 2,5 m. The tested configuration is made of this single room served by a corridor through a door. The door opening is 0,83 m wide and 2,04 m high. A window is placed on another wall, facing a space connected with the outside. All this arrangement is shown on Figure B.1.

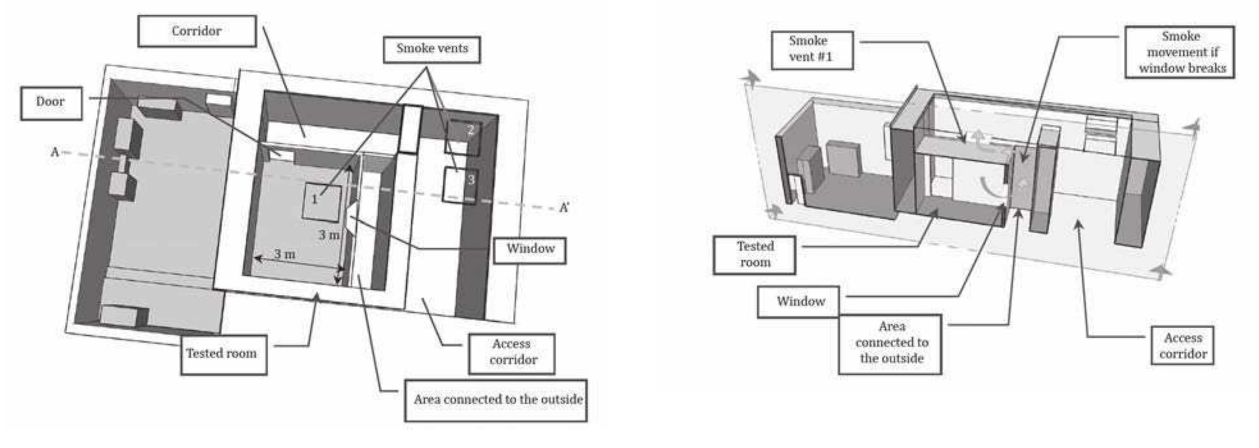

a) Top view **b) Cut sectional view according to A-A'**

Figure B.1 — top and cut sectional view of the test arrangement

To mimic real life conditions, the test room is decorated, furnished and equipped with objects encountered in everyday life, e.g. a wardrobe, clothes, a desk with paper, books, towels, bed pillow and bed linen. An angle of the room is equipped with a corner sink. Apart from ceiling, a large part of the finishing work is made of PVC products, with the aim of studying the impact of using such chlorinated materials in fire scenarios. Furniture and the everyday life objects are bought in retail stores. They are made of standard materials such as those usually encountered. This arrangement is almost identical for both sets of tests.

Finishing work: Two walls of the test room are made of concrete, while the two others are made of gypsum. All are covered with BA13 gypsum board, which are changed between each series of tests to avoid contamination. The ceiling is materialized at a height of 2,50 m by PPF15 gypsum boards held by steel wires connected to the roof slab. This ceiling covers the test room and the adjacent corridor. As for the walls, ceiling boards are changed between each series of tests to avoid contamination. No decorative coating is applied on the ceiling. The floor of the test room is covered with PVC floor covering. The walls of the test room are covered with a PVC wall covering. The window is a PVC double-glazed frame, 1,20 m x 1,25 m in size, and is topped by a box with a rolling shutter, also in PVC.

Plumbing: The test room is equipped with a corner ceramic sink with metal tap and its system of spinning sewage (in PVC) running along one of the interior sides up to a C-PVC, 150 mm diameter down-comer pipe in the next corner of the room. In addition, the corner with the corner sink (see below) is equipped with PVC panelling on whole height, 1 m wide on each wall from the corner.

Electricity: The test room is equipped with a PVC raceway and fittings, placed at the bottom of the walls except for the door where the raceway runs around the door. The raceway is connected to a socket outlet under the desk, and another one under the bedside table. A switch is installed at a standard hand level at the door. The raceway is empty (neither cables nor insulated conductors inside).

Furnishing: The room is furnished with a bed made of a pine spring-bed, a mattress (cotton-polyester fabric external liner, polyurethane foam padding and polyester), a pillow and a quilt (cotton-polyester fabric, polyester lining), both equipped with a cotton pillowcase. The room also contains a bedside table in solid pine (with fibreboard backside panel) with a lamp, a wardrobe (fibreboard backside panel), an office desk (fibreboard backside panel) over which is a wooden shelf, a metallic wastepaper basket placed on the floor next to the desk, an office chair (polypropylene seat shell) and a cotton rug. All these items were supplied from major retailers, within long term and traceable collections.

In addition to finishing and furniture, objects of everyday life were placed in the test room. Clothes are arranged in the wardrobe and a gym bag containing a wool sweater is placed on it. The wardrobe is left ajar for tests. A towel and a bottle of shower gel are placed on the sink. Paper and CD cases are arranged on the desktop. Books, magazine racks with magazines, small storage boxes and a box of cereal are placed on the shelf.

Detection: Two different models of smoke alarms are placed in the centre of the ceiling. The same couple of alarms is also placed on the centre of corridor's ceiling.

B.3 Test design fire scenario

B.3.1 Fuel load

All combustible elements used in the composition of the interior of the test room were weighed, and the masses sorted by constituting material nature. Results are presented in Table B.1. In this table, the identified portion "PVC" is the gross weight of all combustible parts made in PVC and integrates the mass of fillers, plasticizers, etc, accompanying the pure PVC resin. Results highlight a large proportion of wooden products, about 54 %, followed by PVC-based products.

Table B.1 — fuel mass load in the tested room

Item	Mass (kg)	Proportion
Wood and wooden products	130,3	54 %
PVC-based materials	82,5	34 %
Paper, chipboard	7,3	3 %
PU foams	4,3	2 %

Table B.1 *(continued)*

Item	Mass (kg)	Proportion
Other plastics	9,7	4 %
Misc. (cotton, wool, etc.)	7,1	3 %
Total	**241,2**	**100 %**

B.3.2 Fire scenarios and tests analysed

Two series of tests from reference[10] are presented. The first test ("Test 1C") consists in a night dwelling scenario in a closed room. Ignition sequence is performed on the mattress equipped with its bedding components. The test room is decorated, furnished and equipped with objects of everyday life, as described previously. Ignition source is a #5 crib according to British Standard BS 6807[11]. Room door remains closed during all test duration.

The second test ("Tests 2B") is the situation of a ventilated fire in a small living space. The window remains closed, but the door is opened 2 min 30 s after ignition, to consider the delay of reconnaissance, pre-movement and escape of an occupant. Ignition sequence consists in a scenario of an accidental fire in the wastepaper basket, at the foot of the office desk. The test room finishing work is renewed. Then the room is decorated, furnished and equipped with identical objects of everyday life, as described previously. Two paper basket are put under the office desk. Both are filled with 500 g of creased paper balls and a match-like flame burner ignites the fire in one of the wastepaper baskets.

B.3.3 Exposure scenarios

For test 1C, the exposure scenario corresponds to a person asleep. Fire starts on mattress, for example because of a non-extinguished cigarette. The person does not wake up, door and window remain closed during the entire scenario.

For test 2B, the scenario is an accidental fire, starting from a wastepaper basket. Two exposure scenarios are considered. In the first one, it is assumed that the occupant leaves the room quickly, about 2 min 30 s after fire ignition. He opens the door, which remains opened during all the remaining duration of the scenario. In the second one, the studied hypothesis includes another occupant, who remains in the middle of the room during the entire scenario, after the first one has left.

These simple evacuation scenarios are adequate for such small configuration and are representative of the results of the statistical analysis presented at first paragraph.

B.4 Results and interpretations – Test 1C

B.4.1 Results

This standardized crib consists of small wood sticks, with a tissue at the base. This fabric is impregnated with approximatly 1,4 ml of propanol just before the test, then ignited. The crib is placed on the quilt cover, approximately in the centre of the mattress. Events and observations during test are detailed in Table B.2. Test is stopped after more than 28 min: no flames are visible for more than 10 min and all sensors present a slow evolution (e.g. temperatures are slowly decreasing).

Table B.2 — Time events table for test 1C

Time (hh:mm:ss)	Event
00:00:00	Crib ignition
00:00:16	First visible smoke on the camera covering the bed
00:00:26	Door closing
00:00:44	First visible flames on the camera covering the bed

Table B.2 *(continued)*

Time (hh:mm:ss)	Event
00:02:10	First smoke alarm of the room activates
00:03:27	Smoke alarms starts to have a modification in sound produced
00:04:00	Smoke alarms of the corridor activates
00:28:31	End of test. Intervention order to firefighters

The Figures B.2a) to e) show the yields of carbon monoxide (CO), carbon dioxide (CO_2), hydrogen cyanide (HCN) and hydrogen chloride (HCl) observed during the duration of the test 1C at the headboard (Point FT2) or other locations when specified. The yield of carbon monoxide at 2 m high begins to rise significantly approximately 2 min after ignition of the source (Figure B.2a). It should be highlighted that the first room smoke alarm triggers at 2 min 10 s. The growth rate of CO is very regular and almost linear between 11 min and 28 min 31 s (end of test). The convergence of three analyzers using two different measurement techniques (FTIR and NDIR) excludes any metrological bias for this linearity. The evolution of CO_2 concentration at the headboard is much faster than CO (Figure B.2b): fire is initially well ventilated. Three min 30 s after ignition, the [CO]/[CO_2] ratio increases in favour of carbon monoxide (Figure B.2c). The fire turns gradually to under-ventilated conditions. After 3 min, the hydrogen cyanide (HCN) concentration increases at the headboard (Figure B.2d). This increase is likely due to the degradation of the polyurethane foam of the mattress. The concentration of hydrogen chloride (HCl) in the room is likely due to the combustion of PVC products. It increases measurably from 11 min after ignition (Figure B.2e) to the end of the test. HCl concentration, however, remains very low (near detection limits), which explains the large dispersion in measurements. Results also highlight the presence of nitrogen monoxide (NO). Traces of ammonia (NH_3) were observed too, where nitrogen dioxide (NO_2) was under limit of quantification (see Figure B.2f) for ammonia and nitrogen monoxide. Figure B.2g) presents results for other gases. It highlights significant concentrations of hydrocarbons, which correspond to the release of unburnt pyrolysis gases. The contribution of irritant gases other than HCl on the FEC is deemed negligible, and the FEC has been calculated from HCl values only. Figure B.2h) presents the variation of dioxygen concentration. It shows a rapid stabilization of oxygen in the enclosure at 16 %. This concentration is in the order of magnitude of critical concentrations to stop combustion at such temperatures. It means that fire probably stopped because of the lack of oxygen available for combustion.

The Figures B.3a) to b) present results for the temperature measured with the thermocouple trees at two locations in the room (Figure B.3a) for point ATC3, close to the door, and Figure B.3b) for point ATC4, on the mattress. These two series of results are very close and the system should be considered as horizontally homogenous. Temperature rises quickly to about 160 °C -180 °C, then decreases to stabilize around 50 °C. During the first 3 min of the test, temperature increases at ceiling and smoke layer develops, but a fresh air layer remains in the lower volume of the room. Between 3 min and 7 min, a vertical temperature gradient exists, but temperature started to increase on the lower volume. Smoke starts to mix with air and stratification is broken, which is confirmed by visual observation. After 8 min, temperature is homogeneous in the room from floor to ceiling. Temperature decreases slowly at this time from 80 °C to 50 °C during the next 20 min. Results are consistent with preliminary simulations, with a peak at 4 min and a slow decay.

Figure B.4) presents results of smoke opacity. Unfortunately, the opacimeters located at 1,1 m and 0,7 m stopped working after respectively 2 min 17 s and 2 min 30 s. The signal starts to grow for all sensors between 1 min 41 s and 2 min 30 s, as smoke is filling the room. The optical density then increases with the fire growth until around 4 min, which corresponds to the peak temperature and an oxygen level of 16 %, as seen respectively on Figures B.3) and B.2h). The opacity presents later a second significant increase with a maximum at 12 min, when all other variables are stagnant or decreasing. These measurements show the changing nature of the soot and increased production rates when combustion changed to under ventilated regime. After this second maximum, values decrease slowly to the end of the test. The fire source is probably too weak for the size of the room to lead to a strongly stratified situation. At the beginning, the smoke is well stratified, then thermal convection tends to homogenize the concentration of smoke in the room.

The extent of degradation is used to estimate the amount of burned polyurethane foam. This quantity is about 1 kg. The slatted bed base was slightly impacted during the combustion of the mattress. Finally, the bed frame has been slightly degraded. The wall closest to the fire shows slight damage to the PVC panelling. This localized degradation could explain the presence of hydrogen chloride (HCl) in the smoke from the 11th minute after ignition. The rest of the room seems unaffected, except for the soot deposit on all horizontal surfaces.

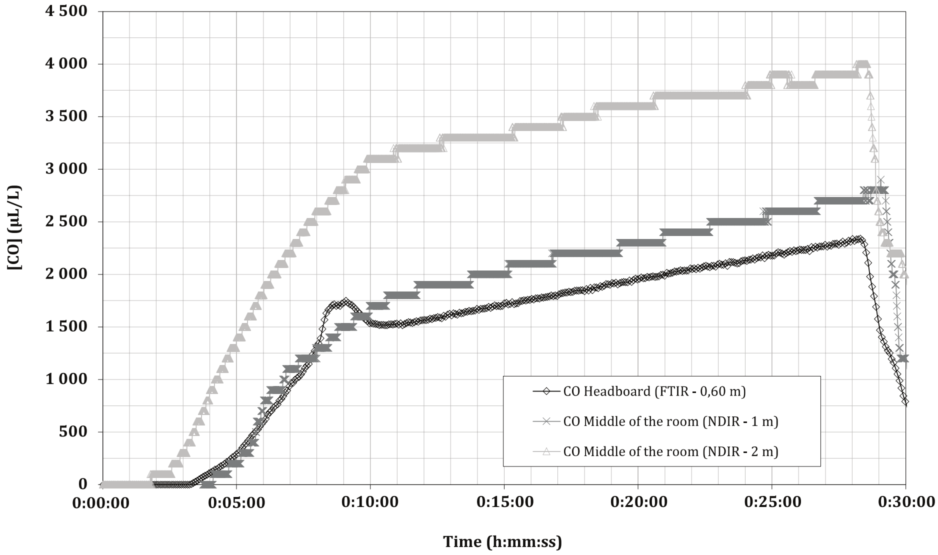

a) CO concentration

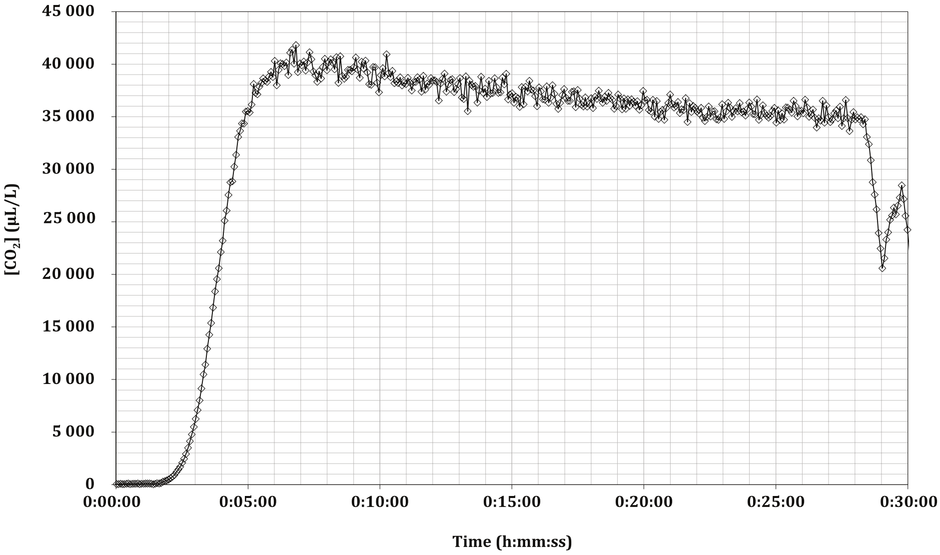

b) CO_2 concentration (headboard)

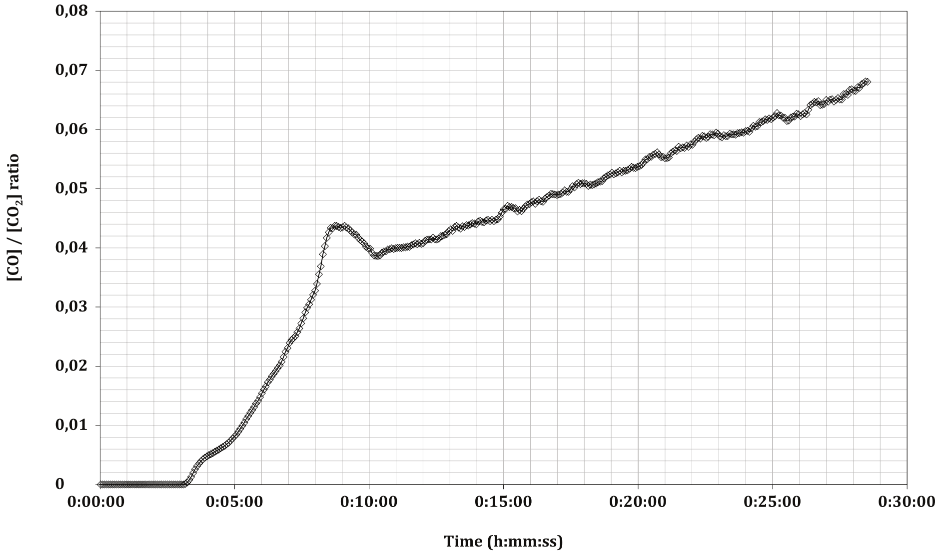

c) [CO] / [CO_2] ratio

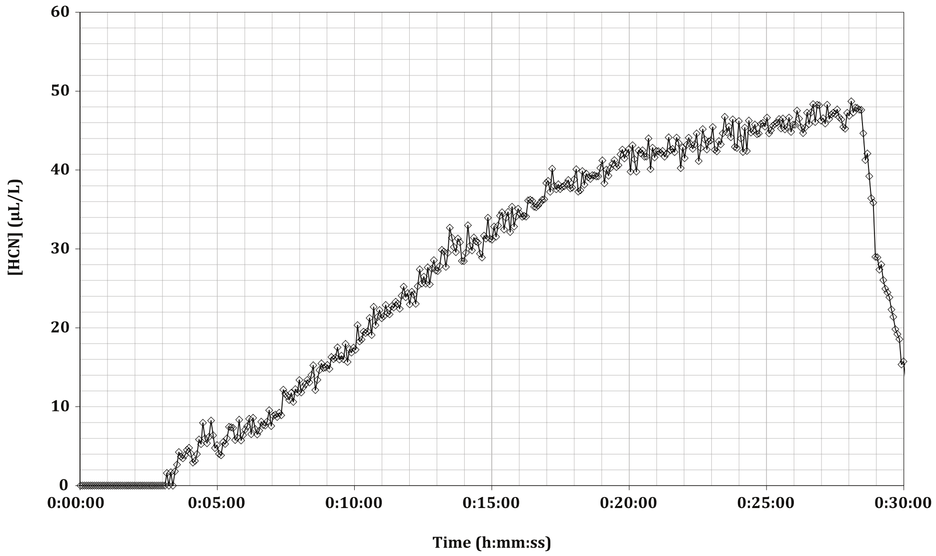

d) HCN concentration (headboard)

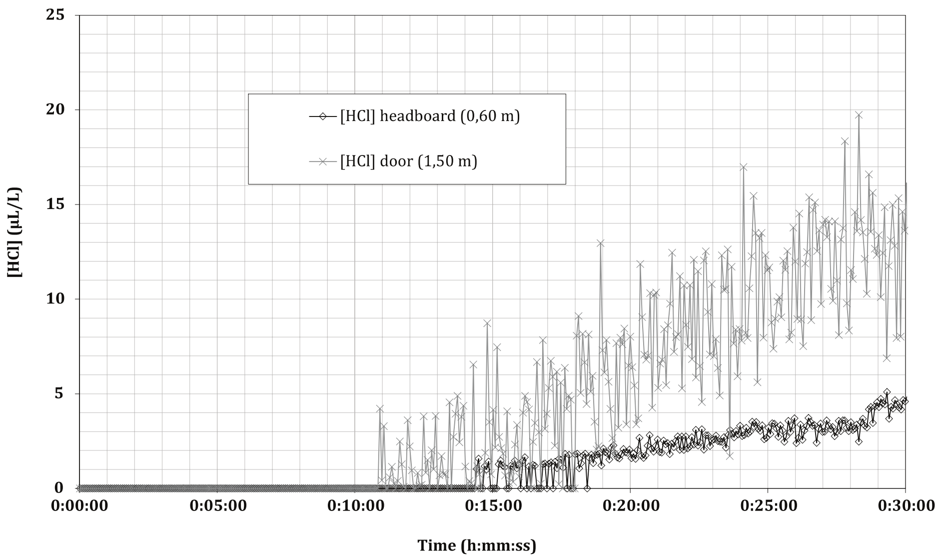

e) HCl concentration

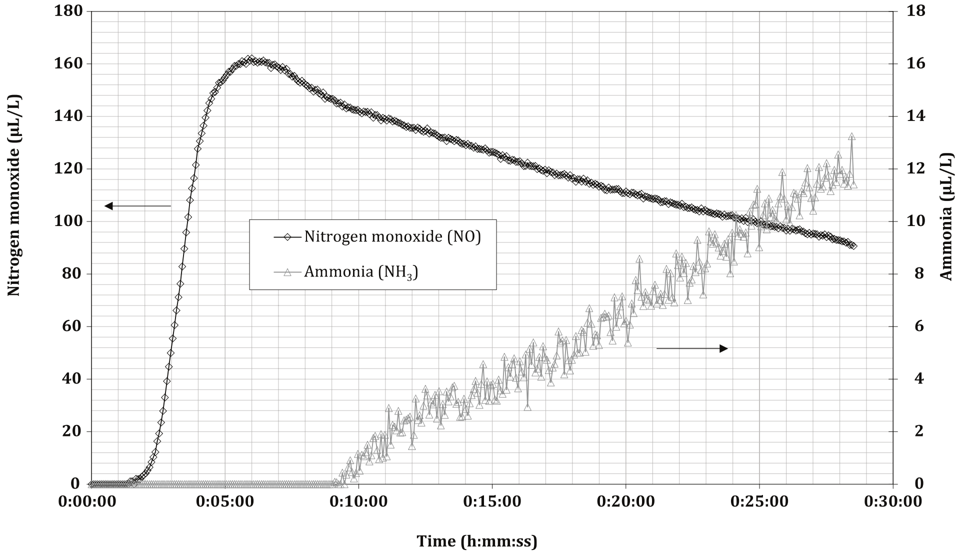

f) Nitric oxides and ammonia (at door)

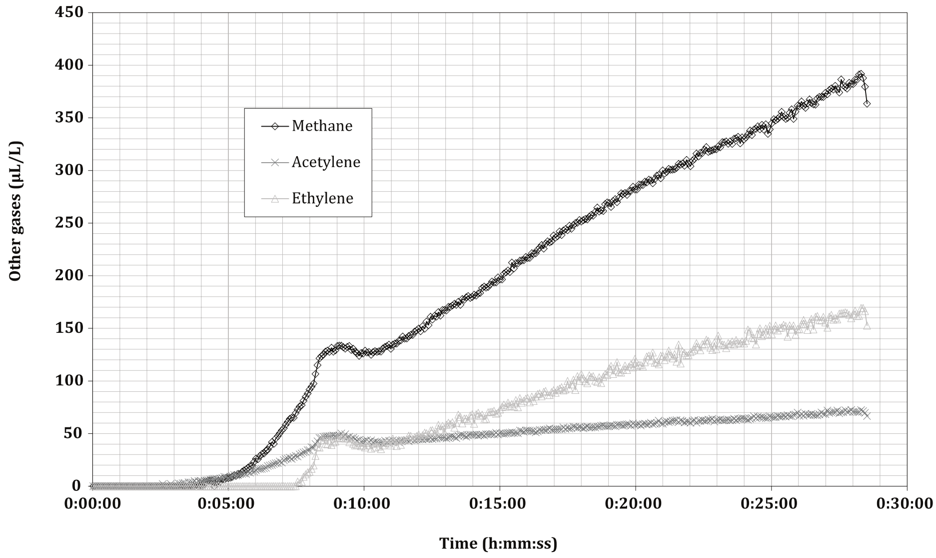

g) Other gases (at door)

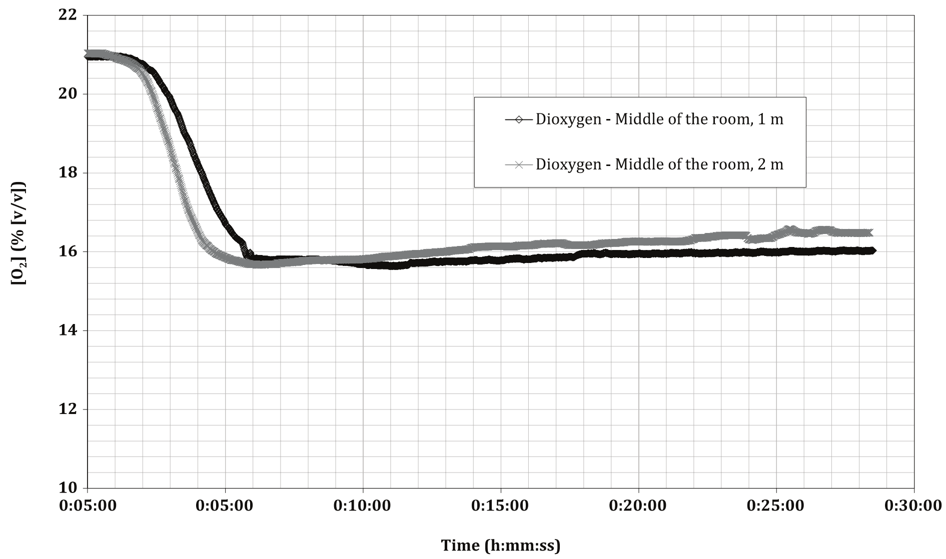

h) O_2 concentration

Figure B.2 — measurement results for gases, test 1C

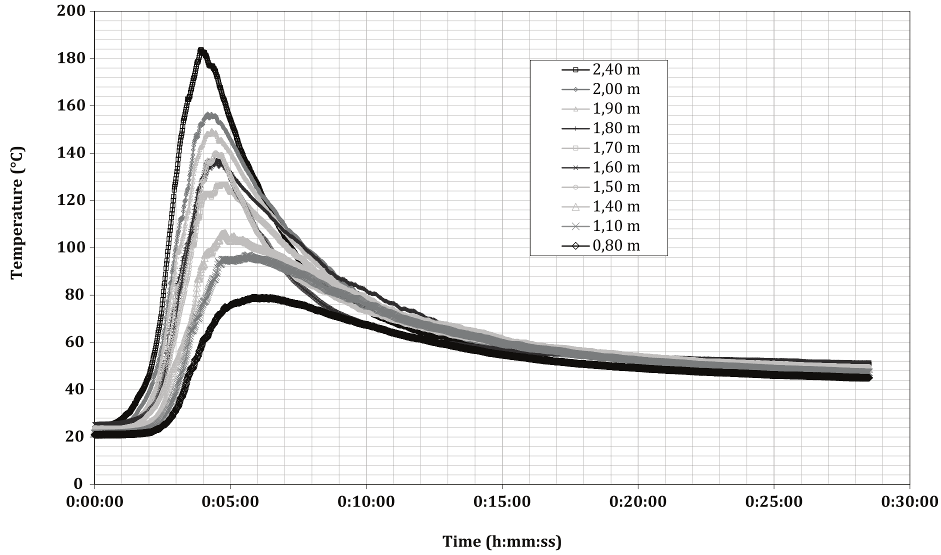

a) Temperature tree, point ATC3 (close to the door)

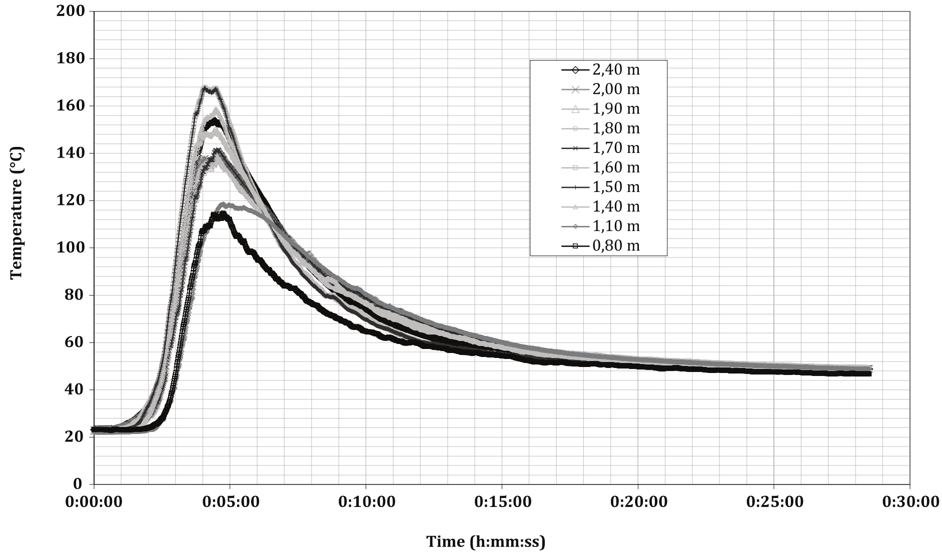

b) Temperature tree, point ATC4 (close to the window)

Figure B.3 — measurement results for temperatures, test 1C

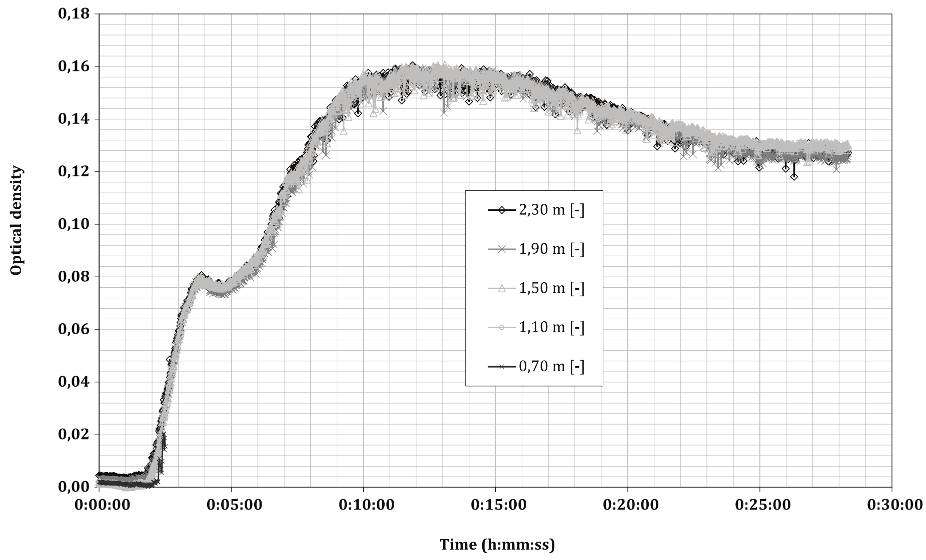

Figure B.4 — measurement results for opacimeters, test 1C

B.4.2 Interpretation according to ISO 13571

The scenario of the test 1C is an accidental fire on a mattress, ignited by an occupant smoking, then falling asleep. The occupant does not wake up and does not evacuate. The openings (doors, windows) remain closed. Figure B.5 shows the interpretation of the results according to ISO 13571, considering the exposed individual with head at the pillow level. Figure B.5a) shows the results of FED/FEC, while Figure B.5b) interprets these results in terms of proportion of the population that is affected, assuming a lognormal distribution of the sensitivity in population. In this interpretation, the effects of asphyxiant (narcotic) gases (CO, HCN) are predominant. The effects of temperature impact a lower percentage of population (except between 4 min and 7 min when the thermal impact curve is slightly higher than the curve of impact from asphyxiant gases). Finally, the irritating effects are not significant, among which those of hydrogen chloride due to the combustion of PVC. Oxygen concentration reaches about 16 % in 4 min. Such oxygen concentration is likely to compromise tenability. It should be noted that smoke alarms are activated early, about 3 min before the onset of asphyxiating effects.

Smoke optical density reaches values that could compromise evacuation for an unknown travel path after 3 min (DO = 0,06 according to[12]or DO = 0,08 according to[13]), when limit for a known path is not reached (DO = 0,2 according to[12]).

Within the frame of this test, the conditions of its execution and the interpretation of measurement data according to ISO 13571, it is possible to conclude:

— At the end of the test, about 9 out of 10 people facing this exposure scenario are in compromised tenability conditions, as a result of the action of the asphyxiant gases (CO and HCN);

— Approximately one in six people facing this exposure scenario are in compromised tenability conditions because of thermal effects;

— Less than 1 in 100 people facing this exposure scenario are in compromised tenability conditions due to the action of irritating gases, including hydrogen chloride.

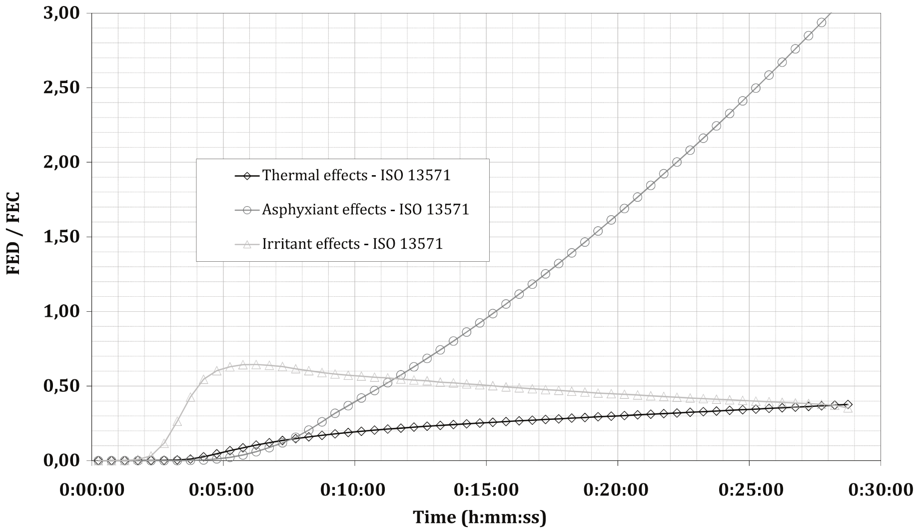

a) FED/FEC calculation according to ISO 13571 **at headboard level**

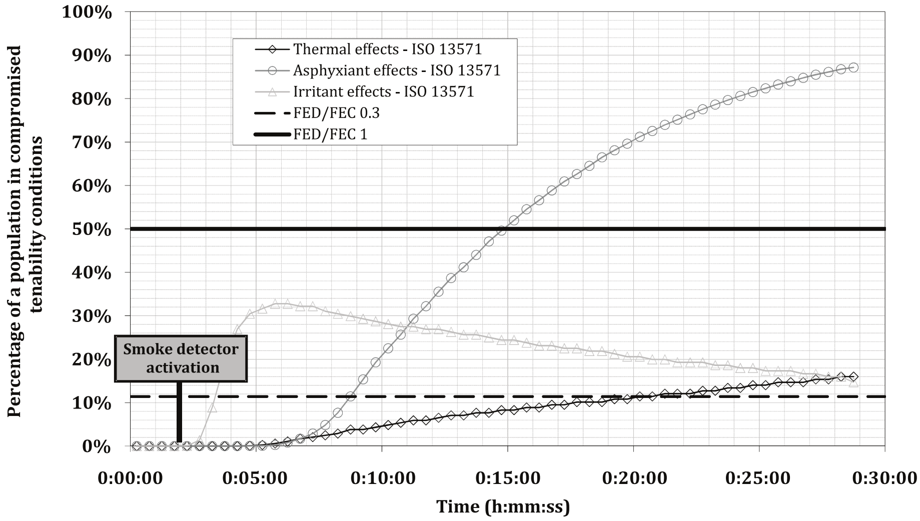

b) Percentage of the population in compromised tenability conditions

Figure B.5 — interpretation of the test 1C according to ISO 13571

B.5 Results and interpretation – Test 2B

B.5.1 Results

Ignition is carried out in the right-side wastepaper basket with a plastic trash bag and 500 g of creased paper balls. The wastepaper basket is placed under the edge of the vertical wall to the right of office. A second identical wastepaper basket is placed next to it under the desk. Ignition is achieved with a small flame simulating a match similar to the EN 597-2 source. The simulated match is placed on the top of the wastepaper basket to cause ignition of the paper. The beginning of the application corresponds to the start of the test (t_0). Test staff then leaves the test room and closes the door.

Events and observations during test are detailed in Table B.3. Test is stopped when 200 °C is reached in the corridor. This is obtained at 6 min and tenability assessment is therefore performed between 0 min and 6 min. Additional information is however available for further model validation purposes from thermocouples and heat flux meters between 6 min and firefighters intervention.

Table B.3 — events table for test 2B

Time (hh:mm:ss)	Event
00:00:00	Beginning of ignition sequence.
00:00:48	End of ignition sequence. Staff leaves the room.
00:01:14	Door closing.
00:02:01	Activation of smoke alarm in room.
00:02:15	Visible flames going out of the volume under the desk.
00:02:31	Second paper basket ignites.
00:03:12	Door opening, 1 min 58 s after its closing.
00:03:22	Fire grows and flame reaches the shelf.
00:03:31	Activation of smoke alarm in corridor.
00:03:42	Flashes of flames from the back side of the desk.
00:04:55	After 10 s of softening, the shell of the seat finally produces flaming drops.
00:04:59	PVC wall panels start to collapse.
00:05:00	Smoke opacimeters are saturated. No optical density data afterwards.
00:05:54	200°C reached in the corridor. First flames visible from the corridor, at the top of the door frame.
00:06:00	End of test. Intervention order given to firefighters.
00:06:15	Growth to flashover.
00:06:34	Visible flames, probably from the bed on fire.
00:08:10	Firefighters intervention.

Figure B.6 presents all the gases measurements results for test 2B. Oxygen decays as CO_2 concentration increases up to flashover, and reaches 8 % at ceiling height (Figures B.6a to 17c). Very few CO is produced during the first minutes, and then CO rises quickly at 5 min 30 s, in pre-flashover phase. Hydrogen chloride (HCl) only appears in small quantities when flashover conditions are reached few seconds before end of test (Figures B.6d and B.6g). Nitrogen monoxide (NO) is present at early stages of fire, as for hydrogen cyanide (HCN), as seen in Figures B.6e and B.6h. These two trends highlight the combustion of nitrogen-containing species, with different local combustion conditions to produce both species. Ammonia is visible on the same figures in first stage of the test, but it is probably consumed after 5 min 30 s, when temperature conditions change in the room. The contribution of irritant gases other than HCl on the FEC is deemed negligible. Therefore the FEC has been calculated from HCl values only, from the beginning to 6 min. Unburnt hydrocarbons remain very low during test, highlighting a complete combustion of pyrolysis gases before flashover (Figures B.6f and B.6i).

Figure B.7 presents temperature measurements at each location of thermocouples trees. Temperature of gases in upper parts starts to increase after 3 min. Until 5 min 30 s, the system is stratified, with also no temperature rise at 1,1 m and 0,8 m. The interface is located between 1,1 m and 1,4 m. Then, temperature rises rapidly in one minute, to reach about 700 °C to 900 °C at each location and each height. Regarding temperatures, flashover conditions are reached from 6 min 15 s. Temperature in the corridor follows the same trend, with a difference of about 100 °C with the room. Again, it is interesting to note that the experimental observations on the fire behaviour meet forecasts of numerical simulations before the intervention of firefighters. The temperature in the room has reached more than 900 °C at the ceiling: the simulation indicates temperatures of the same order, with a flashover occurring in the same time period. Figure B.8 presents the measured total heat fluxes. Flashover conditions are reached when a heat flux from ceiling to floor reaches between 10 kW/m^2 and 20 kW/m^2, according to literature[14]. These conditions are reached after 6 min 15 s. Previously, the heat flux sensor located at door sees an important increase of heat flux, corresponding to an important but localized fire growth, from 5 min 30 s to 6 min 15 s. Post-flashover conditions at the end of test present heat fluxes over 100 kW/m^2 at 8 min.

Figure B.9 presents results for optical density. The smoke opacimeter device fails after 5 min, no optical density values are available then after. First smoke rise is detected on the highest sensor (2,30 m) after 3 min 20 s, then followed by the 1,90 m sensor at 3 min 35 s and by the 1,50 m sensor at 3 min 52 s. After 4 min, the 1,50 m high sensor indicates a variable signal that could correspond to the presence of the interface between air and smoke. There is no smoke under 1,10 m during the whole measurement period. For the period of data collection, it is interesting to note the gradient of optical density (and hence concentration of soot) from top to bottom, with an interface established close to 1,5 m.

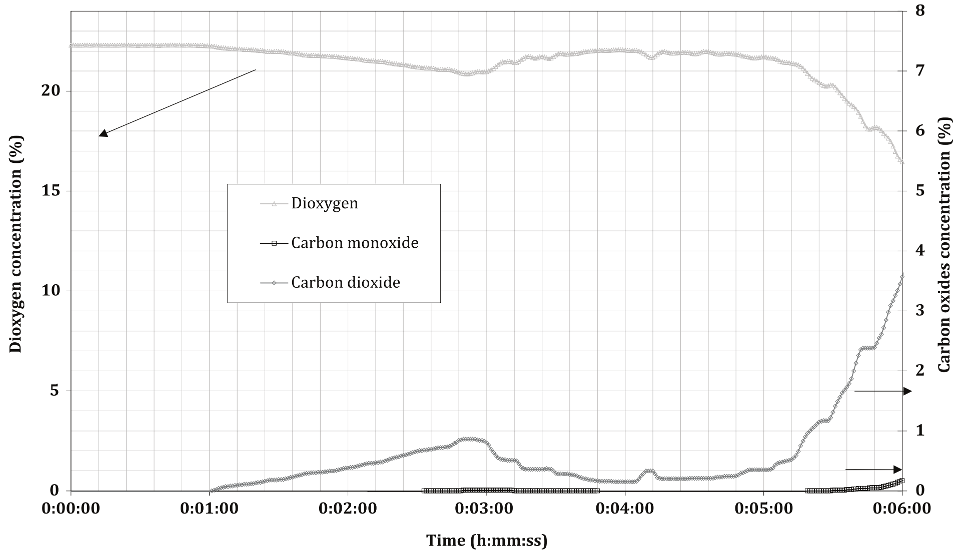

a) O_2, CO and CO_2 concentration, point C1 (middle of the room, 1m high)

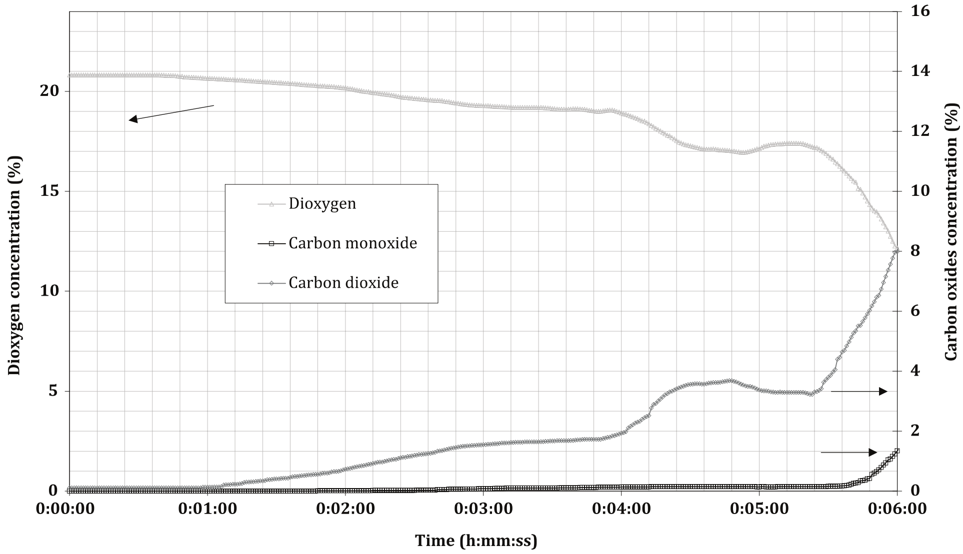

b) O_2, CO and CO_2 concentration, point C2 (middle of the room, 2m high)

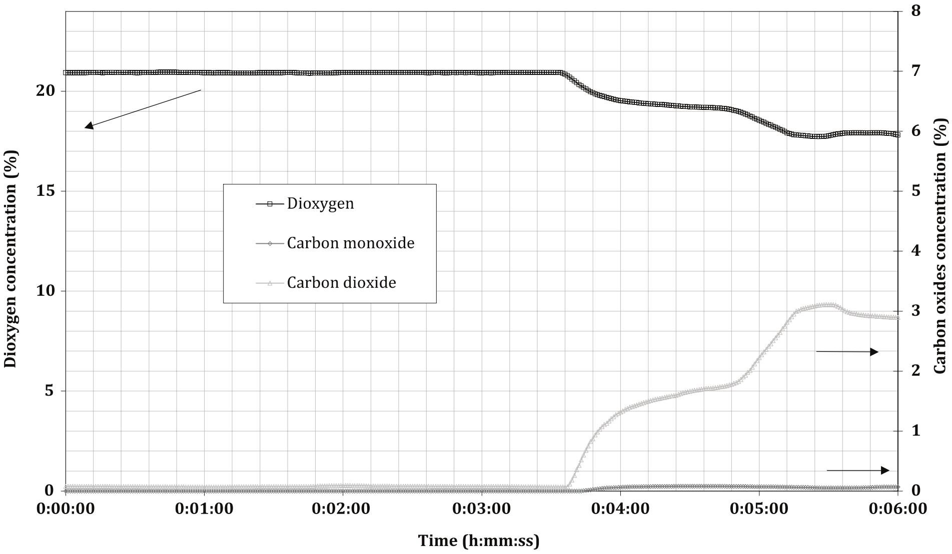

c) O_2, CO and CO_2 concentration, point C3 (corridor, 2 m high)

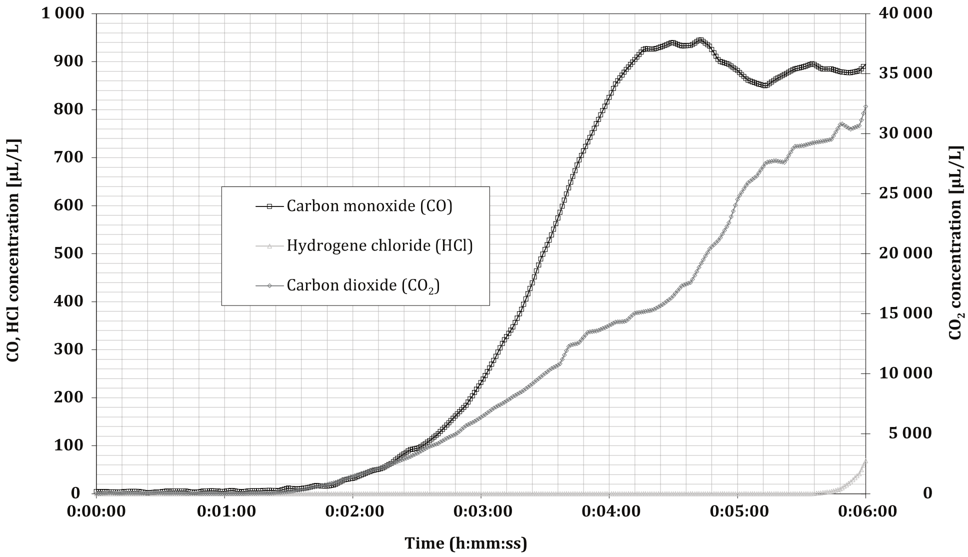

d) FTIR gases concentration (CO, CO_2, HCl), point FT1 (middle of the room, 1,5 m high)

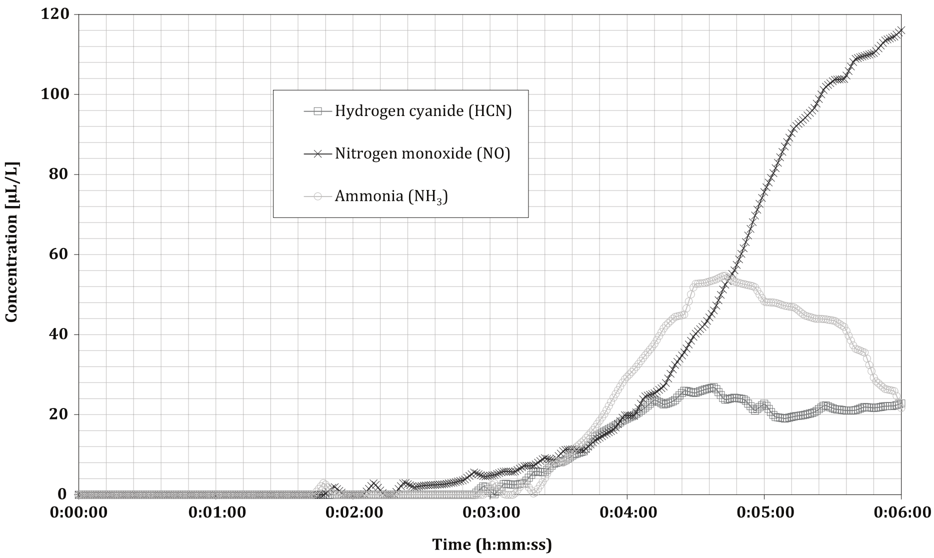

e) FTIR gases concentration (HCN, NO, NH_3), point FT1 (middle of the room, 1,5 m high)

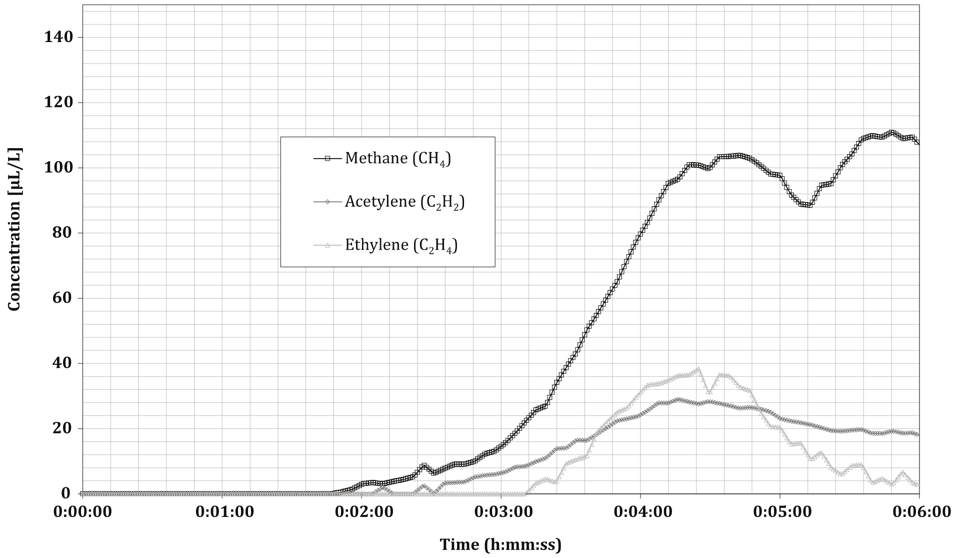

f) FTIR gases concentration (Hydrocarbons), point FT1 (middle of the room, 1,5 m high)

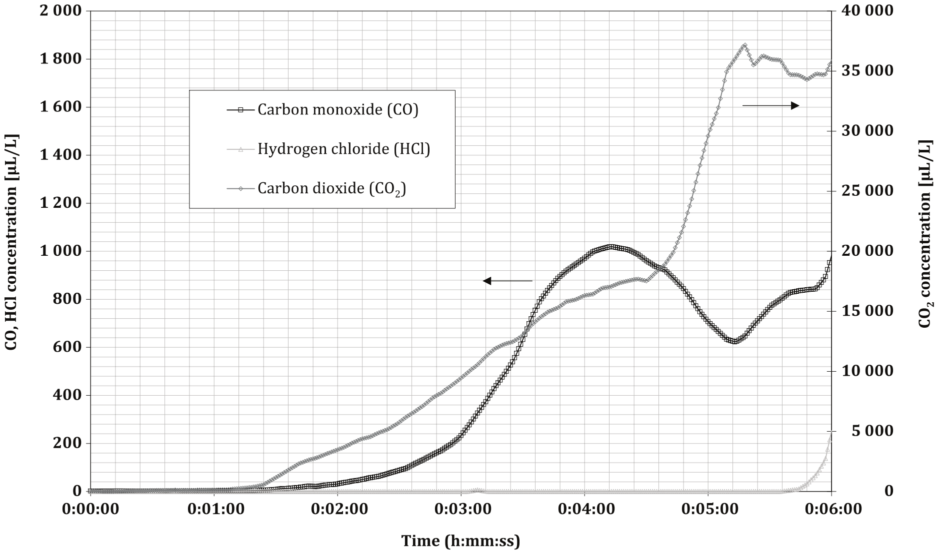

g) FTIR gases concentration (CO, CO_2, HCl), point FT2 (door, 1,5 m high)

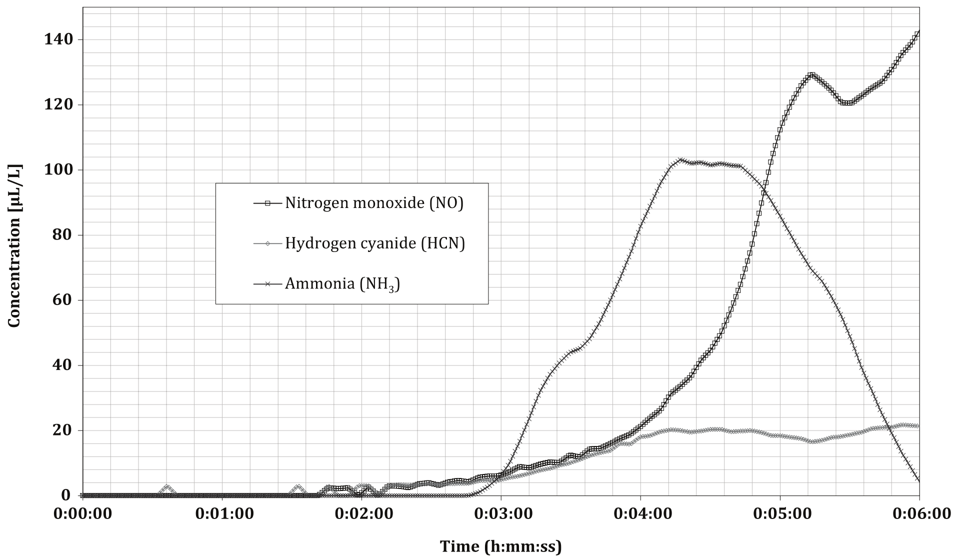

h) FTIR gases concentration (HCN, NO, NH_3), point FT2 (door, 1,5 m high)

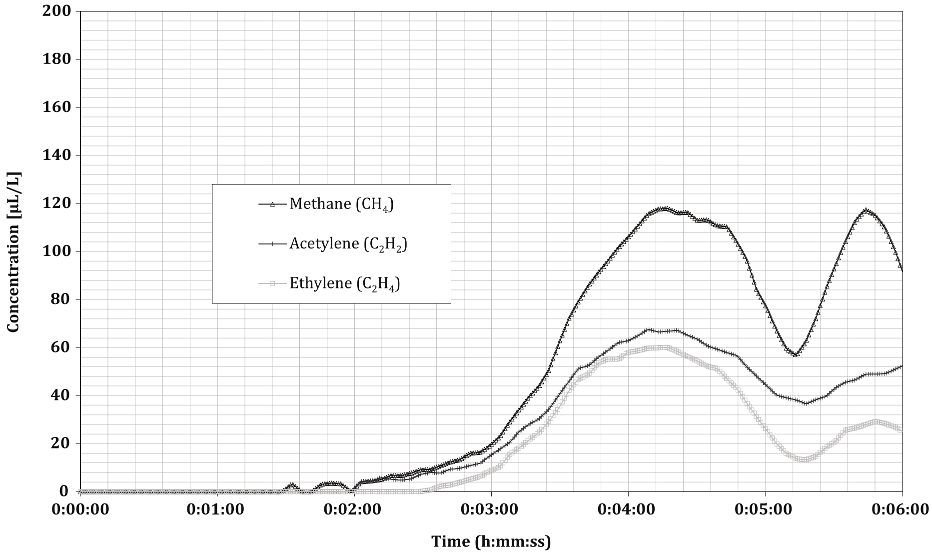

i) FTIR gases concentration (Hydrocarbons), point FT2 (Door, 1,5 m high)

Figure B.6 — measurement results for gases, test 2B

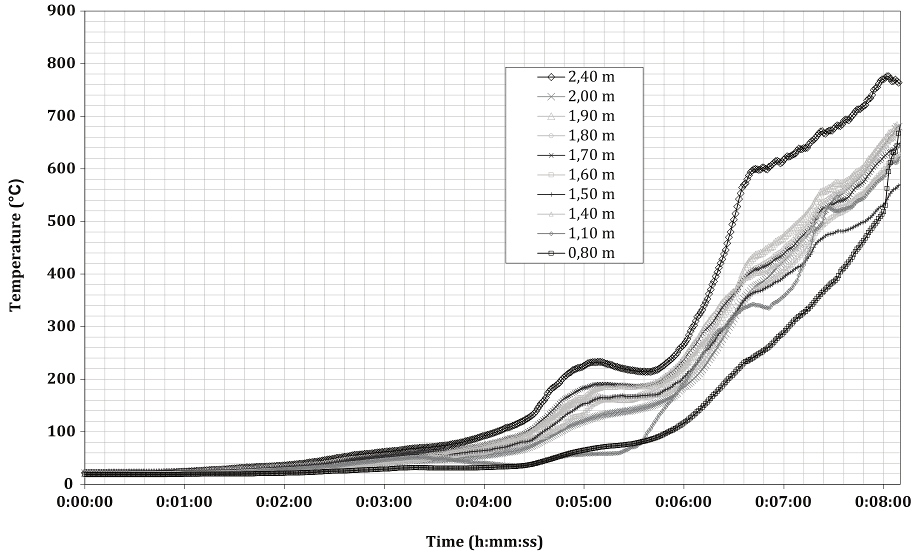

a) Temperature tree, point ATC1 (In the middle of the room)

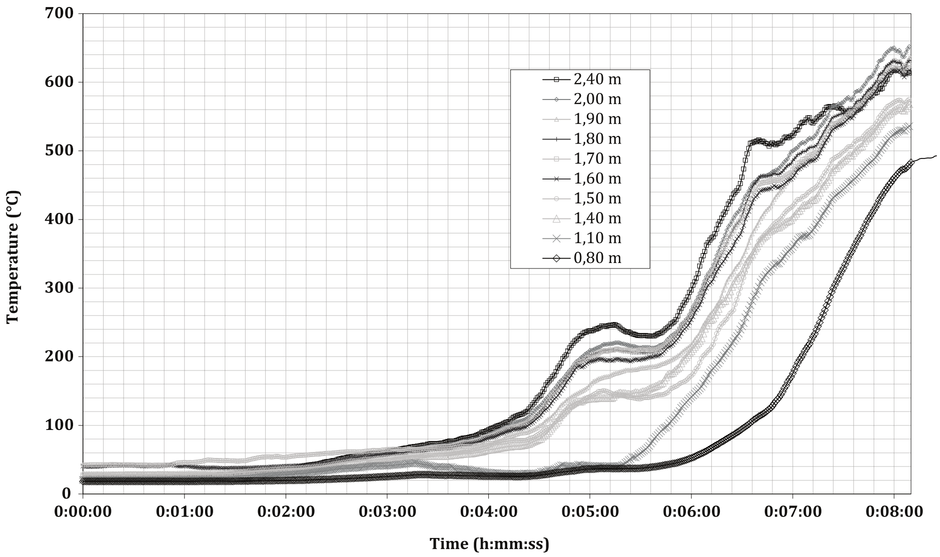

b) Temperature tree, point ATC2 (on the mattress)

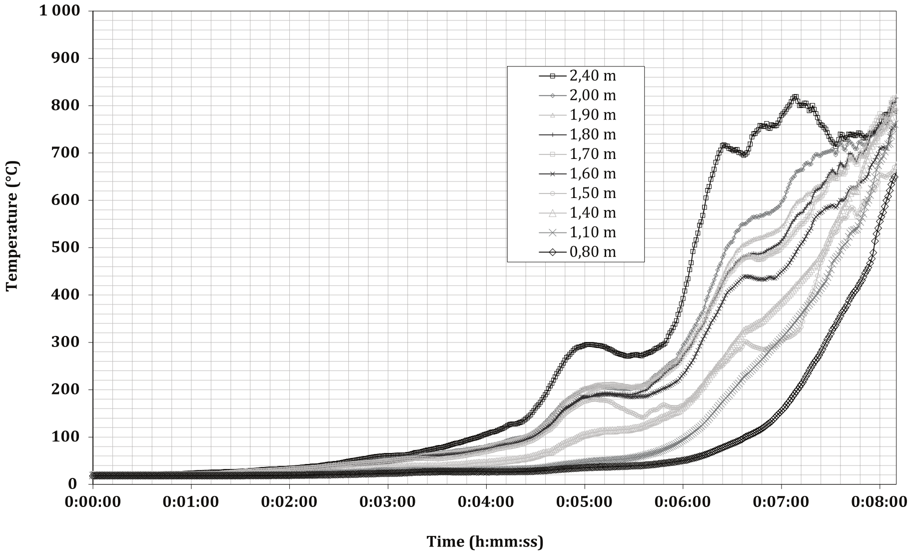

c) Temperature tree, point ATC3 (close to the door)

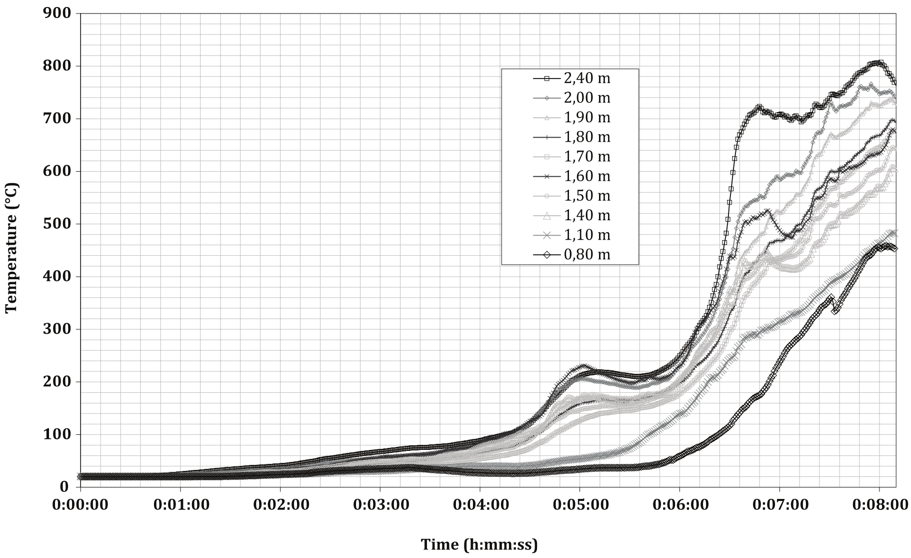

d) Temperature tree, point ATC4 (close to the window)

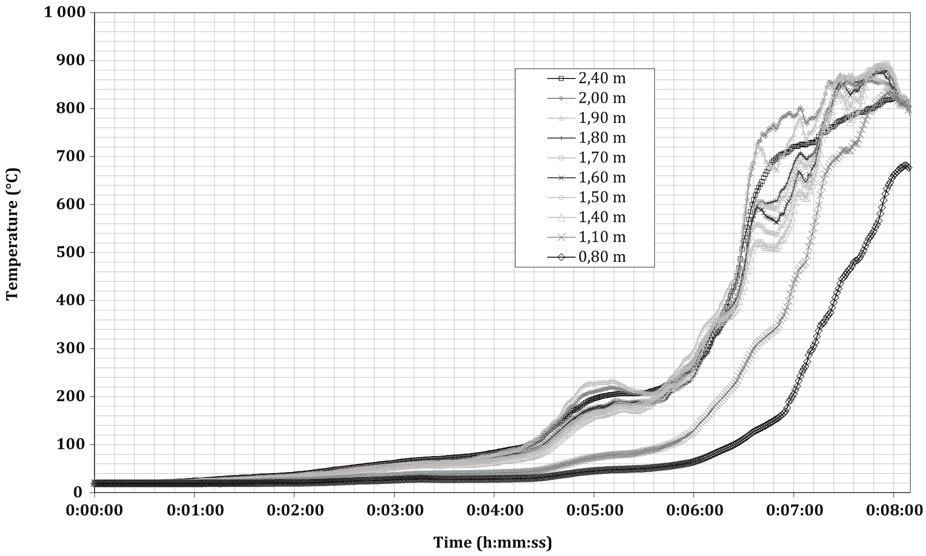

e) Temperature tree, point ATC5 (close to the sink)

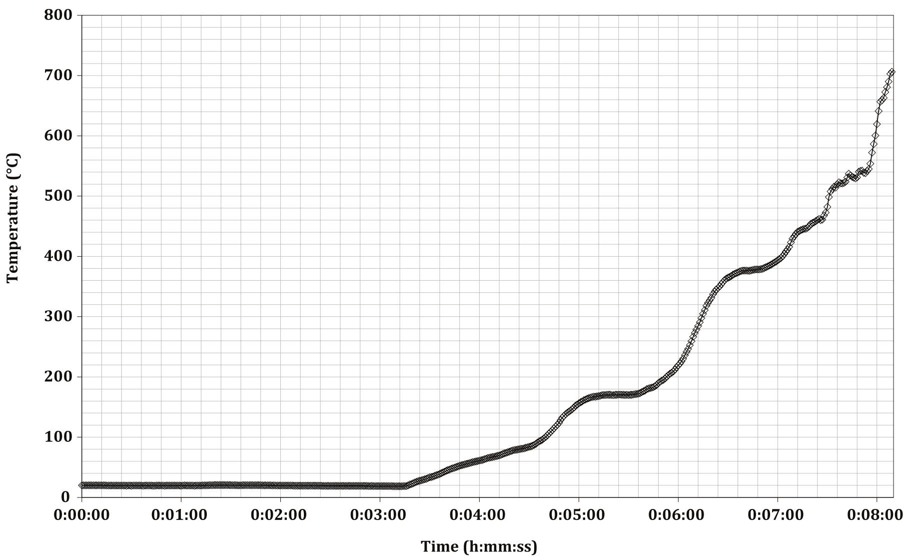

f) Temperature at ceiling level in corridor (point C3)

Figure B.7 — measurement results for temperatures, test 2B

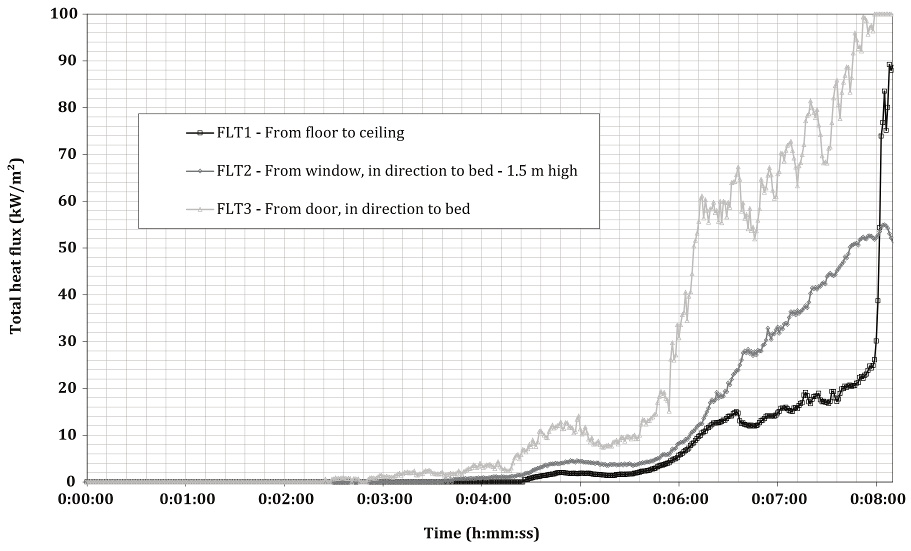

Figure B.8 — measurement results for total heat fluxes, test 2B

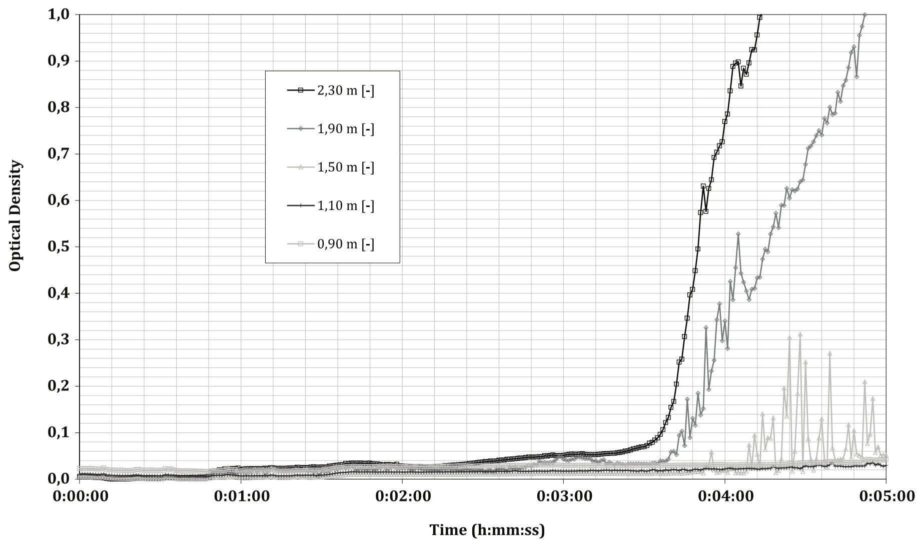

Figure B.9 — measurement results for opacimeters, test 2B

B.5.2 Interpretation according to ISO 13571

The scenario 2B corresponds to an accidental fire in a couple of wastepaper baskets full of paper. In occupancy scenario 2B-I, two minutes after having closed the door, the occupant gets out of the room and leaves the door opened. The window remains closed. In scenario 2B-II, a first occupant escapes in the very same conditions as in scenario 2B-I. A second occupant doesn't evacuate and is standing in the middle of the room. Within the frame of this test 2B, the conditions of its execution and interpretation of measured data according to ISO 13571, it is possible to conclude:

— In scenario 2B-I: except for people with marginal sensitivity to the effects of fire, people who leave the room before 3 min 15 s after the beginning of a fire (or 2 min after closing the door and about 1 min after the activation of the alarm of the test room) do not suffer from deterioration of tenability conditions (See Figure B.10);

— In scenario 2B-II: in such a scenario, the first and main impact on remaining people is the thermal effect of fire effluents. It occurs after 4 min, with a tenability being quickly compromised for the whole population within the following 2 min (See Figure B.11a and Figure B.11b). Asphyxiant and irritant gases effects appear around 6 min, when the tenability is already compromised for the whole population by thermal effects. Smoke opacity remains low under 1,50 m for the first 5 min.

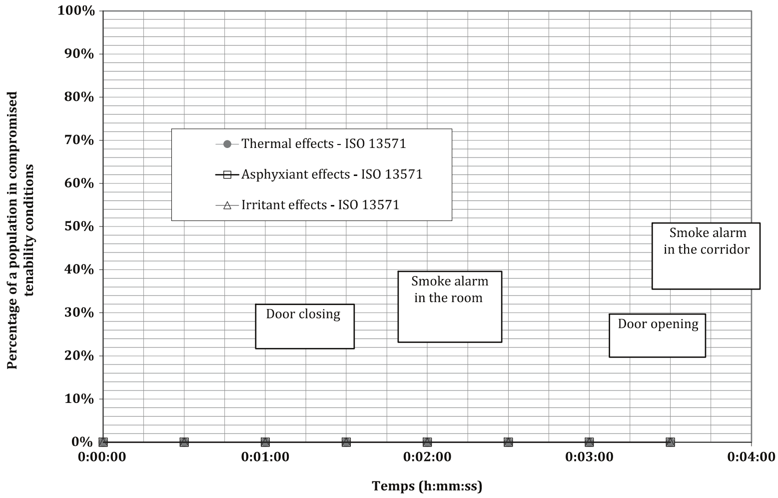

Figure B.10 — interpretation according to ISO 13571: Scenario 2B-I

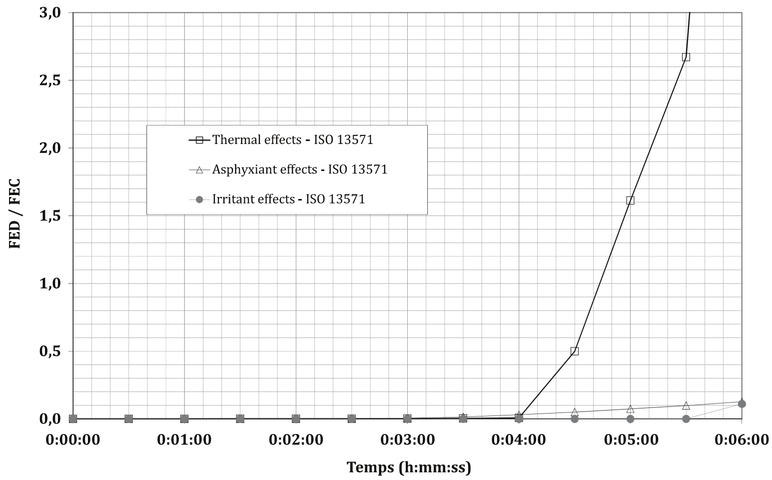

a) FED/FEC calculation according to ISO 13571 at room centre

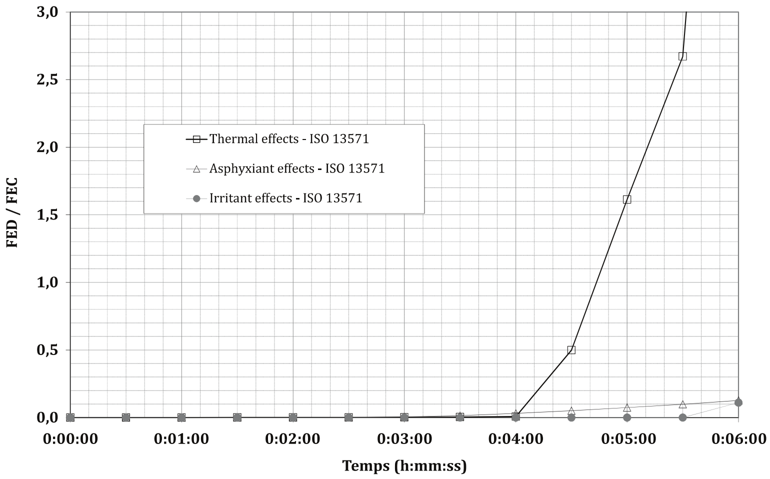

b) Percentage of the population in compromised tenability conditions

Figure B.11 — interpretation according to ISO 13571: Scenario 2B-II

Annex C
(informative)

Methodology for application of ISO 13571 in Fire Safety Engineering approach

The practical methodology making it possible to fulfil the objectives cited in Clause 5 is an adaptation of the methodology covered in ISO 23932, developed in reference[15]. It adds to the general methodology of Fire Safety Engineering the elements necessary for the consideration of toxicity, within the limit of current understanding. The methodology is presented in Figure C.1. Choice of the acceptance criterion indicated in this methodology is made prior to the study to be performed.

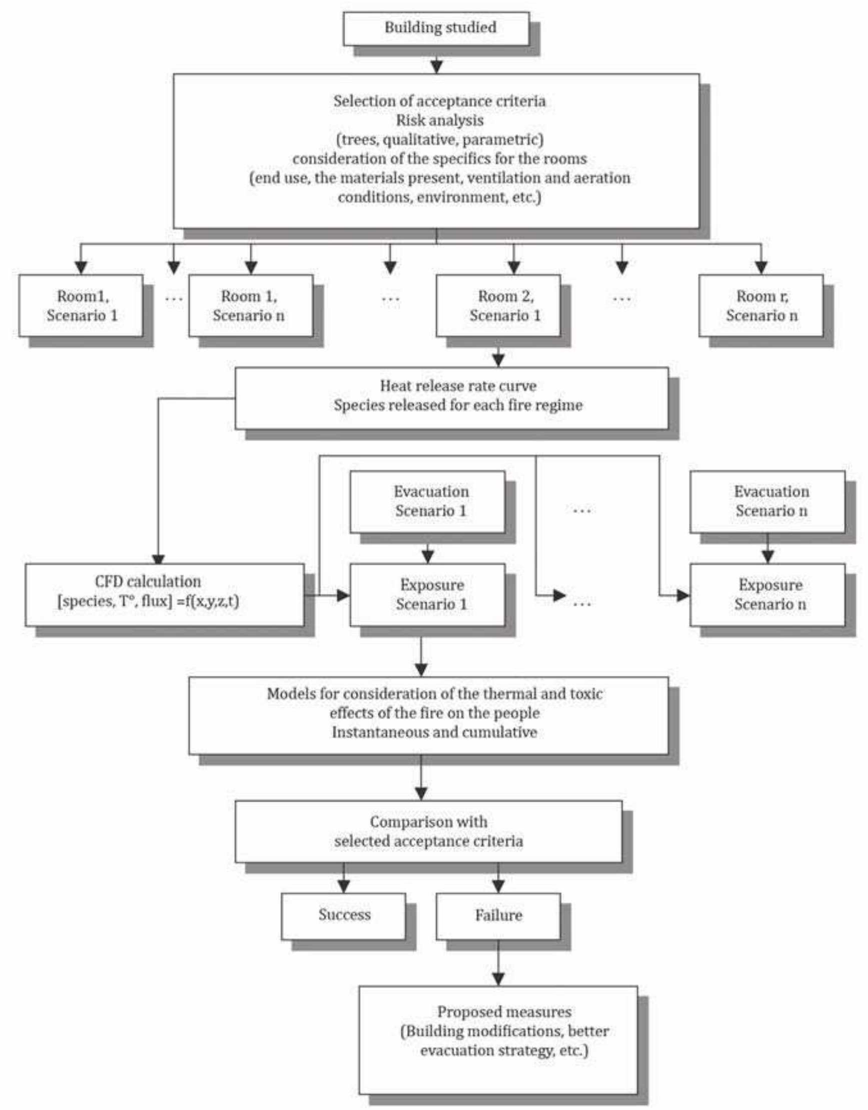

Figure C.1 — Methodology for considering the adverse effects of fire on people

C.1 Risk analysis

During the risk analysis and scenario establishment phase (see ISO 16732 for further details), the traditional scenario selection approach includes an assessment of the risk linked to the smoke's toxicity, for example in the evaluation of the severity of a given scenario. The first step consists of using a risk analysis to uncover the fire scenarios to be studied. Various methods exist like:

— Methods based on failure trees or bow ties

— Qualitative methods (HAZOP, FMEA, etc.)

— Methods making use of parametric studies

Some of these methodologies have been developed for industrial use and need to be adapted to agree with an environment such like dwelling or Public Building.

The parametric study is particularly interesting because it makes it possible – by using simplified tools like zone models – to explore all possible scenarios by using a statistical sampling of several thousands from among these. This type of method then makes it possible to consider:

— Effects of atmospheric conditions inside the room (temperature, pressure, relative humidity)

— Effects of outside atmospheric conditions (temperature, pressure, wind, etc.)

— State of the building's openings (doors, windows – open, closed, part open)

— Ventilation conditions in the areas (AHU, CMV, smoke control, etc.)

— Localization, power and kinetics of primary fire sources

Then, method allows evaluating the consequences in terms of toxicity, temperature in the original room of the fire source and in adjacent or distant rooms.

Thus, by considering the probabilities of occurrence and severity of consequences, it is possible to classify the rooms in descending order of risk.

Whatever the method used, the output data from this step are:

— A list of rooms to be considered for an in-depth study

— The fire scenarios associated with each of the rooms

Currently, five scenario types – divided in two groups – have been uncovered by a general risk analysis is having sufficiently widespread interest for appearing in most of the risk analyses for fires in enclosures. They are:

— Scenarios from group S1 (risk evaluated in the area where the fire source started):

  — Scenario S1a: smouldering fire

  — Scenario S1b: well ventilated fire not leading to a flashover in the initial room of the fire source

— Scenarios from group S2 (risk evaluated in the area adjacent to initial room of the fire source):

  — Scenario S2a: smouldering fire

  — Scenario S2b: well ventilated fire not leading to a flashover

  — Scenario S2c: well ventilated fire leading to a flashover in the initial room of the fire source

Construction of the corresponding fire sources is discussed in the following paragraphs:

— Paragraph C.2.1 for the heat release rate of the fire source

— Paragraph C.2.2, for the rate of production of species associated with each fire regime.

C.2 Source terms of heat and gases

C.2.1 Construction of the heat release rate for the fire source

To establish a toxicity source term for the smoke, it is necessary to first establish a heat release rate source term. The fire development curve (power as a function of time) can then be supplemented by a toxic product production curve. Currently three fire regimes are considered in this methodology. Drawn from ISO 19706, the following fire stages are proposed:

— Smouldering fire

— Well-ventilated fire (growth phase)

— Under-ventilated fire (for example, post flashover)

This number of fire stages can however be easily extended, if a finer analysis proves necessary. The fire stages cited above are used as “building blocks” for reproducing the complete kinetics corresponding to a given scenario for a given room. Thus, all the scenarios demonstrated by the risk analysis for the rooms identified as calling for specific study are built using these “building blocks”.

The transition points in the kinetics of these fire sources, which mark the passage from one fire stage to another, can be determined using analytical formulas. In some cases, using simplified numerical models can usefully help in determining typical magnitudes like the heat release rate necessary for reaching flashover, or the post flashover heat release rate, depending in particular on the openings. References[16][17][18][19] give various methods for establishment of this heat production source term.

C.2.2 Determination of the mass fractions of species produced

It should be noted that this part of the methodology, making it possible to determine the fractions by mass of species produced for each combustion regime and for each material involved can be done well before or at worst in parallel with the risk analysis and building up of the dynamic of the source fire sources.

Thus as time and experience goes by, a more and more complete database will gradually make it possible to reduce the assembly effort that such a database represents.

However, it is appropriate to keep in mind that such a database will be representative of the materials produced at a given period. It will need to be periodically revised to make sure it is representative. Further, it should only be used by experienced users, because of its scope of application and associated limits and because of their experience can make reliable choices concerning the values to be used in a given study.

C.2.2.1 Species production matrices

At the same time as the energy production kinetics – determined using the fire scenario and building blocks presented in the preceding chapter – the source fire source is characterized by production of characteristic species of each combustion regime.

Each material can be characterized by species production “spectrum”: one for each combustion stage. Organization into a matrix makes it possible to easily use these data for simplified characterization, but neglects the necessary synergies of the species produced by a group of material simultaneously involved in the fire source.

Species production matrix, covering three combustion stages, considering 10 gaseous species as proposed for acute toxicity in ISO 13571 is shown in Figure C.2.

Material M	Smouldering Fire (SF)	Well Ventilated Fire (WVF)	Post Flashover Fire (PPF)
CO_2	$CO_{2\,SF}$	$CO_{2\,WVF}$	$CO_{2\,PFF}$
CO	CO_{SF}	CO_{WVF}	CO_{PFF}
HCN	HCN_{SF}	HCN_{WVF}	HCN_{PFF}
HCl	HCl_{SF}	HCl_{WVF}	HCl_{PFF}
HBr	HBr_{SF}	HBr_{WVF}	HBr_{PFF}
HF	HF_{SF}	HF_{WVF}	HF_{PFF}
NO_2	$NO_{2\,SF}$	$NO_{2\,WVF}$	$NO_{2\,PFF}$
SO_2	$SO_{2\,SF}$	$SO_{2\,WVF}$	$SO_{2\,PFF}$
Acrolein (CH_2=CH-CHO)	$Acrolein_{SF}$	$Acrolein_{WVF}$	$Acrolein_{PFF}$
Formaldehyde (HCHO)	$Formaldehyde_{SF}$	$Formaldehyde_{WVF}$	$Formaldehyde_{PFF}$

Figure C.2 — Production matrix for the material M in a model with 10 gaseous species and three combustion stages with yields expressed in $kg \cdot kg^{-1}$

In a room, *n* different materials are present. In a simplified approach, a general matrix can be constructed for the room in the following manner:

$$[\ \ ]_{room} = \sum_{i=1}^{n} P_i \times [\ \ ]_{M_i}$$

where:

$[\ \ ]_{room}$ designates the species production matrix for the room being considered

P_i designates the proportion of material *i* in the room (unitless)

$[\ \ ]_{M_i}$ designates the species production matrix for material *i*

In a first approximation the proportion P_i can be considered as the ratio of the mass of the material present in the room to the total mass of all the materials present. A more detailed analysis is however possible, taking into account the mass loss rates of the materials in question in the characteristic environments of the different fire stages. The concept of available exchange surface then becomes important.

The species production matrix for the room can also include scenario data. Thus in the first stages of the fire, only few materials are involved in variable proportion according to the location of the fire source. On the other hand, when flashover occurs all the materials present participate in the production of gaseous species (in practice they even began to contribute to gas generation by pyrolysis before their effective ignition). It is therefore useful to be able to include the scenario data in the species production matrix for the room being studied with the matrix calculation done as follows (in a three stages fire model which would be smouldering, followed by a well-ventilated stage, then a post-flashover stage):

$$[\ ]_{room} = \sum_{i=1}^{n} P_{(i,SF)} \times [\ ]_{M_i} \begin{bmatrix} 1 \\ 0 \\ 0 \end{bmatrix} + \sum_{i=1}^{n} P_{(i,WVF)} \times [\ ]_{M_i} \begin{bmatrix} 0 \\ 1 \\ 0 \end{bmatrix} + \sum_{i=1}^{n} P_{(i,PFF)} \times [\ ]_{M_i} \begin{bmatrix} 0 \\ 0 \\ 1 \end{bmatrix}$$

where:

$[\ ]_{room}$ designates the species production matrix for the room being considered

$P_{i,SF}$ designates the proportion of material *i* in the room, involved in the smouldering fire stage (unitless)

$P_{i,WvF}$ designates the proportion of material *i* in the room, involved in the well ventilated fire stage (unitless)

$P_{i,PFF}$ designates the proportion of material *i* in the room, involved in the post-flashover fire stage (unitless)

$[\ ]_{M_i}$ designates the species production matrix for material *i*

Figure C.3 shows an example of a complex scenario of a bed burning alone in an empty room. In the chart, first three phases apart from the decline are detailed in species production terms.

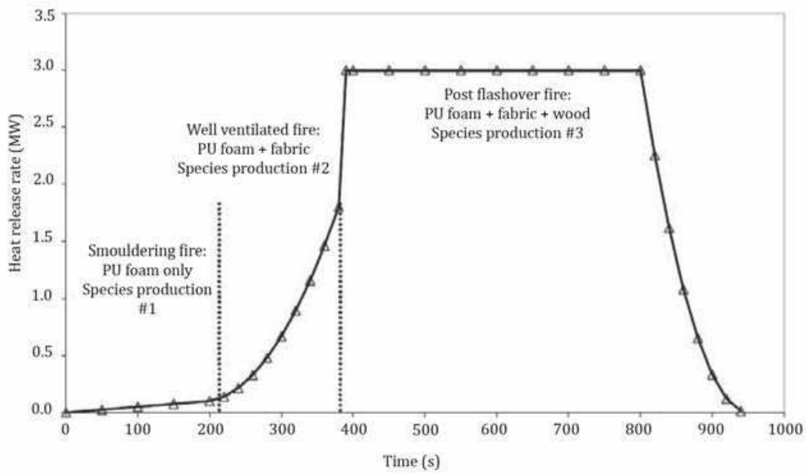

Figure C.3 — Example of fire source including multiple stages (at each stage, the materials involved are different and so are the species produced)

C.2.2.2 Assignment of the species production rates in the matrices

Referring to several types of sources can populate the species production rates that go into these matrices:

— By reference to theoretical values:

— Values extracted from the literature, as References[20][21];

— From fire stages and associated [CO]/[CO_2] ratios proposed in ISO 19706;

  — From theoretical species production rates from Element analysis as proposed in ISO 19703.

— By reference to experimental values such as:

  — Values obtained at bench scale with tube furnace ISO/TS 19700, plus ISO 19702 under various specified ventilation and temperature conditions;

  — Values obtained at bench scale with ISO 5660-1, coupled with ISO 19702, under controlled atmosphere and various heat fluxes;

  — Full-scale and real-scale tests, e.g. ISO 16405;

  — Scalling studies using ISO 29903.

NOTE Cone calorimeter with controlled atmosphere is not standardized at the date of production of this document. Further details on this bench could be obtained in References[22] and[23].

For the theoretical values, it should however be kept in mind that the adequacy of the values found should be considered with prudence. For example in the literature, when the species production table is found, it is not guaranteed that the referenced material is identical to the material that one wishes to characterize. In most cases, it will involve material close to the studied material, but not identical. The values should therefore be considered with prudence. Further, the test conditions used to supply said table are not always clearly stated even though it is only right to use the relevant data for each fire regime.

Furthermore, the values provided by ISO 19703 are theoretical rates based on the assumption that the entirety of the available quantity for a given atom (C, H, O, N, etc.) is converted into the gaseous species considered. There is no consideration of the fire regime in these formulas, no rule for balancing between various competitive species. Thus, CO and CO_2 both use the carbon atoms present in the material studied, but the calculation formulas are disjoint and carbon atoms used twice: once for the production of CO and the second time for the production of CO_2. The calculated rate is therefore a maximum for each of the gaseous species and a high upper bound.

Some additional items are however found in ISO 19706, like for example the $[CO]/[CO_2]$ ratios for each fire regime, which to some extent allows balancing the counts. These ratios are the following:

— Smouldering fire: $[CO]/[CO_2]$ = 0,1 to 1

— Well ventilated fire: $[CO]/[CO_2] < 0,05$

— Post flashover fire: $[CO]/[CO_2]$ = 0,1 to 0,4

For the experimental values, make sure that the tests performed are pertinent to the fire regime studied: for a test to be useful, the combustion environment has to be representative of the fire regime studied. Thus, the results of the tests conducted with under-ventilated conditions are not usable to quantify the gaseous species produced with well-ventilated fire conditions.

Ideally, for each material it would be appropriate to determine the typical combustion reaction equation in a given environment: the stoichiometric coefficients balancing these equations would then be known and make it possible to determine the production rates for each species from them. However pragmatically, it is possible to determine these production rates by species on the basis of tests under well specified conditions.

The experimental methods proposed from ISO/TR 16312-2, References[24] and[25] allowing measurement of these species production rates are described in Annex F, Table C.1 proposes recommended test conditions for measuring the gaseous species produced. They are inspired by the definitions from ISO 19706 and combine a thermal degradation with ISO 5660-1 cone calorimeter under controlled atmosphere with measurement of gaseous species done using ISO 19702 (or alternatively ISO 19701).

Table C.1 — Cone calorimeter test conditions under controlled atmosphere and analysed with Fourier Transform Infrared spectrometry

Fire stage	Heat flux density at the sample surface (kW/m²)	O_2 Oxygen Concentration (%)
Smouldering Fire (SF)	CHF – 5	21 %
Well Ventilated Fire (WVF)	50	21 %
Post Flashover Fire (PPF)	75	15 %
CHF: Critical Heat Flux, critical flux for ignition		

C.2.3 Quantification of source term (calculations)

For this part of the methodology, any CFD software capable of simulating combustion, trace species propagation and outputting data on the concentrations, temperatures and radiative fluxes can be used.

To incorporate the various combustion regimes and the associated species production spectra, it is possible to assign a tracer species for each fire regime existing in the fire scenario.

In actual fire models, each stage could therefore be characterized by a tracer species specific to the regime, and which does not interfere with the other aspects of the CFD calculation and the combustion. This tracer species is produced only when the fire stage, which it represents is reached, and at a mass production rate corresponding to the mass loss rate linked to the heat release rate of the fire source by the enthalpy of combustion. An example with three fire regimes and three tracer species is shown in Figure C.4.

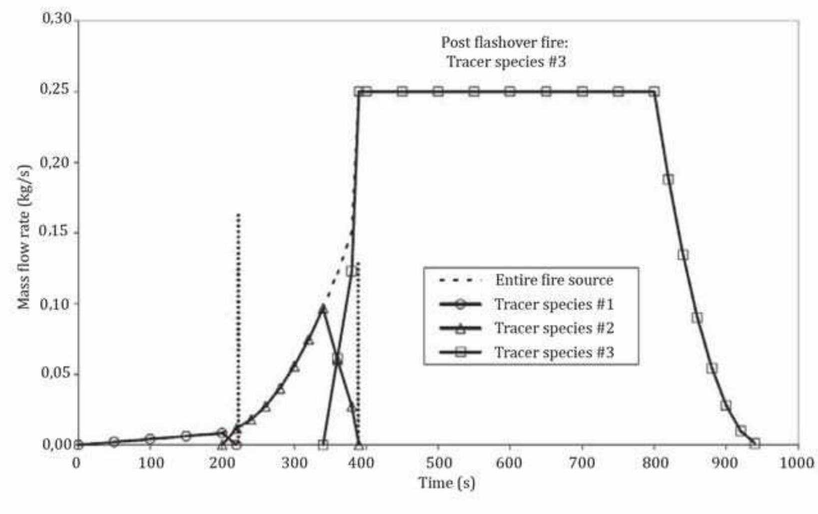

Figure C.4 — Tracer species mass production rate

All these tracer species follow the gas movements as calculated by the CFD software used and it therefore becomes possible to determine the concentration of each tracer species at any point in space and for each time step used. The concentration in actual gaseous species is then calculated by simple linear combination.

Example for carbon monoxide, CO:

$$[CO]_{(x,y,z,t)} = [Tracer_{SF}]_{(x,y,z,t)} \ x\ CO_{SF.room} + [Tracer_{VWF}]_{(x,y,z,t)} \ x\ CO_{VWF.room} + [Tracer_{PFF}]_{(x,y,z,t)} \ x\ CO_{PFF.room}$$

where:

$[CO]_{(x,y,z,t)}$ designates the carbon monoxide concentration (kg·kg^{-1}; kg of CO per kg of atmosphere) at time t and point x, y, z

$[Tracer_{SF}]_{(x,y,z,t)}$ designates the atmospheric concentration of the tracer species which represents the smouldering fire regime (kg·kg−1; kg of tracer species per kg of atmosphere) at time t and point x, y, z

$[Tracer_{VWF}]_{(x,y,z,t)}$ designates the atmospheric concentration of the tracer species which represents the well ventilated fire regime (kg·kg−1; kg of tracer species per kg of atmosphere) at time t and point x, y, z

$[Tracer_{PFF}]_{(x,y,z,t)}$ designates the atmospheric concentration of the tracer species which represents the post-flashover fire regime (kg·kg−1; kg of tracer species per kg of atmosphere) at time t and point x, y, z

$CO_{SF.room}$ designates the carbon monoxide production rate in the species production matrix for the room for the smouldering fire regime (kg·kg−1; kg of CO produced per kg of burned matter)

$CO_{VWF.room}$ designates the carbon monoxide production rate in the species production matrix for the room for the well-ventilated fire regime (kg·kg−1; kg of CO produced per kg of burned matter)

$CO_{PFF.room}$ designates the carbon monoxide production rate in the species production matrix for the room for the post-flashover fire regime (kg·kg−1; kg of CO produced per kg of burned matter)

The same type of equation applies for all the gaseous species considered in the model.

The data output from this step are:

— The spatial-temporal cartography of the gaseous species concentrations for consideration of the toxic effects

— Spatial-temporal cartography of the temperature of the gases and radiative fluxes, for consideration of the thermal effects

C.3 Evacuation

Knowing the cartography of the elements generating effects on people, it becomes possible to calculate the evacuation scenarios according to ISO/TR 16738. Two types of tools could be used to estimate evacuation calculation (time and route).

The first type covers the analytical formulas as described in Reference [26] and which include:

— Time for detecting the fire

— Pre-movement time

— Time to move to reach a zone of relative or absolute safety (in the case of a zone of relative safety, other times will need to be included for reaching a zone of absolute safety)

The CFD calculation results make it possible to get the thermal, toxic and visibility effects at each point in space and time. These can have an impact on the evacuation path and speed and should therefore be considered[8].

It is also important to include the behavioural aspects, especially those of group affiliation, precedence, etc. which have a notable impact on the evacuation. Further, Reference[26] reports that behaviour in the face of fire and smoke is complex and balances the perception of danger against the estimated ability of reaching an exit through exposure to that danger. Thus, despite the knowledge of the dangers connected with smoke, a large portion of people in an evacuation situation persists in crossing the smoke-filled zones they encounter. Reference[26] therefore reminds that people are often prepared to have to cross smoke, and that the percentages found by experience range from 60 % in small residential buildings to about 95 % in the case of the bomb attack on the World Trade Center in 1993.

Two main reasons are discussed:

— Knowing that smoke is dangerous does not correspond to knowing how to correctly evaluate the danger level;

— The fact of knowing that a nearby exit is beyond the smoke-filled zone is sufficient motivation for driving a behaviour of attempting to cross through it.

Other sources of information concerning human behavioural responses to fire and smoke could be found in References[27],[28] and[29]. Reference[30] states also that typically when people state that they panicked, that just means that they were scared, but not that they became crazy or irrational.

The second type of tools covers the numerous software packages for evacuation calculation, which may or may not be coupled to CFD calculation software in order to measure evacuation times. It should be noted that these enable a parametric approach by testing for a given evacuation strategy many evacuation scenarios by using populations selected and placed randomly in the various rooms accessible to people in the building study. It should however be kept in mind that the software do not all operate on the same scientific bases and can lead to different results.

The output data from this step is the one or more evacuation scenarios allowing access to the positions of people as a function of time.

C.4 Conclusions

The methodology example proposed in complement to ISO 23932 above makes it possible to consider toxicity in fire safety engineering studies, incorporating:

— Extensive number of gaseous species, modularly, enabling subsequent development if necessary

— All the combustibles with characteristic concentrations as a function of the fire regimes and fire scenarios

— Dispersion of species locally and at a distance by CFD calculation, for determining $[tox_i; therm_i] = f(x,y,z,t,i)$

— Thermal effects and visibility

— Evacuation scenarios incorporating the results of the CFD step

This methodology makes it possible to deduce all of these data from more realistic exposure scenarios and to evaluate instantaneous effects and the effects from accumulation of toxic species and thermal stress during the evacuation phase using the thermal and toxic models from the ISO 13571 standards.

However, it remains a simplified representation of the conditions encountered in a fire situation. Its modular structure will make it possible all the same to improve the incorporation of the fire's effects, as knowledge improves and data accumulates.

Thus:

— Additional gases can be simply introduced in the species production matrix by adding new rows

— The fire steps can be more detailed, including sub-phases for incorporating more finely the power rise of the fire source and the recruitment of new materials. The matrices can accept as many columns as necessary for processing very detailed scenarios.

— Similarly, the species production is currently correlated to the heat generation rate and could therefore need to detail more finely the fire scenarios steps to incorporate the propensity of certain species to be released early for example.

— Models incorporating effects are separated from other parts of the methodology and can therefore be refined independently. The same is true for the evacuation.

Some improvements could also be undertaken with the improvement of calculation means: the strong coupling evacuation/fire development is an example of this. For now remaining in the research domain and impractical for routine use because of the statistical considerations that go with this problem and the calculation time, this coupling nonetheless remains a long term objective and one for which it is appropriate to prepare solid bases now.

Annex D
(informative)

Example of application to Fire Safety Engineering–Case Nr 1 – hotel room and corridor

D.1 Description of case study

Annex D presents the application of the methodology to a practical case. The choice fell to a fire impact study in a hotel type building. The hotel has a set of standard dimension rooms served by a central corridor.

D.1.1 Hotel room

The room occupies about 22 m^2. The measured dimensions are about 6,75 m × 3,30 m by about 2,70 m under ceiling height. For the purposes of the simulation, done with a 0,20 m resolution, these dimensions are rounded to 6,80 m × 3,20 m × 2,80 m.

The room includes a bathroom and CMV equipped toilets. It includes:

— A single 1,3 m × 1,8 m window whose lower part is about 0,6 m above the floor. For the purposes of the simulation, in terms of resolution, these dimensions are rounded to 1,40 m x 1,80 m

— A 0,85 m × 2,0 m door opening onto the corridor. For the purposes of the simulation, in terms of resolution, these dimensions are rounded to 0,80 m x 2,00 m

Together the furniture represents a heat release load of about 10 000 MJ (evaluated on the basis of the LHV), mostly from particleboard (whose enthalpy of combustion, ΔH_c, is about 16 800 kJ/kg). The heat release load per unit surface area is about 460 MJ/m^2.

D.1.2 Corridor

Corridor dimensions are 20 m × 1,6 m. In compliance with smoke control classical design, it is equipped with an air supply opening and an air extraction opening.

The room door is located in the middle of the corridor, centred at 10 m from corridor extremity.

D.1.3 Comfort mechanical ventilation – AHU

The bathroom and also the toilets are equipped with CMV (15 m^3/h each). The room portion is equipped with an AHU (30 m^3/h supply, high up). According to various regulations, the AHU is stopped upon detecting a fire (the opinion is that it does not contribute to smoke removal). Since firebreak caps were very rarely seen, it was thought that the CMV continues to run after the fire starts (continuous operation of the fan).

D.1.4 Smoke control

Hypothesis is made on a typical hotel which is equipped with a fire safety system. Triggering the fire alarm can be time delayed; the triggering of an actuated fire alarm is done without time delay. Therefore in the corridor, extraction is started upon detecting the fire.

Its flow rate is equal to 0,5 m^3/s per actual exit unit. The corridor has a width of 1,60 m, there are two actual exit units, and hence a volumetric flow rate of 1 m/s^3 between an air inlet opening and an extraction opening. The two openings are arranged:

— One at about 2,5 m from the beginning of the corridor

— The other at about 17,5 m.

D.1.5 Smoke detectors

In the corridors: the first detector is installed 5 m from the end and then every 10 m to 12 m. In the rooms: if the surface area is < 80 m^2, then there is one detector, otherwise one per 60 m^2. In the case being studied, two detectors are therefore placed in the corridor at 5 m and 15 m.

D.1.6 Summary

The rooms described above (room + corridor) have been modelled using FDS software version 5. Figure D.1 shows a view of the rooms being modelled.

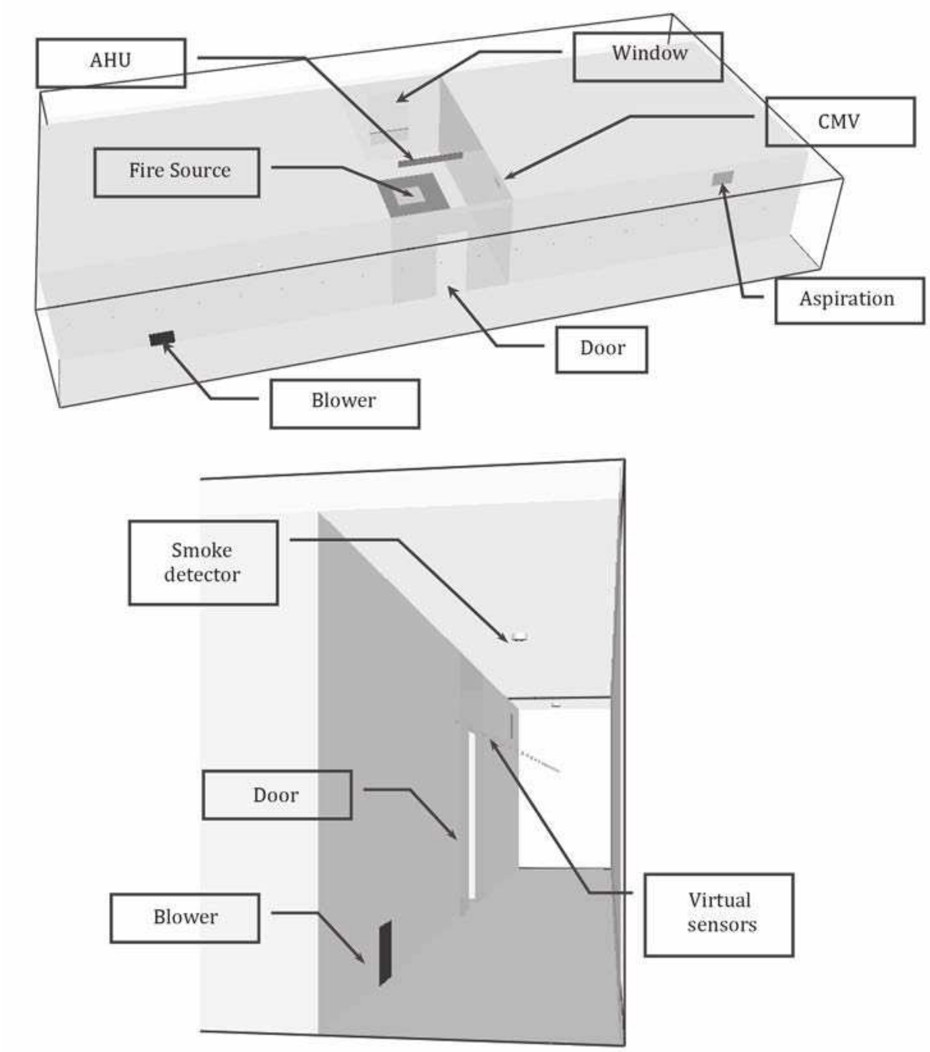

Figure D.1 — General- and closed-up views of the room and the corridor

D.2 Performance criteria

A limit value of 0,3 for FEC, FED_{toxic} and $FED_{thermal}$ according to ISO 13571 is chosen as reference for determining the success or failure of a given evacuation scenario.

D.2.1 Risk analysis

Out of concern for simplification in the context of this sample application, a single scenario is studied, which has not been the subject of a complete risk analysis on an existing hotel. The selection of the fire scenario was made among the typical scenarios coming from a generic risk analysis.

Table D.1 — Selected scenario for hotel room example case

Fire source	Scenario	Comments
Well ventilated fire leading to a flash-over	Scenario S2c	Risk evaluated in the courtroom

The scenario considered here (See Table D.1) is an intentionally set fire. In a rented room, an occupant sets fire to the mattress and then flees after blocking the door open which thereby enables the supply of the fire source with oxygen (in addition to that from the AHU) and the propagation of the effluents to the central corridor. The fire next spreads to adjoining items, thereby involving other materials, and then gradually spreads to the entire room. Upon detection of smoke in the corridor, the AHU is cut, but not the CMV.

D.3 Construction of the fire source kinetics

In light of the scenario considered, the source fire source is broken down as follows:

— Growth with $\dot{Q} = \pm.t^2$ until reaching $\dot{Q}_{FO}$ (heat release rate at flashover calculated per McCaffrey, resolutions per various authors, and if compatible with $\dot{Q}_{MAX}$ calculated with only the door being open, by the method of Petterson).

— At flashover, the window glass breaks and sudden growth from $\dot{Q}_{FO}$ to $\dot{Q}_{MAX}$ (post-flashover heat release rate calculated per Petterson formula, door and window open)

  — Combustion time according to the available heat release load (with 80 % combustion efficiency)

— Extinction (with inverted $\dot{Q} = \pm \times t^2$, rapid)

  — ΔH_c function of the combustibles present (tabulated)

  — Calculated rate of toxic species production changing for the various phases of the fire

NOTE In the state-of-the-art, there is no reliable criterion that makes it possible to determine the moment when breakage of the window glass occurs. First, it depends on many parameters, and second, with constant parameters, the glass breakage is not repeatable. The glass breakage proposed here is therefore the result of a reasonable assumption, which it would be appropriate to look at in detail earlier in an actual study

D.3.1 Growth $\dot{Q} = \pm \times t^2$

In the scenario studied, the value selected is that of the polyurethane mattress, with α = 0,0469 kW/s².

D.3.2 Maximum release rates, $\dot{Q}_{MAX}$ Petterson method

According to the Petterson method, $\dot{Q}_c = 0,09 \cdot A_W \times \sqrt{H} \times \Delta H_c$

In the case of an expert report prepared for real hotel room, the total heat release load was about 10 000 MJ, for about 600 kg combustible material which represents about 16 700 kJ/kg. The ratio between LHV (used for calculating the heat release load) and the chemical combustion enthalpy is on average about 0,7. The enthalpy of combustion selected is therefore about 11 800 kJ/kg.

Under these conditions, and including the door and window as defined above:

— With door alone: $\dot{Q}_{MAX}$ = 2 596 kW or 2,6 MW

— With door and window (after flashover occurs): $\dot{Q}_{MAX}$ = 5 924 kW or 5,9 MW

D.3.3 Heat release rate at flashover per McCaffrey

The heat release rate necessary to lead to flashover is calculated by McCaffrey's method according to the solution of various authors, as stated in Table D.2.

Table D.2 — Heat release rate necessary for flashover, solution according to different authors

Solution	Heat release rate necessary for flashover	Waiting time ($\alpha \cdot t^2$ curve)
Thomas solution	1,7 MW	190 s
Drysdale solution	2,8 MW	244 s
Peacock solution	3,4 MW	269 s
Hägglund and Babrauskas solution	2,2 MW	216 s

The values calculated here are compatible with the maximum rate calculated with door alone. Therefore a flashover does occur, the window breaks at that moment and a rise from $\dot{Q}_{MAX}$ (door only) to $\dot{Q}_{MAX}$ (door + window).

D.3.4 Decline $\dot{Q} = \pm \times (t_f - t)^2$

The value selected for ± is the largest sign of rapid decline, once a majority of the fuel has been exhausted, or 0,1876 kW/s^2. Under these conditions, the decline lasts about 3 min (178 seconds).

D.3.5 Length of the plateau

Considering the value chosen for α, the growth period, from 0 s to $\dot{Q}_{MAX}$ (door open) takes place in about 235 s. Total energy released by the combustion is then about 204 MJ (obtained by integration of the heat release rate over the interval [0 ; 235 s]). Similarly, the decline from $\dot{Q}_{MAX}$ (door + window) to 0 kW is done in about 178 s and represents about 351 MJ. The rise from $\dot{Q}_{MAX}$ (door only) to $\dot{Q}_{MAX}$ (door + window), estimated to take place in 30 s, represents about 128 MJ.

The total heat load is about 10 000 MJ and the combustion efficiency considered is 80 %. There therefore remains about 7 300 MJ available for combustion during the flashover. Considering that the $\dot{Q}_{MAX}$ (door + window) was previously calculated at 5,9 MW, the plateau therefore lasts about 20 min.

D.3.6 Summary

The fire source thus calculated is characterized by the curve of Figure D.2. Schematically this fire is broken down into three phases:

— A first, well ventilated, growth phase from 0 s to 235 s principally involving a polyurethane mattress

— A second phase of rising to a flashover and then flashover, under ventilated, and involving all the materials in the room, and extending from 235 s to 1 470 s

— A third phase of well ventilated descent involving all the materials in the room and lasting from 1 470 s to 1 650 s

The total duration of the fire in the room (excluding any propagation outside) is therefore about 27 min 30 s.

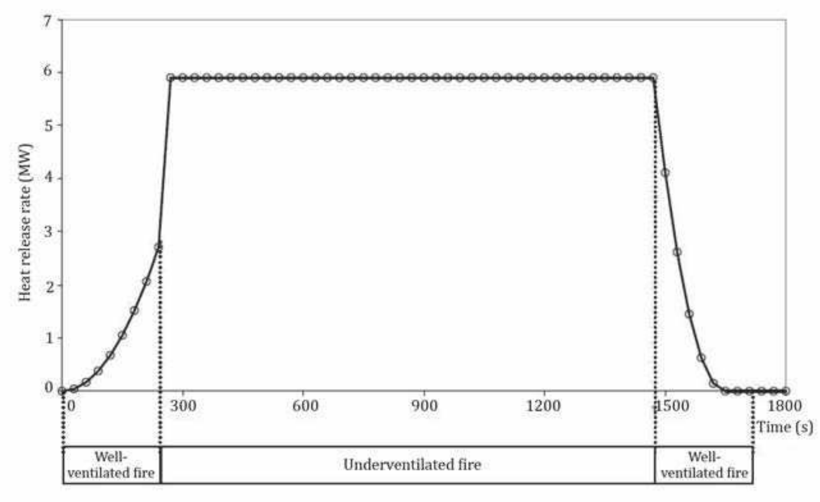

Figure D.2 — Heat release rate for the fire source of the hotel room

D.4 Determination of the fractions by mass of species produced

From Figure D.2, three fire stages can be separated. The species production matrix for each material will therefore include three columns, for which the first and third columns are equivalent, as shown in Figure D.3 below. Out of concern for simplification in this example, only five gases are concerned.

Material M	*Well Ventilated Fire (WVF1)*	*Post Flashover Fire (PPF)*	*Well Ventilated Fire (WVF2)*
CO	CO_{WVF}	CO_{PFF}	CO_{WVF}
CO_2	$CO_{2\ WVF}$	$CO_{2\ PFF}$	$CO_{2\ WVF}$
HCN	HCN_{WVF}	HCN_{PFF}	HCN_{WVF}
HCl	HCl_{WVF}	HCl_{PFF}	HCl_{WVF}
NO_2	$NO_{2\ WVF}$	$NO_{2\ PFF}$	$NO_{2\ WVF}$

Figure D.3 — Structure of matrix used in the example

Only the principal materials are considered in this example. They are listed in Table D.2. These materials represent more than 80 % of the overall heat release load. Without experimental data for these materials, measured according to the test conditions, the corresponding matrices have been determined in order to obtain combustible production rates compatible with the bulk formula of the materials and the ventilation conditions, all based on conservative assumptions.

Table D.2 — Main materials of the hotel room as a function of the heat release load

Material	Heat load	Proportion of the total heat load
Particleboard + melamine decoration (furniture, cabinets, etc.)	3 700 MJ	37 %
Wood (pine, oak, etc.; especially for box springs)	2 300 MJ	23 %
Polypropylene + Latex (carpet backing) polyamide (area carpet)	900 MJ	9 %
Polyurethane (mattress, sofa, chair, etc.)	800 MJ	8 %
Loaded polyester (bathtub, bathroom elements)	500 MJ	5 %

The following assumptions are considered:

— Soot production was negligible Carbon normally consumed by soot is therefore available for production of CO, CO_2 and HCN and therefore leads to maximizing them.

— A significant portion of the nitrogen coming from the material is released in the form of molecular nitrogen, N_2[31]. Thus, in the cone calorimeter, values as low as about 3 % have been found. Also it is considered here that 10 % of the nitrogen initially present in the material is released in the form of NO_2 and HCN.

— In the branches applicable to the CO/CO_2 ratios depending on the ventilation conditions, the value selected is the one which tends to favour the production of carbon monoxide (CO) to the detriment of the less toxic carbon dioxide (CO_2). Thus:

  — Well ventilated fire: $[CO]/[CO_2] = 0{,}05$

  — Post flashover fire: $[CO]/[CO_2] = 0{,}4$

To determine the values necessary to establish the species production matrices in a practical manner, the following methodology was used:

— All the species produced (here there are five of them: CO, CO_2, HCl, HCN, and NO_2) share elements presents in the bulk formula of the material considered ($C_aH_bO_cN_dCl_e$). No part of these elements was considered to be linked to other gases.

— Since HCN enters into the balance for carbon and nitrogen, it was considered first. Thus:

  — The remaining nitrogen (N) will be entirely converted to NO_2.

  — The remaining carbon will be entirely converted to CO and CO_2 in the relative proportions obeying the ratio $[CO]/[CO_2]$ chosen for a given combustion regime.

— Without more precise information, the rate of release for HCN is determined as follows:

  — For the under ventilated fire (post-flashover), the value is extracted from databases for tube furnace tests on similar materials under air at 600 °C according to the NF X 70-100-1 and-2 standards. As an example, the average HCN production the polyurethane foam during these tests is 25 mg/g (25 mg of HCN produced from 1 g of material burnt). This assumption is based on the fact that the ventilation conditions in the tube furnace (air renewal at 2 l/min) are not sufficient for assuring a well-ventilated flame.

  — For the well ventilated fire: HCN is a product of incomplete combustion and seldom appears under conditions of sufficient ventilation[31]: Even if it is produced at the base of the flames, it is re-burnt and the final products are principally nitrogen oxides (NO_x). However it does not disappear completely because evening conditions of globally sufficient ventilation one can expect to find zones in the flame where the ventilation is not sufficient. Thus, to reflect this point, it is estimated that 1/10 the value used for the under ventilated fire is produced in a well-ventilated fire.

— The NO_2 concentration is calculated on the basis of the nitrogen remaining after consumption by HCN. Other nitrogen species are of course produced (notably NO_x and NH_3):

  — These other species are not considered in this example.

  — Using NO_2 as a substitute for the NO_x is conservative, as the critical concentrations for NO_2, is even well below those of NO[2].

  — The HCN value used come from tube furnace tests where many other nitrogen species besides NO_x and NH_3 are produced. Consequently, using the remaining nitrogen to calculate the concentration of NO_2 produced is conservative.

— HCl is calculated on the basis of the available chlorine.

— CO and CO_2 are calculated on the basis of the carbon remaining after consumption for the production of HCN, and in the relative proportions obeying the ratio [CO]/[CO_2] chosen for a given combustion regime.

It is clearly understood that the present methodology for calculating the levels of species produced is a simplified example relying on conservative assumptions. The representativeness of the values calculated by following this simplified methodology is not guaranteed, and therefore excludes applicability outside of this illustrative example.

The Figure D.4 presents the matrices obtained for the various materials:

Particleboard + melamine	Well Ventilated Fire (WVF1)	Post Flashover Fire (PPF)	Well Ventilated Fire (WVF2)
CO ($kg \cdot kg^{-1}$)	0,071	0,375	0,071
CO_2 ($kg \cdot kg^{-1}$)	1,427	0,939	1,427
HCN ($kg \cdot kg^{-1}$)	0,001	0,007	0,001
HCl ($kg \cdot kg^{-1}$)	0,000	0,000	0,000
NO_2 ($kg \cdot kg^{-1}$)	0,014	0,003	0,014

Wood	Well Ventilated Fire (WVF1)	Post Flashover Fire (PPF)	Well Ventilated Fire (WVF2)
CO ($kg \cdot kg^{-1}$)	0,076	0,401	0,076
CO_2 ($kg \cdot kg^{-1}$)	1,513	1,002	1,513
HCN ($kg \cdot kg^{-1}$)	0,000	0,000	0,000
HCl ($kg \cdot kg^{-1}$)	0,000	0,000	0,000
NO_2 ($kg \cdot kg^{-1}$)	0,000	0,000	0,000

Polypropylene + latex + polyamide (carpet)	Well Ventilated Fire (WVF1)	Post Flashover Fire (PPF)	Well Ventilated Fire (WVF2)
CO ($kg \cdot kg^{-1}$)	0,136	0,717	0,136
CO_2 ($kg \cdot kg^{-1}$)	2,717	1,792	2,717
HCN ($kg \cdot kg^{-1}$)	0,001	0,008	0,001
HCl ($kg \cdot kg^{-1}$)	0,000	0,000	0,000
NO_2 ($kg \cdot kg^{-1}$)	0,013	0,001	0,013

Polyurethane foam	Well Ventilated Fire (WVF1)	Post Flashover Fire (PPF)	Well Ventilated Fire (WVF2)
CO ($kg \cdot kg^{-1}$)	0,101	0,524	0,101
CO_2 ($kg \cdot kg^{-1}$)	2,014	1,311	2,014
HCN ($kg \cdot kg^{-1}$)	0,003	0,025	0,003
HCl ($kg \cdot kg^{-1}$)	0,000	0,000	0,000
NO_2 ($kg \cdot kg^{-1}$)	0,009	0,000	0,009

Polyester	Well Ventilated Fire (WVF1)	Post Flashover Fire (PPF)	Well Ventilated Fire (WVF2)
CO ($kg \cdot kg^{-1}$)	0,121	0,639	0,121
CO_2 ($kg \cdot kg^{-1}$)	2,413	1,598	2,413
HCN ($kg \cdot kg^{-1}$)	0,000	0,000	0,000
HCl ($kg \cdot kg^{-1}$)	0,000	0,000	0,000
NO_2 ($kg \cdot kg^{-1}$)	0,000	0,000	0,000

Figure D.4 — Input data used in the example, for various materials

The data from the fire scenario making it possible to calculate the characteristic matrix for the room are given in the Table D.3.

— In the first part of the fire (setting fire to the mattress), only the polyurethane foam contributes significantly. The bed's box springs is also affected, but to a lesser extent.

— In the second part (post-flashover), all the materials contribute to the heat release load of the room, each according to its relative weight.

— In the last part (descent), all the materials contribute except for the mattress which, since it was the primary source of the fire, was completely consumed in the plateau phase.

Table D.3 — Contribution of the materials present, according to the stage of development of the fire in the room

Material	Growth + rising	Plateau	Descent
Particleboard + melamine decoration	0 %	47 %	50 %
Wood (pine, oak, etc.)	10 %	29 %	31 %
Polyurethane (mattress)	90 %	7 %	0 %
Polypropylene + Latex (carpet backing)	0 %	8 %	8 %
Loaded polyester (bathtub)	0 %	6 %	7 %
Polyamide (carpet)	0 %	4 %	4 %
Total	**100 %**	**100 %**	**100 %**

All of these contributions are calculated for compatibility with the heat load, which represents:

— Each of the development stages of the fire (consumption);

— Each of the materials (contribution).

With the assignment of these proportionality factors, it is possible to calculate the species production matrix for the room using the following formula:

$$[\ ]_{Room} = \sum_{i=1}^{n} P_{(i,SF)} \times [\ ]_{M_i} \begin{bmatrix} 1 \\ 0 \\ 0 \end{bmatrix} + \sum_{i=1}^{n} P_{(i,WVF)} \times [\ ]_{M_i} \begin{bmatrix} 0 \\ 1 \\ 0 \end{bmatrix} + \sum_{i=1}^{n} P_{(i,PFF)} \times [\ ]_{M_i} \begin{bmatrix} 0 \\ 0 \\ 1 \end{bmatrix}$$

This is the resulting matrix for the hotel room, as stated in Figure D.5.

Room	Well Ventilated Fire (WVF1)	Post Flashover Fire (PPF)	Well Ventilated Fire (WVF2)
CO (kg·kg^{-1})	0,098	0,449	0,084
CO_2 (kg·kg^{-1})	1,964	1,122	1,679
HCN (kg·kg^{-1})	0,002	0,006	0,000
HCl (kg·kg^{-1})	0,000	0,000	0,000
NO_2 (kg·kg^{-1})	0,008	0,001	0,008

Figure D.5 — Matrix for the whole hotel room

The HCN value at the post flashover fire stage is 0,006 kg.kg^{-1}, which could seem low in comparison with the value 0,025 kg.kg^{-1} assigned to the polyurethane foam for this phase. However, it only contributes 7 % to the release of species at this stage of the fire (compared to 90 % in the first phase), and this value, which appears to be low, does not mean a low production in terms of total quantity released. In fact, the heat release rate is much greater in the post flashover phase of fire than in the first phase, and the mass production rate of gas is therefore also higher. From this it follows that the total HCN production does follow the quantity likely to be released by the polyurethane foam (and the other HCN contributors).

As an example, the CO_2 value for the well-ventilated fire WVF1 is calculated in the following way

— 10 % contribution from the wood, with a production rate of 1,573 $g.g^{-1}$

— 90 % of the polyurethane foam with a production rate of 2,014 $g.g^{-1}$

It follows that $[CO_2]_{WVF1}$ = 0,1 × 1,573 + 0,9 × 2,014 = 1,964 $g.g^{-1}$.

This matrix calculated for the room makes it possible to now calculate, as a function of the quantity of each tracer species measured at one point and one moment, the final quantity for each of the gases considered.

D.5 Evacuation and effects of the fire

The evacuation scenario in the selected example is deliberately simplified. This example considers two people who start their evacuation at different moments: The time referred to as pre-movement can in fact vary enormously according to the individuals, and the activities they were involved in at the moment the alarm sounds.

The first person who goes right through the corridor decides to leave 100 s after the fire starts, or about one minute after the fire alarm is triggered; this is very short and corresponds, for example, to an alert person who knows the area well, the fire instructions and the dangers inherent in this type of situation, and is not involved in an engrossing activity. Despite the quick reaction and the starting of the smoke removal device, the visibility conditions have already noticeably worsened (see Figure D.6). Also, the speed of the person is impacted, and speed of their movement is reduced to 0,5 $m.s^{-1}$[26].

The second person, which takes his same path, decides to do so much later. He starts to take the corridor at about 400 s, or nearly six minutes after the alarm sounds. Here again the visibility conditions have worsened (see Figure D.7) but not much worse than for the person who evacuated early. Also the same speed of movement, 0,5 $m.s^{-1}$, is used.

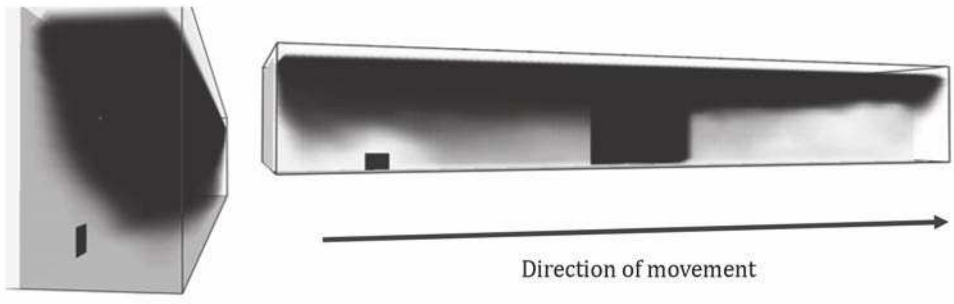

Figure D.6 — Worsening of the visibility in the corridor at t_0 + 100 s

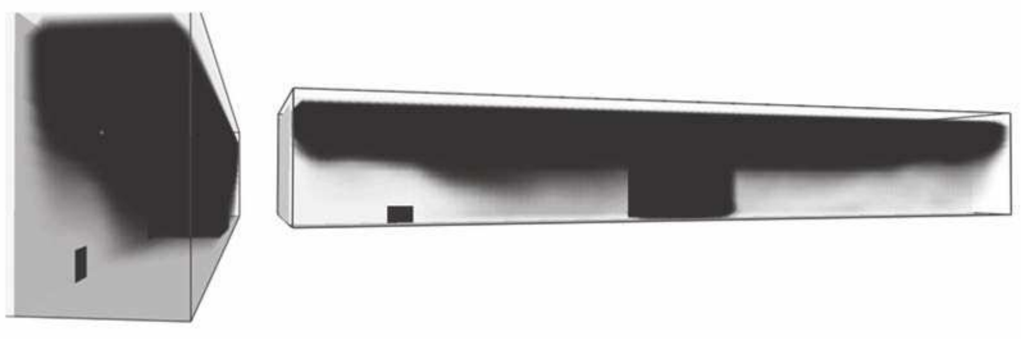

Figure D.7 — Worsening of the visibility in the corridor at t_0 + 400 s

Under these evacuation conditions, the trace species levels and the temperatures and characteristic flows, as encountered during the person's passage, are considered and the FED (asphyxiating and thermal) and FEC (irritating) are calculated continuously. The results are presented graphically in Figure D.8 (for beginning of evacuation at 100 s) and Figure D.9 (for beginning of evacuation at 400 s).

The first occupant who travels the corridor at t = 100 s does not encounter any specific difficulty until near the door: the fire has not yet reached flashover and the concentrations found in the corridor are due to the first phase of the fire. Since the conditions are well ventilated, there is relatively little CO and the $FED_{asphyxiating}$ is only rising slowly and remains well below the limit of one or even 0,3. While passing in front of the door, this person is subject to significant thermal effects, but not incapacitating: $FED_{thermal}$ undergoes a sudden rise at this point, but remains below 0,3. In contrast, this person is subject to a fairly significant concentration of irritating gases, which could compromise their evacuation. The FEC reaches 0,57, which is below 1, but above 0,3. Some people could be incapacitated at this point, and irritant effects are those who could compromise tenability.

The second occupant who travels in the corridor later is subject to a lower proportion of irritating gases: the FEC is systematically below that experienced by the first occupant. In fact at 400 s, the proportion of gas coming from the first phase of well-ventilated fire has become very small. These gases were transported away from the fire source and taken by the smoke removal ventilation. The residual concentration in the core door is low. In contrast, the gases coming from the second phase of the fire are very present. Hence, the first phase of the fire is, in proportion, a greater contributor of irritating gases (NO_2) than the second phase, which is characterized by a greater production of asphyxiating gases (CO, HCN). Close to the door, thermal ambiance is excessive and this criteria compromises the tenability first for this scenario.

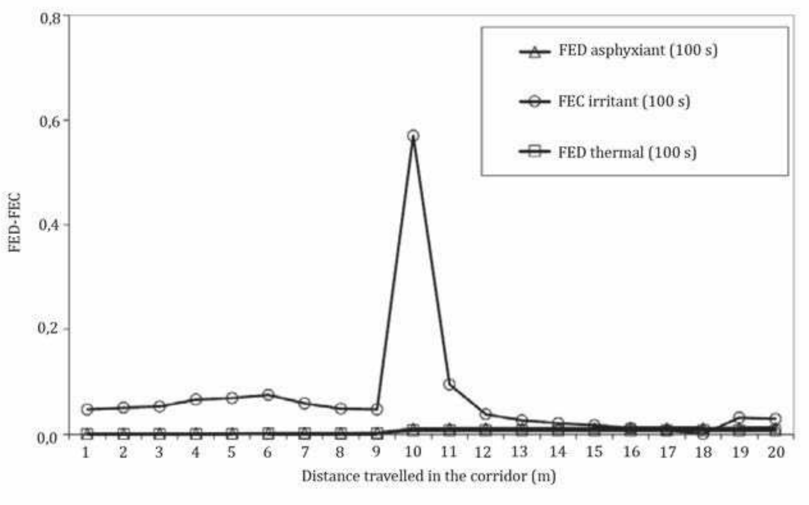

Figure D.8 — Progression of the FED and FEC according to distance travelled in the corridor – case of early start at t_0+100s

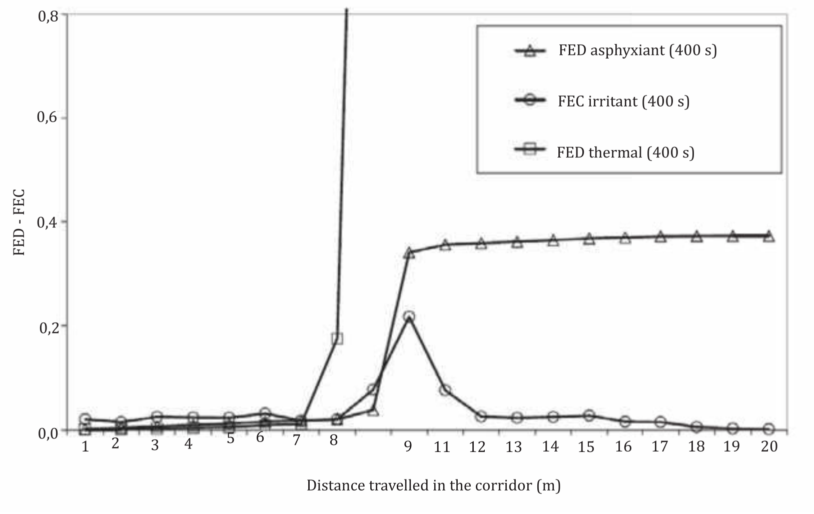

Figure D.9 — Progression of the FED and FEC according to distance travelled in the corridor – case of late start at t_0+400s

Furthermore, the evacuation as dealt with in these first two examples is partially decorrelated from the effects: only the visibility was briefly considered for adjusting the speed of movement of the two occupants considered. On the other hand, both occupants continued to move forward in the corridor, even if and including when the concentration of irritants and thermal effects experienced could have dissuaded them from it. This point remains however to be argued, as Reference [26] states that in most cases, people in an evacuation situation expect to have to cross smoke filled zones and even though they know that smoke kills will nonetheless pass through it. In fact knowing that smoke can prove deadly does not mean knowing how to estimate to what extent and further the knowledge of a nearby exit can prove a sufficiently strong motivation to venture into the smoke.

In order to study the effect of a change in behaviour linked to the quantity of smoke and the perceived effects, a new scenario is studied, considering that the occupant start to evacuate at 400 s, then decides to turn back and not cross the smoke perceived as very dense and not providing visibility into the condition of the corridor behind it. By making the assumption that the occupant decides to turn back even though the occupant has gone 6 m in the corridor, Figure D.10 presents curves obtained for the FED and FEC experienced by the occupant.

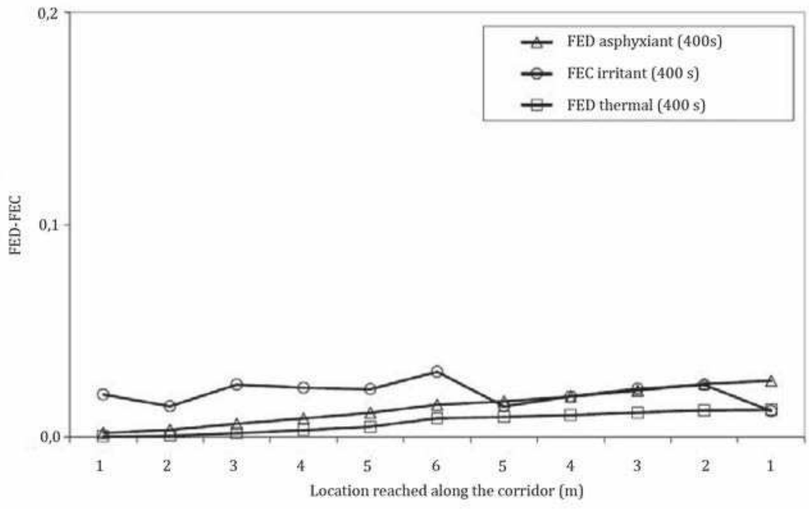

Figure D.10 — Progression of FED and FEC, according to point reached in the corridor – case of late start at t_0+400s and turn back after 6 m

Figure D.10 shows that the decision was beneficial for the occupant: the quantities of asphyxiants and irritants encountered are insufficient to cause incapacitation. Similarly, the thermal dose received stays far below the limit value of 0,3. The occupant would therefore be able to continue their evacuation towards another exit.

Note however, as emphasized above, this type of behaviour is not necessarily the most common despite being very suitable to the situation.

In Figure D.10, it is also appropriate to remark that the $FED_{thermal}$ progresses less quickly than $FED_{asphyxiating}$. This point supports the fact that when one is sufficiently far from the fire source to not experience its direct thermal effects (convective and radiative), then the danger related to smoke toxicity becomes dominant.

Annex E
(informative)

Example of application to Fire Safety Engineering – Case Nr 2 – restaurant

E.1 Introduction

This annex presents the application of the methodology to a second practical case. Only in this sample application the scenario of a fire in the dishwashing room at this restaurant, located in immediate contact with the public, is considered. Furthermore, only the main rooms are given in detail.

E.2 Properties of the rooms

The restaurant has an entry hall leading into the "scramble", a zone where the plates, meal trays and table settings are laid-out. The restaurant has a kitchen block opening onto the scramble and a dining room which has a total surface area of about 570 m^2. The cash registers are located at the interface between these two zones. The room studied in this example is the laundry room, in direct contact with the dining hall, and in the area surrounding it the trays are arranged on a conveyor system at the end of the meal. Numbers on Figure E.1 indicate escape routes.

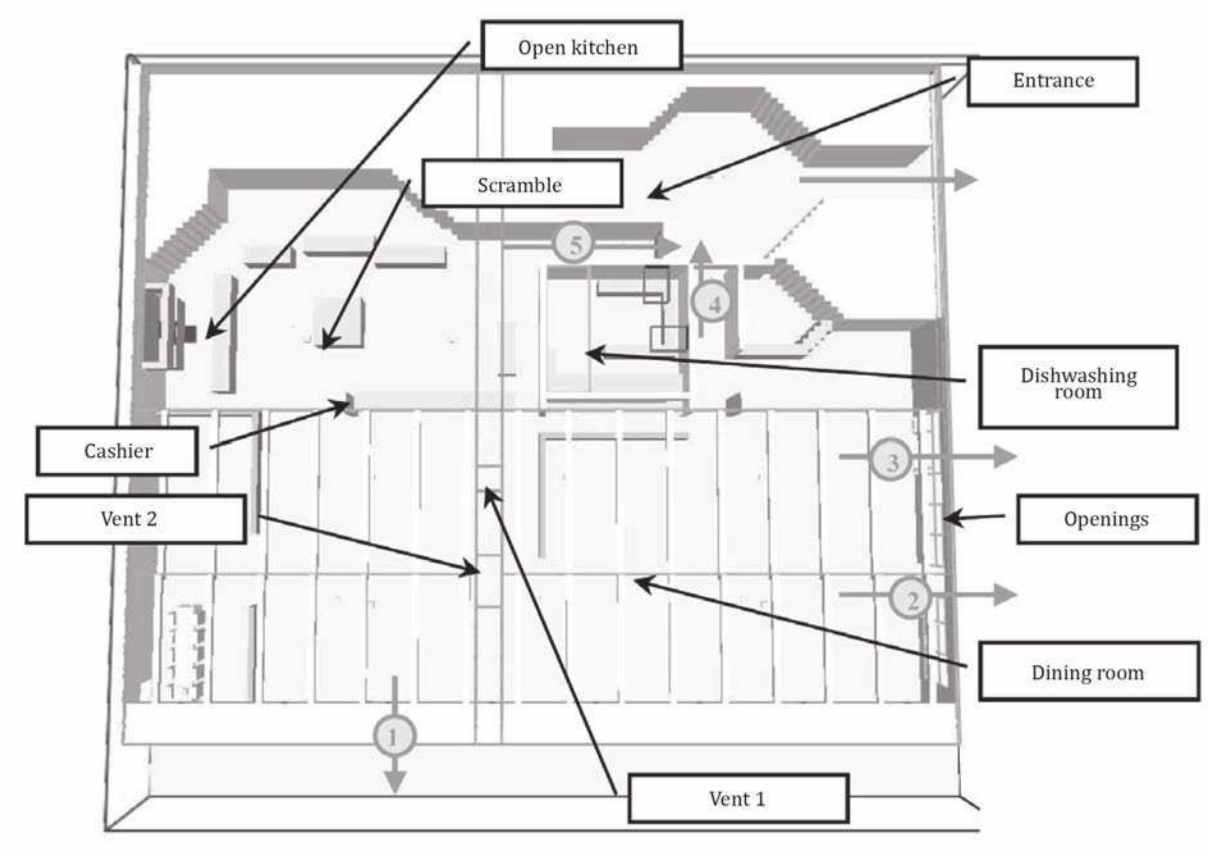

Figure E.1 — Plan the restaurant being studied – Ground-floor

E.2.1 Dishwashing room

The dishwashing room is 5,75 m × 5,25 m with a height under the ceiling of about 2,70 m. The extraction hoods which are there serve both for extraction of steam and smoke removal because they are equipped with a smoke removal blower with a minimal resistance of 400 °C for two hours with a protected power supply. The extraction is done with a nominal flow rate of 3 500 m^3/h. The blower is implemented in the upper part with a flow rate of 3 000 m^3/h. Apart from the door to the room, which is closed during service, the only opening is the tray pass-through which is 0,75 m × 0,75 m and located at a height 1 m above the ground.

E.2.2 Open kitchen

The open kitchen has smoke removal at a rate of 6 500 m^3/h, through cooking steam evacuation hoods and is also equipped with a 400 °C-two hours smoke removal blower with protected power supply. It is separated from the dining room by a ceiling screen with a height of more than 50 cm.

E.2.3 Dining room

The dining room has a surface area of 570 m^2 and a height under the ceiling varying from 3,25 m to 3,50 m. The long axis of the dining room is about 32 m. It has:

— three smoke removal openings with dimensions of 0,59 m × 1,12 m

— two vents with respective dimensions of 1 m × 1 m and 2 m × 1 m

The smoke removal openings are located on the right façade of the building.

Additionally, this dining room is equipped with a Air Handling Unit (AHU) delivering a flow rate of 9 000 m^3/h. Air circulation is provided in the upper part of the room by:

— 16 blower vents (eight vents of 0,036 m^2 and eight vents of 0,26 m^2)

— two extraction vents with 0,325 m^2 geometric surface area and one extraction vent (café space) with 0,16 m^2 geometric surface area

E.2.4 Grid

The grid used in the simulation is a homogeneous cubic Cartesian grid, whose unit cells are 25 cm on a side. In full rigor, the influence of this grid should have been studied to evaluate the impact on the final result. However, considering that the fire sources used are imposed standard fire sources (in contrast to fire sources with calculated development), this resolution is suited for the study of the movement of the smoke and gas released. The grid is therefore made up of about 300 000 unit cells.

E.3 Performance criteria

According to ISO 13571, a limit value of 0,3 for the FEC, FED_{toxic} and $FED_{thermal}$ is chosen as reference for determining the success or failure of a given evacuation scenario.

E.4 Risk analysis

The risk analysis enable to uncover several areas of this restaurant which could present an immediate risk to the public. Out of concern for simplification in the context of this sample application, a single scenario is studied, which is that of fire starting in the dishwashing room of the restaurant, identified as one of the two significant scenarios in the initial study[15]. This scenario is described in Table E.1.

Table E.1 — Selected scenario for example case 2

Fire source	Scenario	Comments
Well ventilated fire leading to a flashover	Scenario S2c	Risk evaluated outside of the dishwashing room

The main equipment for this room is the washing machine which has three paths over which the baskets carrying the trays, plates and table settings move. These paths have polyamide rollers (about 40, for a total of about 70 kg of material). The interior of the machine comprises electronic cards in epoxy and cables and conductors in polyolefin conduits. The mass involved is however minor compared to the other combustibles.

The washing baskets are polypropylene. The meal trays are fibreglass reinforced polyester. Other combustible materials are present in the room in minor quantities (food waste, trash bags, etc.); most of the furniture is stainless steel for obvious reasons of hygiene and ease of maintenance. The washing baskets are stored high on a shelf located above one of the washing machine paths, and represent about 30 kg of combustible material. The meal trays are nearby (about 20 kg combustible material).

It should be noted that the kitchen staff is not continuously present in this room. A fire breaking out could therefore benefit from some lapse of time before being discovered.

The following is therefore the selected fire scenario:

— Following a machine failure in the absence of personnel, the electric elements overheat and lead to the ignition of the initial fire source.

— This initial fire source propagates to the polypropylene baskets immediately involved and propagates from basket to basket at a moderate speed. The polyamide rollers participate in the combustion as the fire source extends. The heat release rate increases.

— Because of the nature of the combustibles from the tray carriers (thermofusible polypropylene) the fire gives rise to the appearance of an inflamed layer. The rise in power of the fire source accelerates.

— At this stage, the FPETOOLS 2.0 fire simulator tool from NIST indicates the possibility of a flashover occurring in this room in consideration of the characteristic parameters of the room (combustible, ventilations, geometry, etc.) At this moment:

— The maximum heat release rate depends on the supply of combustion agent, and therefore on the ventilation (mechanical ventilation in presence of the opening). It should be noted that the mechanical ventilation for this room, which participates in the smoke removal, does not stop during the entire time of the fire.

— Length of the combustion depends on the quantity of combustible and the available services.

— The end of the combustion is reached when the majority of combustible is exhausted

— Considering the heat release load present and the length of the incident resulting from it (less than 15 min.), the closed-door to the dishwashing room is considered to resist the fire and therefore remain closed during the entire length of the fire. Furthermore, since no combustible material outside the room was at a sufficiently short distance for it to have propagated, the fire remains enclosed in the dishwashing.

It should be noted that in the restaurant:

— The AHU for the dining room and the washroom, and also the washroom and grill hoods, which have a blower resisting 400 °C for two hours, operate at high speed the entire duration of the fire. No emergency cutoff device is provided for stopping their operation in case of triggering natural smoke removal.

— The vents, openings and/or units leading to the outside are actuated or open 2 min 30 s after the start of the fire (detection time + time preparing for movement + travel time for the first people arriving at the doors, and the staff at the vent and opening actuating system).

— The door on the cafeteria side is more directly impacted by the smoke so it is considered that it is restricted to never being opened.

E.5 Construction of the fire source kinetics

Here, Petterson method used in the previous application example cannot be used as is because of the presence of mechanical ventilation. The system encountered here is complex, because it has:

— A forced air supply using mechanical ventilation with an entering flow rate of 3 000 m^3/h;

— A forced extraction with an exiting flow rate of 3 500 m^3/h;

— A passive opening (the tray pass-through) located 1 m above the ground and whose size is 0,75 m × 0,75 m.

Considering the temperature rise because of the fire source, the density difference of the hot air extracted relative to the fresh air supplied, the two mechanical ventilation systems and the passive opening, the system is beyond a simple analysis. As an alternative to the analytical methods previously used, the source fire source will therefore be entirely determined using zone type simulation software. Since the room is likely to go from a two-zone situation (hot layer and cold layer) to a one-zone situation (room overcome with smoke), Ozone software for the University of Liège is chosen.

E.5.1 Fire source features

The data to be supplied to the Ozone software to define the fire source are:

— The fire source growth factor, seen previously

— The maximum surface area affected by the extension of the fire source

— The maximum heat release rate per unit surface area

— The heat release load per unit surface area

— The average enthalpy of combustion

— The combustion efficiency

— The combustion model

E.5.2 Growth $\dot{Q}$ = ±×t²

In the scenario studied, the value selected for α is that corresponding to polyurethane pallets, which are similar in chemical nature and arrangement to the polypropylene tray carriers present in the dish washing room, in other words α = 0,0469 kW/s^2.

E.5.2.1 Maximum surface area affected by the extension of the fire source

Considering the formation of a flaming pool due to the polypropylene tray carrier, and the placement of the washing machine in the room (in U-shape), the assumption of a maximum surface area of 15 m^2, which is half of the room, seems to be a reasonable assumption.

E.5.2.2 Maximum heat release rate per rnit rurface

The maximum heat release rate used is 500 kW/m^2: this value is the high-end value for the range currently used for smoke removal studies. In fact, the combustibles present are highly energetic.

E.5.2.3 Heat release load per unit surface area

All of the materials in total have a heat release load of about 3500 MJ. This heat release load is distributed over the entire surface extent of the fire source, which is 15 m^2. The factor $^{3}{}_{q,1}$ introduced by Ozone at this stage, and which has the value 1,15, is incorporated in the calculation. The heat load per unit surface area is then about 205 MJ/m^2.

E.5.2.4 Average enthalpy of combustion

The calculation of the average enthalpy of combustion is done by using the data stated in Table E.2. The average (weighted) heat of combustion resulting from these data are about 30 MJ/kg.

NOTE The heat of combustion depends on the conditions under which the combustion takes place and therefore varies according to the regime reached. The value calculated here, and assumed constant, it is therefore useful to give an indication.

Table E.2 — Heat of combustion for the principal materials involved in the fire source

Material	Mass (kg)	Heat of combustion (chemical) (kJ/kg)
Polyamide	70	27 950
Polypropylene	30	37 700
Polyester/fibreglass	20	22 440

E.5.2.5 Combustion efficiency

This parameter makes it possible to corporate the difference which exists between the heating power which is determined with a calorimetric bomb and the actual enthalpy of combustion observed in a given combustion regime.

The enthalpy of combustion calculated in the previous chapter already incorporates this parameter. Thus the value of 80 % supplied by default by the software is to be replaced by the value 100 %.

E.5.2.6 Combustion model

Three combustion models are available in the software Ozone used:

— *No Combustion,* in which no influence of the ventilation is considered and principally applicable when the heat release rates and the mass loss have been measured.

— *External Flaming,* in which the influence of the ventilation is considered, but does not limit the mass loss flow rate associated with the heat release rate. Additional combustion takes place outside of the enclosure.

— *Extended Duration,* in which the influence of the ventilation is considered and limits the mass loss rate and heat release rate, leading to a modification of the length of the fire in the room.

In reality, the pyrolysis rate is linked both to the oxygen availability and the net quantity of energy transferred to the materials. Also, it's the *Extended Duration* model which seems best suited to the physical reality of the fire in this room.

E.6 Calculation of the heat release rate

The fire source calculated by Ozone is characterized by the Figure E.2. The progression of the oxygen concentration in the room, assumed uniform, makes it possible to identify the different combustion regimes:

— Between 0 and 220 s, the oxygen concentration is above 15 %, the combustion regime is well ventilated.

— After 220 s, the oxygen concentration drops below 15 % and the combustion regime enters an under ventilated phase.

— At 270 s, flashover conditions are reached in the room and the heat release rate increases dramatically.

— Starting at 990 s, the oxygen concentration returns above 15 % and the combustion regime returns to a well ventilated phase.

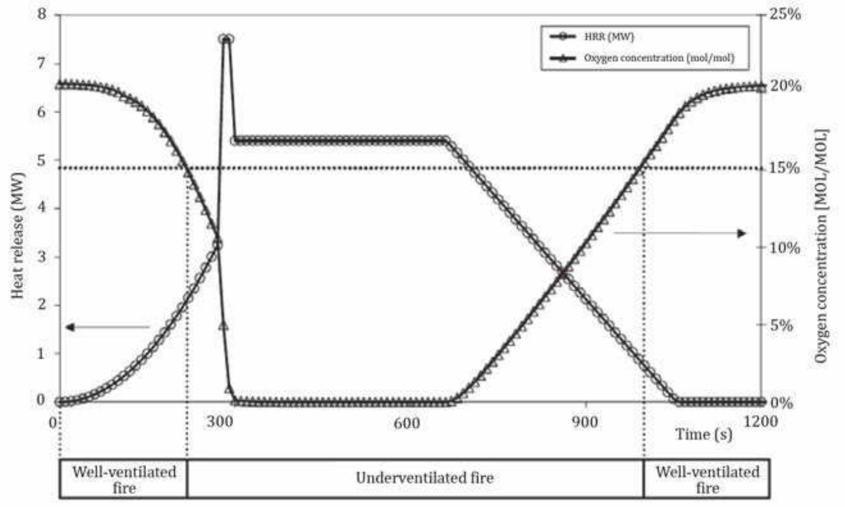

Figure E.2 — Heat release rate and oxygen concentration for the fire source in the dishwashing room

E.7 Participation of the materials, phases of the fire source

According to the scenario given above, the Table E.3 presents materials involved in fire as function of time. Considering the development of the fire, the following assumptions are made:

— Polypropylene trays contribute especially to phases 1 and 2, and relatively less to phase 3 since the majority of the polypropylene has already burned in the earlier phases.

— The polyamide rollers contribute significantly more in phase 3 than in phases 1 and 2.

— Polyester/fibreglass trays only contribute when flashover is reached, meaning starting with phase 3.

Table E.3 — Phasing of the fire source, dishwashing room

Phase	Time	Materials	Combustion
1	from 0 to 220 s	Polypropylene trays Polyamide rollers [a]	Well ventilated, growth stage
2	Between 220 and 270 s	Polypropylene trays Polyamide rollers	Under ventilated, growth stage
3	Between 270 and 990 s	All materials	Under ventilated, post-flashover stage
4	*After 990 s*	*All materials* [b]	*Well ventilated,* *decline stage*

[a] Electronic elements inside the dishwasher are negligible because of their low mass compared to the total.

[b] Because phase 4 only involves less than about 1 % of the total heat release load, it will not be considered in the remainder of the study.

E.8 Determination of the mass fraction of species produced

Three fire stages can be separated. The species production matrix for each material will therefore include three columns, for which the second and third columns are equivalent. It is shown below. Out of concern for simplification in this example, only five gases are considered: CO, CO_2, HCN, HCl and NO_2.Only the principal materials are considered in this example, as presented in Table E.4. Without experimental data for these materials, the corresponding matrices have been determined in the same way as in the previous application example of Annex D.

Table E.4 — Principal materials from the dish washing room, as a function of the heat release load

Material	Heat release load	Proportion of the total heat load
Polyamide	1 960 MJ	55 %
Polypropylene	1 130 MJ	32 %
Polyester/Fibreglass	450 MJ	13 %

The Figure E.3 presents the matrices obtained for the various materials:

Polyamide	Well Ventilated Fire (WVF)	Under Ventilated Fire (PFF1)	Under Ventilated Fire (PFF2)
CO ($kg.kg^{-1}$)	0,108	0,563	0,563
CO_2 ($kg.kg^{-1}$)	2,157	1,408	1,408
HCN ($kg.kg^{-1}$)	0,002	0,023	0,023
HCl ($kg.kg^{-1}$)	0,000	0,000	0,000
NO_2 ($kg.kg^{-1}$)	0,038	0,002	0,002

Polypropylene	Well Ventilated Fire (WVF)	Under Ventilated Fire (PFF1)	Under Ventilated Fire (PFF2)
CO ($kg.kg^{-1}$)	0,146	0,773	0,773
CO_2 ($kg.kg^{-1}$)	2,917	1,932	1,932
HCN ($kg.kg^{-1}$)	0,000	0,000	0,000
HCl ($kg.kg^{-1}$)	0,000	0,000	0,000
NO_2 ($kg.kg^{-1}$)	0,000	0,000	0,000

Polyester/glass	Well Ventilated Fire (WVF)	Under Ventilated Fire (PFF1)	Under Ventilated Fire (PFF2)
CO ($kg.kg^{-1}$)	0,121	0,639	0,639
CO_2 ($kg.kg^{-1}$)	2,413	1,598	1,598
HCN ($kg.kg^{-1}$)	0,000	0,000	0,000
HCl ($kg.kg^{-1}$)	0,000	0,000	0,000
NO_2 ($kg.kg^{-1}$)	0,000	0,000	0,000

Figure E.3 — Matrices used as input data for the calculation

The data from the fire scenario making it possible to calculate the characteristic matrix for the room are given in Table E.5.

Table E.5 — Contribution of the various materials, according to the stage of fire in the room

Material	Phase 1	Phase 2	Phase 3
Polyamide	33 %	33 %	57 %
Polypropylene	67 %	67 %	29 %
Polyester/fibreglass	0 %	0 %	14 %
Total	100 %	100 %	100 %

All of these contributions were calculated for compatibility with the heat release load which represents:

— each of the development stages of the fire (consumption)

— each of the materials (contribution)

With the assignment of these proportionality factors, it is possible to calculate the species production matrix for the room using the formula.

$$[\ ]_{Room} = \sum_{i=1}^{n} P_{(i,SF)} \times [\ ]_{M_i} \begin{bmatrix}1\\0\\0\end{bmatrix} + \sum_{i=1}^{n} P_{(i,WVF)} \times [\ ]_{M_i} \begin{bmatrix}0\\1\\0\end{bmatrix} + \sum_{i=1}^{n} P_{(i,PFF)} \times [\ ]_{M_i} \begin{bmatrix}0\\0\\1\end{bmatrix}$$

The resulting matrix used for calculation is presented as Figure E.4.

Room	Well Ventilated Fire (WVF)	Under Ventilated Fire (PFF1)	Under Ventilated Fire (PFF2)
CO ($kg.kg^{-1}$)	0,133	0,703	0,634
CO_2 ($kg.kg^{-1}$)	2,663	1,757	1,585
HCN ($kg.kg^{-1}$)	0,001	0,008	0,013
HCl ($kg.kg^{-1}$)	0,000	0,000	0,000
NO_2 ($kg.kg^{-1}$)	0,013	0,001	0,001

Figure E.4 — Final matrix for the whole room

This matrix calculated for the room makes it possible to now calculate, as a function of the quantity of each tracer species measured at one point and one moment, the final quantity for each of the gases considered.

E.9 Evacuation

The evacuation scenario in the present application example is here again intentionally simplified. As indicated in the Annex C dealing with methodology, it would be appropriate to incorporate human behaviour, the phenomena of precedence, affiliation, etc. especially since the people present in this restaurant could reach several hundred (up to 570 people theoretically on the basis of one person per square meter for the public, since the employees have their own evacuation routes.

In particular, the question of the route taken to evacuate deserves to be raised here because several evacuation routes are available: Frequently people leave a room by the route they took when they entered; a route which can be longer than using a nearby emergency exit.

Further, here the evacuation conditions are complicated because of the large number of people involved and because all of the available exits will not necessarily be used. Exits 1 and 2 are in fact never used in normal service. Exit 3 is known and regularly used. Exit 4 is the normal exit route, but it is quickly neutralized because of its proximity to the fire source. Exit 5 corresponds to going out by the route used to enter the building (see Figure E.5).

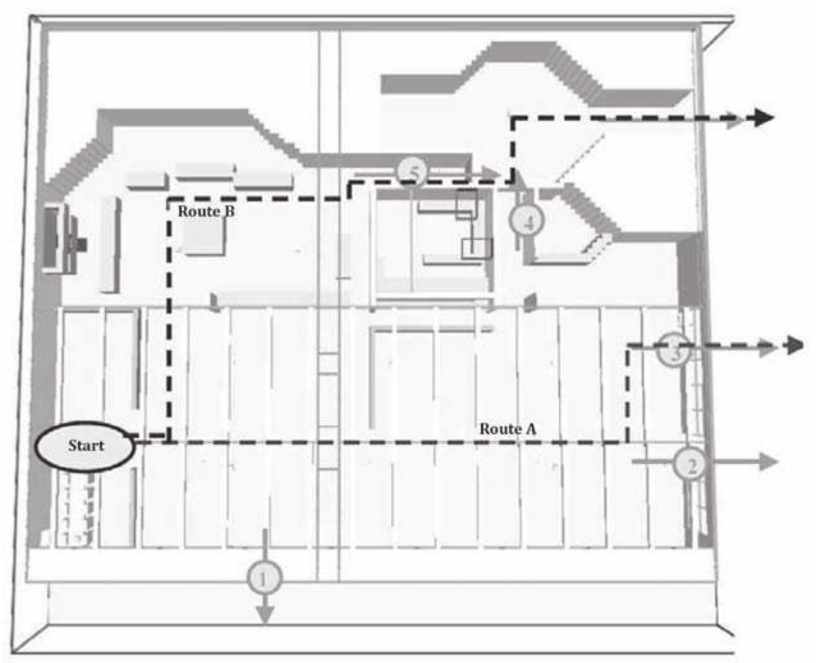

Figure E.5 — Restaurant exits and evacuation paths evaluated

Complete analysis of the evacuation would call for evaluating the evacuation conditions for each of the people present incorporating the characteristic evacuation times (detection, alert, pre-movement, movement, etc.) and their variability in particular because of congestion phenomena.

Additionally, a further level of analysis could make use of parametric tools to make it possible to test several thousand evacuation situations and to evaluate the evacuation conditions according to the corresponding exposure scenarios for each person in each of the situations. It would then be possible to uncover the probabilities of success or failure, the time objectives, evacuation strategies and to test several scenarios.

The context of the present simplified example, we will only consider for people distributed on two paths. The four people leave from the “Start” zone as follows:

— Two take the red route (**Route A**), which goes through the dining room to reach exit 3, normally used in regular service (unlike exits 1 and 2).

— The two other people take the blue route (**Route B**), which never goes in the area around the dishwashing room, and which avoids it by the back (exit 5). This path corresponds to leaving the business by the route taken to enter it.

For each path, the two people start their evacuation at different moments: the time referred to as pre-movement can in fact vary enormously according to the individuals, and the activities they were involved in at the moment the alarm sounded.

E.9.1 Delay in detecting the fire

The moment of detection corresponds to the moment when the smoke starts to leave the room by the tray pass-through. This time is pessimistic because people regularly return their tray to the dishwashing room. The visibility to the inside of the dishwashing room is however poor. The calculation highlights that first smoke going out of the dishwashing room to the main hall becomes visible at about $t = t_0 + 60$ s. Therefore this 60 s time will be used as a reference for the detection delay.

E.9.2 Alarm time

Starting from the moment when this fire source is discovered, the time necessary to remove any doubt and then trigger the alarm is estimated at one minute for the purposes of this application example.

E.9.3 Pre-movement time

This time is needed for the information to spread from the discovery site to all of the room and for the people there to decide to start moving.

This time is different for each occupant evacuating. ISO/TR 16738, Annex E of gives some data on the distribution of pre-movement times and their derivatives. From this it follows that the distribution of pre-movement times follows approximately a log-normal distribution whose profile depends on the quality of the fire safety management.For the purposes of this application example, this time was set to the minimum at one min. For each path study, the first occupant will therefore not leave before 180 s.

NOTE The lower the levels of fire safety management, the longer the pre-movement times of the first occupants who evacuate and the distribution of pre-movement times which follow from it.

E.9.4 Escape routes

The evacuation takes place under movement conditions which depend on the degree of congestion of the aisles and exits and also on the visibility conditions.

Data concerning the movement speeds are provided in ISO/TR 16738, Annex G. In particular, the Nelson and Mowrer equation connects the density of people and the movement speed, S, between the limits of 0,54 people/m^2 and 3,8 people/m^2.

$$S = k - a \cdot k \cdot D$$

where:

D is the density, expressed in number of people per square meter

k is 1,4 for horizontal movement

a is equal to 0,266

Thus, by considering an average density of two people per square meter, a movement speed of 0,65 m.s^{-1} results, and 0,28 m.s^{-1} for three people per square meter Above 3,8 people per square meter, the movement speed is zero. Reference [26] cites normal speeds of order 1 m.s^{-1} for movement in conditions of good visibility, 0,5 m.s^{-1} in case of poor visibility and between 0,2 and 0,4 m.s^{-1} for very poor visibility. A simple method is using 1 m.s^{-1} for clear visibility, 0,5 m.s^{-1} for very limited visibility, and 0,3 m.s^{-1} for no visibility.

There are however no precise guides enabling incorporating the two phenomena simultaneously. Also, in the context of this example, the following simplified values are taken for the evacuation speed, considering simultaneously the visibility and moderate congestion of the evacuation aisles.

— Good visibility (≥10 m): movement speed = 0,5 m.s^{-1}

— Poor visibility (<10 m): movement speed = 0,25 m.s^{-1}

The Figure E.6 shows the progression of the visibility starting from 180 s and in steps of 60 s (the blue square corresponds to the dishwashing room), at the average height of human vision (1,5 m). The zones where the visibility is best (30 m) are red, the zones where the visibility is minimal are in dark blue. The 10 m visibility limit is shown in black.

It emerges from these illustrations that the visibility is good up to 4 min. after the fire starts, but then worsens a lot over the entire business. The optimal conditions for movement therefore occur between 180 s (first occupant to leave) and 240 s.

The smoke remains better stratified in the area around the dishwashing room: hotter, it has a greater buoyancy and accumulates in the upper part. Further, the proximity of the vents make it possible to extract a large part of it.

In the other areas of the restaurant, the combination of the loss of buoyancy of the smoke due to their cooling, and mixing of the ambient air linked to the AHU leads to massive destratification of the smoke.

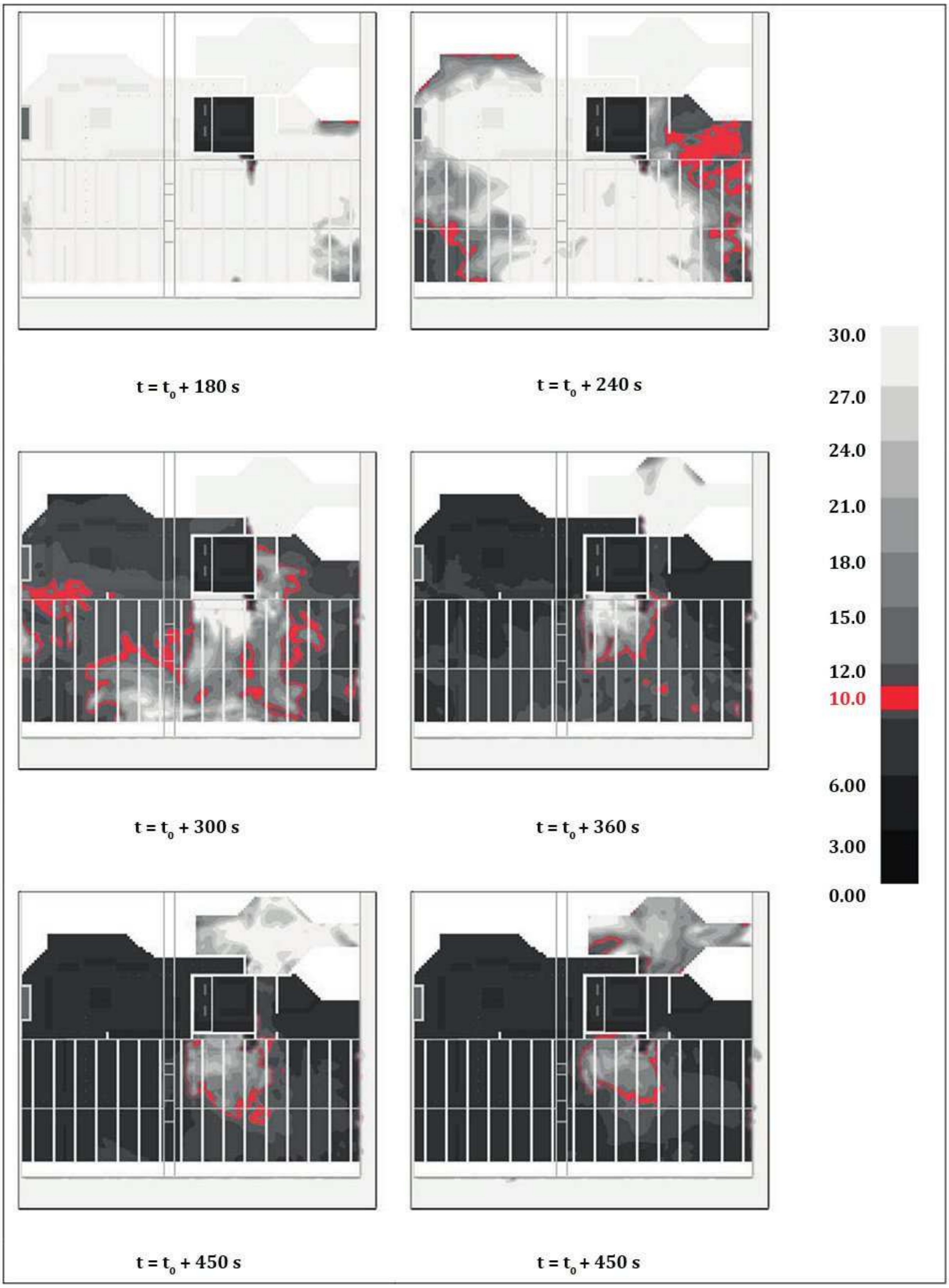

Figure E.6 — Progression of the visibility in the restaurant (red shows the 10 m visibility limit)

For each route, consider the departure of an occupant at t_0 + 200 s and the departure of an occupant at t_0 + 400 s. The speed of movement takes into consideration the visibility conditions. The two occupants taking the **route A** will be designated **A200** and **A400** according to the departure time. The two occupants taking the **route B** will be designated **B200** and **B400** according to the departure time.

For route A:

Figure E.7 presents the results obtained for various FED formulas, for route A and movement starting after 200 s. The first occupant A200 – who leaves at 200 s – covers the distance necessary for his evacuation without experiencing notable effect. The largest value is reached by exposure to irritating gases near the end of their travel. The FEC value reached however remains well below the 0,3 limit. For this occupant, evacuation is completed without difficulty.

NOTE The thermal and asphyxiating FED are not 0 at the moment of starting, because they integrate the dose received in the 200 s pre-movement phase.

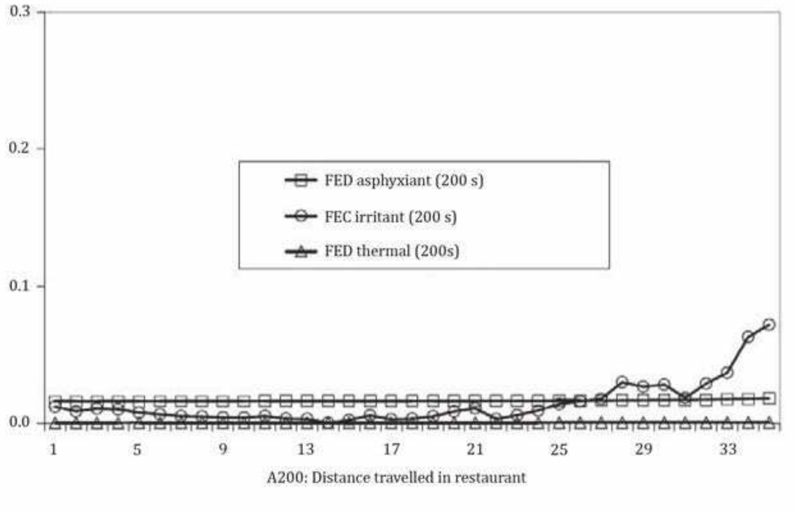

Figure E.7 — Effects experienced by the first occupant (route A, 200 s)

Figure E.8 presents the results obtained for various FED formulas, for route A and movement starting after 400 s. The second occupant – taking this path and starting at 400 s (A400) experiences major thermal effects which compromise his evacuation. All the temperatures that he experiences before per 40°C to 50°C with a relatively weak convective effect, the incident flux to which he is subject rises to more than 4 kW/m^2 right by the dishwashing room. The smoke escaping by the tray pass-through is in fact very hot: it then rises to the ceiling and is then channelled by beams which concentrated it in a band going from the tray pass-through to the wall of the building, while going over the evacuation path A. The flux it radiates downward is then sufficient for compromising the evacuation. Over this portion of the path, the relatively hot smoke remains under the ceiling because of buoyancy, and in this area, the toxic concentration remains moderate: this explains why the rise in $FED_{asphyxiating}$ is less strong than $FED_{thermal}$. All the same $FED_{asphyxiating}$ rises above the 0,3 limit at the end of the route, which means that if the person were properly protected against the thermal effects, but without an isolating respiratory device (for example a fire-fighter without SCBA), they would end by being incapacitated by the toxic effects of the gases.

It is also appropriate to note that $FED_{asphyxiating}$ is already high at the beginning of the route, but not $FED_{thermal}$: remaining in place protects the occupant thermally, but not from toxic effects. If this occupant remained in place for too long, he would end up being incapacitated by toxic effects without having moved. This is for example particularly interesting in the case of sleepy areas, whether they are located in public buildings or in residential areas.

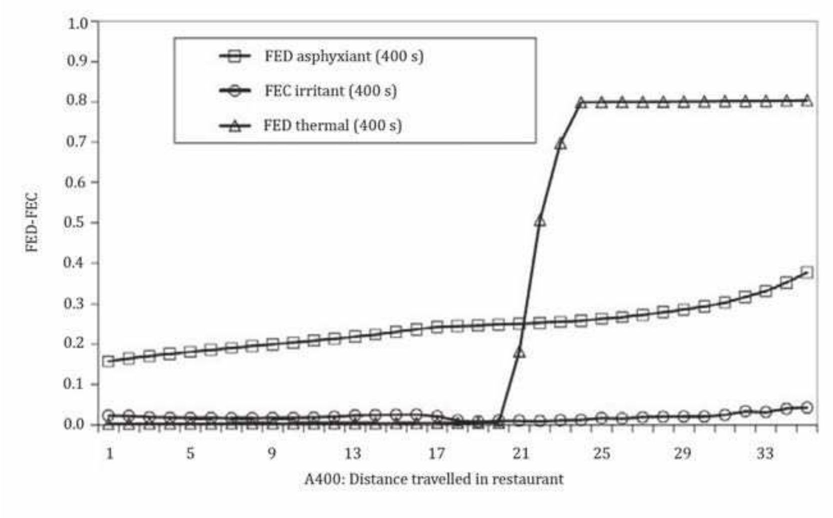

Figure E.8 — Effects experienced by the second occupant (route A, 400 s)

For route B

Figure E.9 presents the results obtained for various FED formulas, for route B and movement starting after 200 s. Like the first occupant on route A, the first occupant on route B – B200 who leaves at 200 s – covers a distance necessary for his evacuation without experiencing notable effect. For the occupant B200, the evacuation is completed without difficulty.

NOTE The thermal and asphyxiating FED are not 0 at the moment of starting, because they integrate the dose received in the 200 s pre-movement phase.

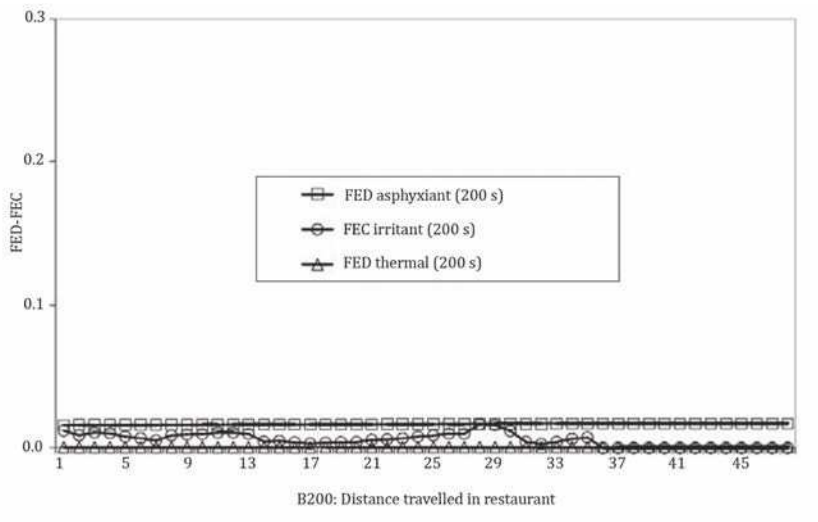

Figure E.9 — Effects experienced by the first occupant (route B, 200 s)

Figure E-10 presents the results obtained for various FED formulas, for route B and movement starting after 400 s. contrary to earlier start (B200), exposure to toxic gases is incapacitating before occupant can complete his evacuation. This occupant goes far from the hot smoke; he is only affected by the toxic gases: $FED_{thermal}$ remains far below 0,1 whereas $FED_{asphyxiating}$ exceeds the threshold of 0,3 even though no one is in the area of the scramble.

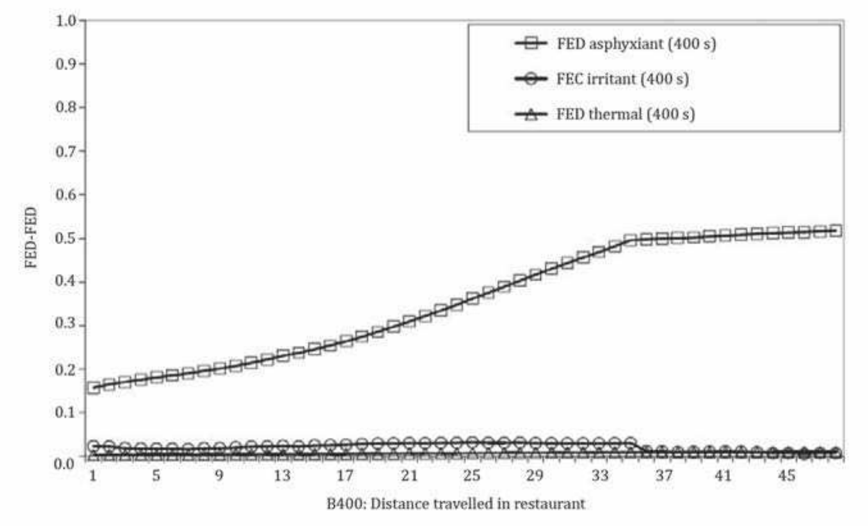

Figure — E-10 — Effects experienced by the second occupant (route B, 400 s)

Note that if the person could move that far, the passage by door #5 (inflexion after 35 m travel on the Figure E-10) would lead to a notably smaller exposure, because the zone located after door #5 is notably less smoky: the FEC drops suddenly after this point, and the $FED_{asphyxiating}$ curve has a discontinuity in the slope at the same point. However, even though they arrive in an area with less smoke, the gases present would continue to produce their effects.

In fact, one could imagine the case of person leaving by door #5 being just under the threshold of incapacitation. They could feel relatively safe because they encounter much better conditions, but find themselves incapacitated by the small increase in asphyxiating gas dose in this area.

For this occupant, incapacitation takes place because of the toxic effects; the thermal effects are nearly nonexistent for him.

Progression of the FEC and FED according to the moment of starting.

Figure E.11 shows progression of FED and FEC along the route used and the time since starting to leave. The chart incorporates the progression of the visibility conditions for determining the travel speed each point.

It is observed that the evacuation along route A can be done successfully if the departure time is below about 290 s. Beyond that, the thermal problems encountered on the path at the time of passage under the hot smoke lead to rapid incapacitation and evacuation become impossible because of thermal effects of fire.

For route B, evacuation remains possible until 330 s. Beyond that, the asphyxiant effect becomes too significant, the person is incapacitated before being able to complete his evacuation. On the other hand, along route B, the thermal dose never compromises evacuation whatever the moment of departure.

The importance of the evacuation management strategy therefore emerges from this analysis: an evacuation strategy suited to this establishment leads to the departure of all the occupants before these time windows. Otherwise, the strategy is not suitable, and it is appropriate to implement substantial modifications, either to the evacuation management, or to the establishment itself, for example by implementing additional smoke control devices such as vents or openings.

The technique presented for analysing the development of the FED and FEC as a function of the behaviour of the individual makes it possible to not only analyse the conditions encountered during the evacuation, but can of course serve to test the evacuation strategies.

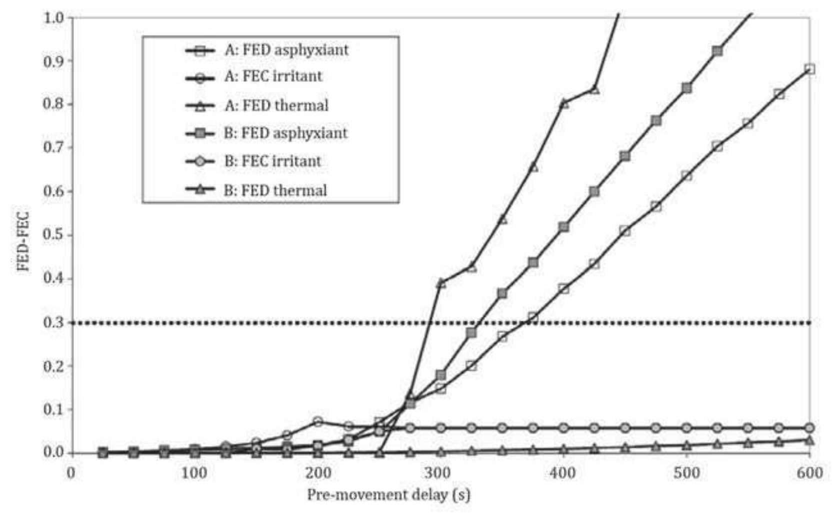

Figure E.11 — Progression of the effects on people along the route taken and the time since leaving

Annex F
(informative)

Determination of data for matrix

F.1 General

Species production matrices covered in Annexes C to E can be fulfilled with several types of sources, some theoretical (e.g. ISO 19706, and ISO 19703), and others experimental.

Theoretical values should however be considered with caution because they suffer from significant limitations.

— Values found in the literature can relate to similar materials, which are not identical to the materials actually present, and the test conditions are often not specified. These latter can therefore be removed from the conditions that one seeks to characterize.

— The values coming from ISO 19703 are maximized theoretical rates, which do not take into account the combustion equation and the sharing of the atoms composing the combustible molecules between various species produced, nor the fire regime.

— The values coming from ISO 19706 are too fragmentary and are particularly interesting for the [CO]/[CO_2] ratios for each fire regime.

This is why the following test conditions for measuring the gaseous species produced, inspired by the definitions from ISO 19706, are recommended.

The thermal attack with cone calorimeter (ISO 5660-1) under controlled atmosphere with measurement of gaseous species is done using a Fourier transform infrared (FTIR) analyser (ISO 19702) or classical analysers (ISO 19701). In Table C-1, the value of CHF or Critical Heat Flux designates the critical flux at piloted ignition determinable for a given material by the Tewarson method which connects the incident flux density to the square root of the inverse of the ignition time measured according to a linear relation. The critical flux at piloted ignition designates therefore the flux density such that ignition of the material occurs after an infinite time.

F.2 Test devices and measurement procedures

F.2.1 Thermal attack device

The test samples are subjected to an incident thermal flux which is principally radiative in nature. This control thermal flux is produced by a conical electric furnace, described in ISO 5660-1.

The protocol consists of heating up the material subjected to this controlled source for sufficient time to reach thermal equilibrium. A first incident flux is tried. If the material catches fire in less than 30 min., a smaller flux is tried. Otherwise, a larger flux is tested. Near the flux limit, the flux increment is 1 kW/m^2. The first value of incident flux corresponding to the non-ignition of the material is then confirmed by a second test. For large fluxes, the increment is 10 kW/m^2. Since the tested fluxes are representative of the pre-flashover phase of the fire, the maximum value currently studied is 50 kW/m^2. However, for the present purposes, the 75 kW/m^2 flux is used to study the materials in post flashover fire situation.

NOTE In order to facilitate the ignition of the pyrolyzed gases produced, an electric spark plug is placed at the surface of the test sample.

The test sample is placed in the standardized sample holder and then exposed to the flux from a radiator, according to the requirements of ISO 5660-1. The standardized sample holder is placed on a previously tared continuous weighing scale. The surface of the test sample is subjected to the thermal flux (previously adjusted using a calibrated terminal fluxmeter) emitted by the heating resistance of a comic radiator. The distance between the radiator and the surface of the sample is adjusted to 25 mm, per the recommendation of the ISO 5660-1 standard. For all the tests, the test samples are conditioned in advance for 48 h at 23 ± 2°C and 50 ± 5 % relative humidity.

F.2.2 Energy parameters

Cone calorimeter combustion makes it possible to calculate various energy parameters and also the material's fire behaviour parameters.

— The material's heat release rate characterizes its aptitude to release heat during its combustion. It is evaluated from the oxygen consumption necessary for this combustion.

— The opacity of the smoke produced is determined continuously during the test. It is obtained by measuring the light intensity attenuation of the beam of a helium neon laser.

— The mass lost from the test sample is measured continuously during the test. It makes it possible to characterize the speed of degradation of the material.

F.2.3 Tests under controlled atmosphere

The behaviour of material can also be studied under different sub-oxygenation conditions. Thus, beyond the conditions of normal ventilation (20,95 % O_2) we will also consider those corresponding to an O_2 level set at 15 %.To generate the working atmosphere; the device comprises a pre-mixing chamber making it possible to precisely mix controlled quantities of nitrogen and ambient air. This mixture is then injected directly into the combustion chamber. This is formed from a sealed housing with a lockable access door, in which a normalized support balance is placed. A conical radiator, originating the thermal breakdown of the test material, is placed under the roof of the housing. Before each test the oxygen concentration is verified using the oxygen analyser installed in the test bench.

F.3 Fire effluents analyses

F.3.1 Analysis by Fourier Transform Infrared (FTIR) Spectrometer

Combustion effluents are sampled at a constant rate in the main conduit from the cone calorimeter, and routed to the gas cell of a Fourier transform infrared spectrometer. The infrared beam passing through this cell makes it possible to obtain the absorption spectrum of the chemical species which have a dipole moment.

A quantitative analysis of the chemical species produced during thermal breakdown of the sample is done in a first step by comparison of the collected infrared spectra with spectra of pure gases in a computer library.

This qualitative analysis is then supplemented by a quantitative analysis. Conventionally this is done using the calculation program called "Classical Least Square". This program is fed with both the spectra of the samples and also a set of standard spectra of pure gases. For the quantitative analysis as for the calibration, the signal measurement is done for each gas in a specific spectral zone which is free of interference from other gases

Qualitative analyses performed on all the spectra collected during the test makes it possible to establish the production kinetics of each chemical species. The integration of these kinetics makes it possible to estimate the quantity of gas produced per unit mass of material used.

More details on this technique are available in ISO 19702.

F.3.2 Analysis of aldehydes by High-Performance Liquid Chromatography (HPLC)

The effluents are sampled at a constant rate in the main conduit of the cone calorimeter throughout the live combustion by means of a tube containing a specific chemical reagent (2,4-dinitrophenylhydrazine).

The hydrazones formed are subsequently dissolved in acetonitrile. High-performance liquid chromatography (HPLC) at 360 nm is used for qualitative and quantitative analysis of formaldehyde, acetaldehyde, acrolein, acetone and propionaldehyde hydrazone.

More details on this technique are available in ISO 19701.

F.4 Critical flux

The critical flux of the product tested and also its thermal response can be determined by means of the Tewarson relation. In the equation, t_{ig} designs ignition delay (s), q''_e the incident flux (kW/m^2), CHF the critical heat flux (kW/m^2) and TRP the thermal response parameter (kJ·s$^{-0.5}$·m^{-2}). The relation is used by measuring the ignition delay of the test sample at different flux levels from the conical heater.

F.5 Alternative fire model for effluents: ISO/TS 19700

The test device described in the ISO/TS 19700 standard is a tube furnace traversed by a quartz tube and opens into a mixing and measurement chamber. A mechanism makes it possible to push a nacelle containing the sample to be tested, reduced to small size and homogenized in the nacelle, at a controlled speed such that the mass pushed in the tube per unit time is the most constant possible.

The air flow rate at the inlet to the quartz tube is fixed as is the secondary airflow rate in the mixing chamber. This contains a device for measuring the opacity of the smoke.

The analyses are done using analytical methods described in the standards ISO 19701 and ISO 19702. To reproduce the various fire regimes, the following are the recommended test conditions:

F.5.1 Oxidative pyrolysis

Linear density sampling of 25 mg·mm^{-1} in the nacelle, setting of the tube furnace to 350°C, and primary air flow rate at 2 l·min^{-1}. In case of ignition, the furnace's temperature setting is lowered until obtaining pyrolysis without ignition during the entire length of the test's cruising regime.

NOTE This condition can also be obtained if necessary with the cone calorimeter under controlled atmosphere by conducting the test under nitrogen.

F.5.2 Combustion in well-ventilated environment

Linear density sampling of 25 mg·mm^{-1} in the nacelle, regulation of the tube furnace to 650 °C, primary air flow rate at 10 l·min^{-1}, and secondary airflow rate at 40 l·min^{-1}. The test is valid for oxygen depletion included between 1,8 % to 3,14 % otherwise it is necessary to adapt the sampling. If no ignition occurs, the temperature is increased by 25 °C and the test redone until obtaining combustion during the entire length of the tests cruising regime.

F.5.3 Under-ventilated fire

The conditions are similar to those of the well ventilated fire, since the primary air flow rate is adapted according to the oxygen depletion obtained during combustion in well ventilated environment.

Here again, if there is no ignition, the temperature is adjusted in steps of 25 °C.

F.5.4 Combustion in post-flashover conditions

This case is identical to the preceding, except for the furnace temperature which is set at 825 °C.

Bibliography

[1] Guillaume E., & Chivas C. *Fire models used in toxicity testing*, Proceedings of Hazards of Combustion Products conference, Ed. V. Babrauskas, R.G. Gann and S. Grayson, London, 10/11 November 2008, ISBN 978-0-9556548-2-4, Interscience Communications Ltd, London (2008)

[2] Guillaume E Toxicité des Fumées d'Incendie. Techniques de l'Ingénieur, SE2060 (in French)

[3] Gottuk D.T., & Lattimer B.Y. Effects of Combustion Conditions on Species production, SFPE Handbook of Fire Protection Engineering 4th edition, NFPA, Quincy Massachusetts USA, 2008, section 2-5

[4] Advances in Combustion Toxicology. ed. G. Hartzell, Technomic Publishing Company, ISBN 87762-590-5 (vol. 1), 87762-591-3 (vol. 2), 87762-886-6 (vol. 3)

[5] Fire Toxicity. ed. A.A. Stec, R.T. Hull. Woodhead Publishing Ltd / CRC Press LLC, 2010

[6] Su J.Z., Bénichou N., Bwalya A.C., Lougheed G.D., Taber B.C., Leroux P. Unprotected Floor Assemblies and Tenability Conditions in a Test House Under Two Basement Fire Scenarios. Fire Technology, **Vol. 47**, 2011, pp. 631–64.

[7] American Society for Testing and Materials. Standard Test Method for Fire Testing of Upholstered Furniture, ASTM E1537-02a. ASTM, West Conshohoken, PA, 2002

[8] Purser D. A. - Assessment of Hazards to Occupants from Smoke, Toxic Gases, and Heat. In: The SFPE Handbook of Fire Protection Engineering, (DiNenno P.J., Drysdale D., Beyler C.L., Walton W.D., Custer R.L.P., Hall J.R. eds.). Society of Fire Protection Engineers /National Fire Protection Association, Quincy, Massachusetts, Fourth Edition, 2008

[9] Wieczorek C.J., & Dembsey N.A. Human Variability Correction Factors for Use with Simplified Engineering Tools for Predicting Pain and Second Degree Skin Burns. J. Fire Prot. Eng. 2001, **11** pp. 88–111

[10] Guillaume E., Didieux F., Thiry A., Bellivier A. Real-scale fire tests of one-room apartments with regard to tenability assessment. Fire Saf. J. 2014, **70** pp. 81–97

[11] BS 6807:2006, *Methods of test for assessment of ignitability of mattresses, upholstered divans and upholstered bed bases with flaming types of primary and secondary sources of ignition*

[12] Jin T. Studies of Emotional Instability in Smoke from Fires, Journal Fire and. Flammability. 1981, **12** pp. 130–142

[13] Rasbash D.J. Sensitivity Criteria for Detectors Used to Protect Life. Fire International. 1975, **5** (40) pp. 30–49

[14] Peacock R.D., Reneke P.A., Bukowski R.W., Babrauskas V. Defining flashover for fire hazard calculations. Fire Saf. J. 1999, **32** (4) pp. 331–345

[15] Guillaume E., Verlinden G., Gensous F., Muller A., Bonhomme M., Joyeux D., Lecoq-Jammes O., Cornillon T., Oraison J.M., Labarthe J.C., Van Niel K., Bellivier A., Chivas-Joly C., Didieux F., Rochat B., Detraz P., Chaudron B., Parisse D., Le Madec B., Lacoste J.F., Heuzé B., Rémy A., Hourqueig R. Etude de la prise en compte de la toxicité des fumées en cas d'incendie. Rapport final du Groupe de Travail « Toxicité » du Comité d'Etudes et Classification des Matériaux vis à vis du risque Incendie (CECMI – Ministère de l'Intérieur, Direction de la Sécurité Civile). Technical report available on http://www.lne.fr/publications/guides-documents-techniques/rapport-toxicite-fumees-incendie-final.pdf, 2010

[16] Drysdale D. An Introduction to Fire Dynamics. John Wiley & Sons, Chichester, UK, Second Edition, 1998, pp. 296–323.

[17] BS PD 7974-1:2003 "Application of fire safety engineering principles to the design of buildings. Initiation and development of fire within the enclosure of origin (Sub-system 1)

[18] EN 1991-1-2:2002 "Eurocode 1: Actions on structures – Part 1-2: General actions – Actions on structures exposed to fire", ICS 53.020.20;91.080.10

[19] Babrauskas V., & Walton W.D. A simplified characterization of upholstered furniture heat release rates. Fire Saf. J. 1986, **11** (2) pp. 181–192

[20] Gann R.G., Averill J.D., Butler K.M., Jones W.W., Mulholland G.W., Neviaser J.L., Ohlemiller T.J., Peacock R.D., Reneke P.A., Hall J.R. International Study of the Sublethal Effects of Fire Smoke on Survivability and Health (SFES), NIST Technical Note 1439, NFPA, Quincy, MA 02269-9101, August 2001

[21] Gann R.G., Averill J.D., Johnsson E.L., Nyden M.R., Peacock R.D. Fire effluent component yields from room-scale fire tests. J. Fire & Materials. 2010, **34** (6) pp. 285–314

[22] Babrauskas V., Twilley W.H., Janssens M.L., Yusa S. Cone calorimeter for controlled-atmosphere studies. Fire Mater. 1992 January, **16** (1) pp. 37–43

[23] Leonard J.E., Bowditch P.A., Dowling V.P. Development of a controlled-atmosphere cone calorimeter. Fire Mater. 2000 May, **24** (3) pp. 143–150

[24] Le Tallec Y., & Guillaume E. Fire gases and their chemical measurement, Proceedings of Hazards of Combustion Products conference, Ed. V. Babrauskas, R.G. Gann and S. Grayson, London, 10/11 November 2008, ISBN 978-0-9556548-2-4, Interscience Communications Ltd, London (2008)

[25] Fardell P.J., & Guillaume E. Sampling and measurement of toxic fire effluent. In: A. Stec, R, (Toxicity F. ed.). Woodhead Publishing Ltd, Hull, 2010

[26] Proulx G. Evacuation time, SFPE Handbook of Fire Protection Engineering 4th edition, NFPA, Quincy Massachusetts USA, 2008, section 3-12

[27] Bryan J.L. Behavioral Response to Fire and Smoke, SFPE Handbook of Fire Protection Engineering 4th edition, NFPA, Quincy Massachusetts USA, 2008, section 3-11

[28] Evacuation simulation of tall buildings. Proceedings of the CIB-CTBUH International conference on Tall Buildings, 20-23 October 2003, Malaysia

[29] Kuligowski E.D. The Process of Human Behaviour in Fires. NIST Technical Note 1632. May 2009

[30] Winerman L. Fighting fire with Psychology. Monitor staff, September 2004, Vol. 35, No. 8

[31] Bustamante Valencia L., Rogaume T., Guillaume E., Rein G., Torero J.L. Analysis of principal gas products during combustion of polyether polyurethane foam at different irradiance levels. Fire Saf. J. 2009. DOI:10.1016/j.firesaf.2009.05.003

[32] ISO 16732 (all parts), *Fire safety engineering — Fire risk assessment*

[33] ISO 23932, *Fire safety engineering — General principles*

[34] ISO 19706, *Guidelines for assessing the fire threat to people*

[35] ISO 19701, *Methods for sampling and analysis of fire effluents*

[36] ISO 19703, *Generation and analysis of toxic gases in fire — Calculation of species yields, equivalence ratios and combustion efficiency in experimental fires*

[37] ISO/TR 16312-2, *Guidance for assessing the validity of physical fire models for obtaining fire effluent toxicity data for fire hazard and risk assessment — Part 2: Evaluation of individual physical fire models*

[38] ISO 29903, *Guidance for comparison of toxic gas data between different physical fire models and scales*

[39] ISO/TS 19700, *Controlled equivalence ratio method for the determination of hazardous components of fire effluents*

[40] ISO 16405, *Room corner and open calorimeter — Guidance on sampling and measurement of effluent gas production using FTIR technique*

[41] ISO/TR 16738, *Fire-safety engineering — Technical information on methods for evaluating behaviour and movement of people*

[42] ISO 13943, *Fire safety — Vocabulary*

[43] ISO 13571, *Life-threatening components of fire — Guidelines for the estimation of time to compromised tenability in fires*

[44] ISO 5660-1, *Reaction-to-fire tests — Heat release, smoke production and mass loss rate — Part 1: Heat release rate (cone calorimeter method) and smoke production rate (dynamic measurement)*

ICS 13.220.01
Price based on 86 pages